HEINRICH HEINE
UNIVERSITÄT DÜSSELDORF

Development and Evaluation of Physiologically Based Pharmacokinetic Drug-Disease Models for Carvedilol in Adults and Children by Using Population Based Simulations and Real Data

INAUGURAL-DISSERTATION

zur Erlangung des Doktorgrades

der Mathematisch-Naturwissenschaftlichen Fakultät

der Heinrich-Heine-Universität Düsseldorf

vorgelegt von

Muhammad Fawad Rasool

aus Multan

Düsseldorf, April 2016

Aus dem

Institut für Klinische Pharmazie

und Pharmakotherapie

Gedruckt mit der Genehmigung der

Mathematisch-Naturwissenschaftlichen Fakultät der

Heinrich-Heine-Universität Düsseldorf

Referent: Prof. Dr. Stephanie Läer

Korreferent: Prof. Dr. Jörg Breitkreutz

Tag der mündlichen Prüfung: 18.05.2016

I. Erklärung zur Dissertation

Ich versichere an Eides Statt, dass die Dissertation von mir selbständig und ohne unzulässige fremde Hilfe unter Beachtung der „Grundsätze zur Sicherung guter wissenschaftlicher Praxis an der Heinrich-Heine-Universität Düsseldorf" erstellt worden ist. Die Dissertation wurde in der vorgelegten oder in ähnlicher Form noch bei keiner anderen Institution eingereicht. Ich habe bisher keine erfolglosen Promotionsversuche unternommen.

Düsseldorf den   Muhammad Fawad Rasool

II. Acknowledgement

III. Zusammenfassung

Die zügig voranschreitende Entwicklung im Bereich des Physiologie-basierten pharmakokinetischen (PBPK) Modellierens sowie das stetig wachsende Wissen über pathophysiologische Veränderungen tragen entscheidend zur Entwicklung von Arzneistoff-Krankheitsmodellen bei. Durch Einbindung dieser krankheitsbedingten pathophysiologischen Veränderungen, besteht mittels des PBPK Ansatzes die Möglichkeit Arzneistoff-Krankheitsmodelle zu entwickeln.

Im erste Abschnitt der Dissertation wurden zwei PBPK Modelle entwickelt, welche pathophysiologisch bedingte hämodynamische Änderungen im hepatischen und renalen Blutfluss bei vorliegender Herzinsuffizienz berücksichtigen. Am Beispiel des Modelarzneistoffes Carvedilol wurde gezeigt, dass die entwickelten Modelle eine korrekte Vorhersage der Pharmakokinetik in gesunden und erkrankten Populationen ermöglichen.

Der zweite Teil der Arbeit diente der Modellentwicklung zur Vorhersage der stereo-selektiven Disposition von Carvedilol in Erwachsenen und Kindern mit Herzinsuffizienz. Das entwickelte Model, welches den reduzierten Blutfluss durch die Organe berücksichtigt, konnte erfolgreich die Pharmakokinetik der Carvedilol Enantiomere in gesunden und herzinsuffizienten Erwachsenen zeigen. Im Gegensatz zu Erwachsenen, zeigte sich jedoch, dass bei Kindern bis 12 Jahren die Simulation ohne reduzierten Blutfluss eine genauere Vorhersage erlaubt.

Der Schwerpunkt im dritten Kapitel dieser Arbeit war die Entwicklung und Untersuchung eines PBPK-Carvedilol-Zirrhose Modells, welches fähig ist Dosisempfehlungen zu berechnen. Hierbei wurde vor allem der grundlegende Unterschied an gebundener und gesamter (gebunder und ungebunder) systemischer Carvedilol Konzentration in den unterschiedlichen Schweregraden der Krankheit untersucht.

Diese Dissertation befasst sich mit PBPK Modellierung verschiedener klinischer Szenarien, in welchen der stark über die Leber extrahierte-Arzneistoff Carvedilol in gesunden und erkrankten Populationen zum Einsatz kommt.

IV. Summary

The rapid advancement in physiologically based pharmacokinetic (PBPK) modelling as well as the increasing quantitative knowledge of disease-related pathophysiological changes facilitate building of drug-disease models. By incorporating pathophysiological changes occurring in different diseases, the PBPK approach can be used for developing drug-disease models.

In the first part of this thesis, two PBPK models were developed that were incorporating the pathophysiological changes in hepatic and renal blood flow occurring in adult and pediatric chronic heart failure (CHF) patients. Carvedilol, which undergoes extensive metabolism in the liver, was selected as a model drug. The model has successfully predicted carvedilol PK in healthy and diseased populations.

The aim of second part of thesis was to predict stereo-selective disposition of carvedilol in adult and pediatric CHF patients. The developed model has successfully described PK of carvedilol enantiomers in healthy adults and in CHF patients after the incorporation of reduced organ blood flows. In contrast to adults, pediatric patients up to 12 years of age were better described without the reductions in organ blood flow, whereas older pediatric patients were better described after incorporating organ blood flow reductions.

The focus of third part of the thesis was to develop and evaluate a PBPK-carvedilol-cirrhosis model with the available clinical data in liver cirrhosis patients and to recommend model based drug dosing after exploring the underlying differences in unbound and total (bound and unbound) systemic carvedilol concentrations with the different disease stages.

In short, this thesis focuses on PBPK modelling of different clinical scenarios encountered with the use of high hepatic extraction drug "carvedilol" in healthy and diseased populations.

V. Table of contents

VI. List of Figures

VII. List of Tables

VIII. List of abbreviations

ADAM	advanced dissolution, absorption, and metabolism
ADME	Absorption, Distribution, Metabolism and Elimination
AUC_{0-inf}	area under the plasma concentration-time curve from time zero to infinity
AUC_{last}	area under the plasma concentration-time curve from the first to the last concentration points
B:P ratio	blood-to-plasma concentration ratio
BCS	Biopharmaceutics Classification System
CHF	Chronic Heart Failure
CI	confidence interval
CL	drug clearance
C_{last}	last measured concentration in a plasma profile
Child-Pugh	CP
CL_H	hepatic clearance
CL_{int}	intrinsic clearance
CL_R	renal clearance
C_{max}	maximum concentration
CL_{perm}	permeability clearance
CYP	cytochrome P450
EM	Extensive Metabolizer
EMA	European Medicines Agency
f_a	fraction of drug absorbed
f_g	fraction of drug escaping gut wall metabolism
f_h	fraction of drug escaping hetapic metabolism
F	bioavailability
f_u	fraction unbound
$f_{u,Gut}$	unbound fraction of the drug in the enterocyte
GET	gastric emptying time
iv	Intravenous
k_e	elimination rate constant
K_p	tissue-to-plasma distribution coefficient
LogD	logarithmic distribution coefficient
log$P$	logarithmic octanol-water partition coefficient
MW	molecular weight
NCA	non-compartmental analysis
NYHA	New York Heart Association

P_{eff}	human jejunum permeability
P_{app}	apparent permeability
PBPK	physiologically based pharmacokinetic
PD	pharmacodynamics
PK	pharmacokinetic
pK_a	acid dissociation constant
PM	Poor Metabolizer
Q_{Gut}	a hybrid term predicted by using villous blood flow and permeability clearance
Q_H	hepatic blood flow
$Ratio_{(Obs/Pred)}$	observed to predicted ratio
SD	standard deviation
t_{max}	time of maximum concentration
V_{ss}	steady state volume of drug distribution

IX. Motivation, Rationale, and Aim of the Thesis

In the world of classical pharmacokinetics there was always a need for models that are physiologically realistic and easy to understand. This need was met by the emergence of systems pharmacology which eventually lead to the development of physiologically based pharmacokinetics (PBPK). The PBPK approach utilizes population specific, demographical, anatomical, physiological and genetic data that leads to development of virtual populations. These virtual populations then can be used to explore pharmacokinetics (PK) of different drugs by facilitating incorporation of in-vivo and in-vitro absorption, distribution, metabolism and elimination data (ADME).

In the current PhD research work, PBPK approach was used for building drug-disease models in adult and pediatric populations. The first chapter focuses on development of a PBPK model for the use of high hepatic extraction drug, carvedilol in adult and pediatric chronic heart failure patients (CHF), by incorporating pathophysiological reductions in organ blood flows. Since, carvedilol is administered as a racemic mixture of R and S-enantiomers and both enantiomers have different PK and pharmacodynamics (PD) profiles. Therefore, in the second chapter the previously developed CHF model was upgraded with additional information on tissue/organ blood flow reductions and was used to predict stereo-selective disposition of carvedilol enantiomers in adult and pediatric CHF patients. In the last chapter, a PBPK model was developed in liver cirrhosis patients to explore the PK of carvedilol in this population. The developed carvedilol-cirrhosis PBPK model was evaluated with the only available clinical PK data in Child-Pugh–C patients and after evaluation it was extended to other Child-Pugh populations. Moreover, on the basis of differences between unbound and total (bound and unbound) carvedilol exposure, dose reductions were recommended in different Child-Pugh cirrhosis populations.

Chapter 1:

A physiologically based pharmacokinetic drug-disease model to predict carvedilol exposure in adult and pediatric heart failure patients by incorporating pathophysiological changes in hepatic and renal blood flows

1.1. Introduction

Chronic diseases are associated with pathophysiological changes that could have profound impact on drugs pharmacokinetic behavior with a potential need to modify the administered drug therapy (Boucher et al., 2006). It is important to acknowledge that most patients with chronic illnesses do not have a single, predominant condition but suffer from multiple comorbidities. The rapid advancement in physiologically based pharmacokinetic (PBPK) modelling as well as the increasing quantitative knowledge of disease-related pathophysiological changes facilitate building of drug-disease models that can incorporate these changes to predict their pharmacokinetic impact (Edginton and Willmann, 2008; Johnson et al., 2010; Khalil and Laer, 2011; Rowland Yeo et al., 2011; Li et al., 2012; Sayama et al., 2014; Vogt, 2014). A PBPK model that is modified according to the pathophysiology of a disease could be extended, after its evaluation, to a wide variety of drugs because of its mechanistic nature. An additional gain can be further obtained if an extrapolation from adult patients to special populations, e.g. children, does occur.

However, despite the clinical significance, there are only few published examples of PBPK models incorporating pathophysiological changes occurring with chronic diseases (Edginton and Willmann, 2008; Johnson et al., 2010; Li et al.,

2012; Sayama et al., 2014; Vogt, 2014). Interestingly, there is, up to date, no published report of a drug-disease PBPK model evaluated for predicting drug exposure in chronic heart failure (CHF) adult and pediatric patients after incorporating reduced organ blood flow changes; despite the high prevalence and the clinical importance of this disease. Instead, there are some published PBPK models that explored drug pharmacokinetics with liver cirrhosis (Edginton and Willmann, 2008; Johnson et al., 2010), chronic kidney disease (Rowland Yeo et al., 2011; Li et al., 2012; Sayama et al., 2014), and in patients with low cardiac output syndrome undergoing cardiac surgery (Vogt, 2014). In CHF, there is a gradual decrease in hepatic blood flow with increasing severity of the disease, which was previously quantified in adults (Leithe et al., 1984). Developing and evaluating a PBPK model that can incorporate the relevant hemodynamic changes seen in CHF and that can quantify the impact of those change could be of great use. This is particularly true for drugs with high hepatic extraction ratio, as these are most vulnerable to hepatic blood flow changes resulting in a significant effect on their clearance (Nies et al., 1976). Under intravenous (iv) administration, the change in CL will lead to a direct change of drug exposure, whilst in the case of oral administration, the effect of CL changes on exposure is more complex as it is confounded and compensated, in part, by the change in bioavailability.

In light of this information, to evaluate a PBPK CHF model with incorporated organ blood flow changes, a model drug being used clinically in CHF with high hepatic extraction was searched. Carvedilol, a third generation beta-blocker used in the treatment of various cardiovascular disorders undergoes extensive first pass metabolism with a high hepatic extraction ratio (0.7) and an absolute oral

bioavailability of 22-24% (Neugebauer et al., 1987; Neugebauer et al., 1990; Neugebauer and Neubert, 1991; Abdelaziz et al., 2009). Due to its high hepatic extraction and the availability of observed clinical data in both healthy and CHF adult populations (Neugebauer et al., 1987; von Mollendorff et al., 1987; Tenero et al., 2000; Giessmann et al., 2004), a PBPK model for carvedilol can be developed and evaluated in healthy adults and in adult CHF patients. Furthermore, due to availability of clinical PK data in pediatric CHF patients (Behn, 2001), carvedilol can serve as a model drug to demonstrate if a PBPK disease model can accurately predict the pharmacokinetic changes occurring in adult and pediatric CHF patients.

1.1.1. Objective

The main objective of this study was to develop PBPK models that incorporate the hemodynamic changes in hepatic and renal blood flow occurring in CHF, and to evaluate it in adults and children using carvedilol as a model drug.

1.2.   Methods

1.2.1.   Modeling software and strategy of model building

Simcyp® simulator v.13.1 (Simcyp Ltd, Sheffield, UK) was used to provide the general structure of the developed PBPK models. Simcyp® is a population based PBPK simulator used for bottom up mechanistic drug modeling of absorption, distribution, metabolism and excretion (ADME). This software combines in vitro and in vivo data for drug absorption, distribution, and elimination with its physicochemical properties, in addition to the incorporated anatomical and physiological data to simulate the drug systemic exposure in virtual healthy and diseased populations (Jamei et al., 2009a).

In the presented work, two PBPK models that differed only in terms of the assigned clearance inputs were developed: model-1, in-vitro intrinsic clearances (CL_{int}) based on human liver and intestinal microsomes (HLM and HIM), and model-2, based on CYP-enzyme clearances. The choice of presenting both models were made because fewer assumptions were made with model-1; however, model-2 can offer additional gain of information in the future by allowing the user to incorporate information on the genetic polymorphisms of the metabolizing enzymes.

A systematic approach was used in developing the PBPK models, starting by screening and extracting drug specific input parameters and clinical pharmacokinetic data from published literature, followed by the incorporation of these data into the software and the selection of the underlying physiological models and final model parameters, and ending with the final evaluation of model

predictions of drug disposition and absorption. The model building was done in a stepwise strategy similar to that reported previously (Khalil and Laer, 2014). In this strategy, the iv drug application in healthy adult subjects is first simulated to avoid the complexities of the oral absorption process so that a wide range of drug-dependent parameters that govern the drug disposition, including clearance inputs and the percentage CYP-enzyme contributions, were chosen or optimized. For the oral application, parameters from the previous step were kept plus additional parameters that control and influence drug absorption such as intestinal permeability. In order to do so, one third (n=3, one iv and 2 oral) of the collected observed pharmacokinetic data in adults was used to optimize the model parameterization, two-thirds (n=6) were used later for a subsequent model verification, and all data were used in the final model evaluation. Changes of hepatic and renal blood flows observed in CHF were then incorporated into this adult model to predict carvedilol PK in CHF patients. At the end, the final adult CHF model was then scaled down to children using the pediatric module of Simcyp®. In the adult and pediatric CHF populations, predictions were made in duplicate using both models i.e., with and without incorporating the reduced organ blood flows. The workflow for the development of PBPK models is shown in **Figure 1-1**.
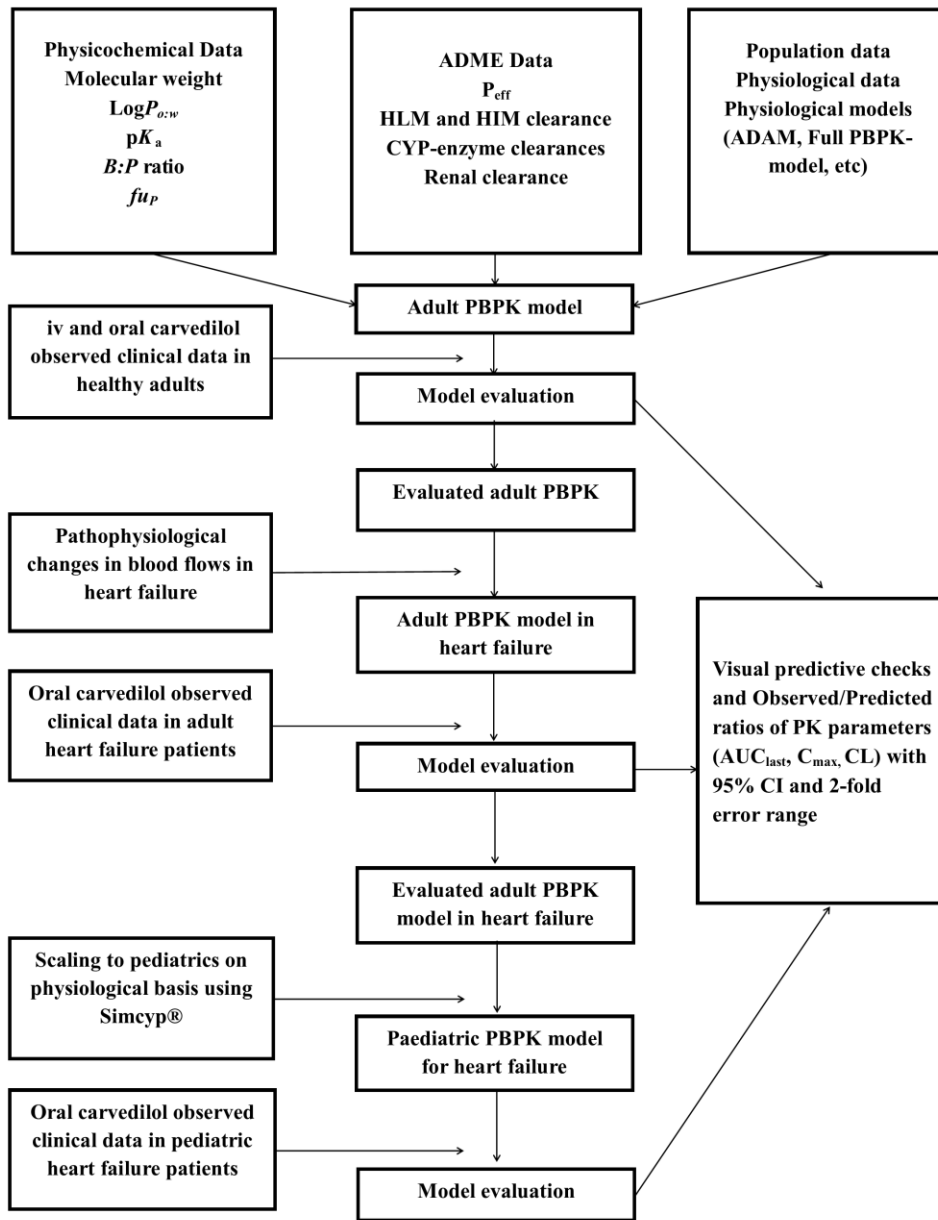
Figure 1-1 Workflow for the development of adult and pediatric PBPK carvedilol heart failure models

LogP$_{o:w}$ octonal-water partition coefficient, *fu$_P$* fraction of unbound drug in plasma, *pK$_a$* acid dissociation constant, *ADME* Absorption, Distribution, Metabolism and Elimination, *P$_{eff,man}$* human jejunum permeability, *HLM* human liver microsomes, *HIM* human intestinal microsomes, *ADAM* Advanced Dissolution Absorption and Metabolism

1.2.2. Model structure and parameterization

A comprehensive literature search was performed to extract necessary in vivo and in vitro ADME data to complete the parameterization of the models. These data include, for e.g., the drug-specific physicochemical properties, drug clearance information, and measures of drug intestinal permeability. The final set of model input parameters are summarized in **Table 1-1**. The two developed models were similar in terms of all the input parameters, except the method used for assigning clearance. A detailed description of the various model components with their parameterization is given below.

1.2.2.1. Absorption

The advanced, dissolution, absorption and metabolism (ADAM) model with the default values of fasting gastric emptying time (mean=0.4h with coefficient of variation (*CV*) 38%) and small intestinal transit times (mean=3.33h with Weibull distribution, α=2.92 and β=4.04) were used to predict drug absorption (Jamei et al., 2009b). The predicted human jejunum permeability ($P_{eff,man}$) of carvedilol was 1.94×10^{-4} (cm/s), which was obtained using in vitro Caco-2 permeability (P_{app}) data calibrated with reference values of propranolol and metoprolol (Bachmakov et al., 2006). In addition, the predicted absorbed fraction of carvedilol was 0.896, which is consistent with carvedilol being a highly permeable drug belonging to BCS class II.

The $P_{eff,man}$ value was increased from 1.94×10^{-4} (cm/s) to 7.4×10^{-4} (cm/s) in all simulations of adults and pediatrics whenever carvedilol was administered as oral suspension due to the observed increase in carvedilol bioavailability. This

optimization was achieved by comparing the predicted pharmacokinetic parameters in healthy adults with the observed data, after administering 50 mg oral capsule and suspension (von Mollendorff et al., 1987). Although fast gastric emptying of liquid dosage formulations is already reported and can, theoretically, be a parameter to adjust (Davis et al., 1986), it was, however, not possible to account for the previously mentioned increase in drug absorption by only reducing the gastric emptying time.

With regard to the active transport, there are some reports suggesting possible role of P-glycoprotein (P-gp) in carvedilol disposition (Kaijser et al., 1997; Giessmann et al., 2004). However, the "International Transporter Consortium" (ITC) has stated in its guidelines and established decision trees that, when the net flux ratio of a drug in a bidirectional transport assay as Caco-2 is less than 2, then it is a poor or non P-gp substrate (Giacomini et al., 2010), which was the case with carvedilol (net flux ratio is 1.3(Bachmakov et al., 2006)). This suggests that carvedilol is a poor substrate to P-gp, which is in harmony with reports stating that carvedilol is a strong P-gp inhibitor but not a good substrate (Wessler et al., 2013). In light of above mentioned information, no P-gp specific data was incorporated in the developed PBPK models.

Table 1-1 Main drug dependent parameters and characteristics of the presented PBPK models

Parameter	Model 1	Model 2	Ref. value	Reference
Molecular weight (g/mol)	406.47	406.47	406.47	PubChem.
Log$P_{o:w}$	4.19	4.19	4.19	PubChem.
pK_a	7.97	7.97	7.97	(Caron et al., 1999)
Absorption				
Model	ADAM			
$P_{eff,man}$ (cm/s) in tablets and capsules[a]	1.94×10^{-4}	1.94×10^{-4}	1.94×10^{-4}	(Bachmakov et al., 2006)
$P_{eff,man}$ (cm/s) in oral suspension[b]	7.4×10^{-4}	7.4×10^{-4}	-	-
Distribution				
Model	Full PBPK			
Prediction method [c]	Poulin and Theil method			
Blood to plasma (*B:P*) ratio	0.69	0.69	0.69	(Fujimaki et al., 1990)
fu$_P$	0.0054	0.0054	0.0054	(Fujimaki et al., 1990)
Elimination				
CL_{iv} (L/h)	-	38	35.34[d]	(von Mollendorff et al., 1987)
HLM CL_{int} (µL/min/mg protein)	246	-	246	(Kilford et al., 2009)
Fraction unbound in microsomal incubation	0.04	-	0.04	(Kilford et al., 2009)

Parameter	Model 1	Model 2	Ref. value	Reference
HIM CL_{int} (µL/min/mg protein)	11.4	-	11.4	(Hanioka et al., 2012)
CYP2D6 CL_{int} (µL/min/mg/pmol of isoform)[e]	-	339.7	-	-
CYP1A2 CL_{int} (µL/min/mg/pmol of isoform)[e]	-	8.71	-	-
CYP2C9 CL_{int} (µL/min/mg/pmol of isoform)[e]	-	3.1	-	-
CYP2E1 CL_{int} (µL/min/mg/pmol of isoform)[e]	-	3.71	-	-
Additional HLM clearance (µL/min/mg protein)[e]	-	906.7	-	-
CL_R (L/h)	0.25	0.25	0.25	(Gehr et al., 1999)

$LogP_{o:w}$ octonal-water partition coefficient, fu_P fraction of unbound drug in plasma, pK_a acid dissociation constant, *ADAM* Advanced, Dissolution, Absorption and Metabolism, CL_{iv} intravenous clearance, CL_R renal clearance, *HLM* human liver microsomes, *HIM* human intestinal microsomes, CL_{int} intrinsic clearance

[a] Human jejunum permeability calculated from P_{app} value of a Caco-2 assay by calibrating with metoprolol and propranolol using Simcyp®

[b] Optimized human jejunum permeability

[c] Poulin and Theil method with the Bierezhkovskiy correction as the prediction method for the volume of distribution and the tissue to plasma partition coefficients (predicted V_{ss} 1.69 L/kg)

[d] CL_{iv} (L/h) range 22.5—50.8

[e] Values calculated by using the retrograde model in Simcyp®

1.2.2.2.   Distribution

The full PBPK model for the prediction of drug distribution was used in both developed models. The drug volume of distribution in steady state (V_{ss}) and the specific tissue to plasma partition coefficients (K_p) were calculated by Poulin and Theil method with the Bierezhkovskiy correction (Berezhkovskiy, 2004). As a result, the predicted V_{ss} value of 1.69 L/kg by this method was comparable to the reported value of 1.62 L/kg[1] in the literature (von Mollendorff et al., 1987).

1.2.2.3.   Elimination

The human liver and human intestinal microsomes intrinsic clearance (CL_{int}) were used for the prediction of drug clearance in model-1 (Kilford et al., 2009; Hanioka et al., 2012). The model-2 uses CYP-enzyme CL_{int} values calculated by the retrograde model for enzyme kinetics in Simcyp®. The retrograde model is one of the models incorporated in Simcyp®, and allows the calculation of intrinsic clearance values of the relevant metabolizing enzymes from an in vivo measured clearance. The detailed description of this model is already published elsewhere (Cubitt et al., 2011; Salem et al., 2014). In brief, the retrograde model utilizes an in vivo measure of the adult iv or oral clearance with known fractions of hepatic, renal, or any additional clearance, the drug fraction unbound (f_u), the blood to plasma ratio of drug concentrations, and the liver blood flow to calculate a total hepatic intrinsic clearance as given in the following equation of the well-stirred liver model:

---

[1] V_{ss} was calculated by using non-compartmental analysis in Phoenix WinNonLin®

$$CL_{int} = \frac{Q_H \times CL_H}{fu_B \times (Q_H - CL_H)}$$ **Equation 1-1**

In a second step, this hepatic CL_{int} value is divided between the involved hepatic elimination pathways (i.e., the different CYP-enzymes) using input information about the percentage contribution of these metabolizing enzymes in drug clearance.

The contributions of the CYP-enzymes that are involved in carvedilol metabolism were guided by the available evidence in the literature. It has been reported that CYP2D6 is the major contributing CYP-enzyme whilst CYP1A2, CYP2C9, CYP2E1, and CYP3A4 are involved with a minor role (Oldham and Clarke, 1997; Giessmann et al., 2004; Sehrt et al., 2011). In the literature, there is no clear information about the relative contributions of the CYP-enzymes to the total carvedilol clearance except for CYP2D6 with 50-62% (Giessmann et al., 2004; Sehrt et al., 2011). From the remaining CYP enzymes believed to be involved in the metabolic pathways of carvedilol, CYP1A2, CYP2C9, and CYP2E1 were reported to be of further importance (Oldham and Clarke, 1997). In light of the above mentioned information and the fact that relative amount of carvedilol-glucuronidation is around 22% (Neugebauer and Neubert, 1991), 80% of total carvedilol clearance was assigned to the following CYP-enzymes: 60% CYP2D6, 10% CYP1A2, 5% CYP2C9 and 5% CYP2E1 and the remaining 20% to glucuronidation as additional clearance. A renal clearance of 0.25 L/h was used in both models 1 and 2 (Gehr et al., 1999).

Three UGT enzymes, UGT1A1, UGT2B4 and UGT2B7 are believed to be involved in the metabolism of carvedilol. In the literature, there is no clear

information about their individual relative contribution to the metabolic clearance of carvedilol, therefore, the collective impact of these UGT enzymes was reflected in an assigned additional clearance that constituted about 20% of the total carvedilol clearance. This is in a good agreement with the reported values of 20-23% in healthy adults (Neugebauer and Neubert, 1991).

The variability in clearance was assigned by a *CV* of 30% to HIM and HLM CL_{int} in model-1. In model-2, a 30% *CV* was assigned to the additional clearance, whereas for the CYP-enzyme CL_{int} values obtained by the retrograde model the seen variability was due to variations in the physiological and anatomical variables such as liver weight, microsomal proteins per gram liver, the abundance of each specific CYP-enzyme, cardiac output and liver blood flow.

The hepatic clearance (CL_H) was predicted by using well stirred liver model (Wilkinson and Shand, 1975) using following equation,

$$CL_H = \frac{Q_H \times fu_B \times CLu_{H,int}}{Q_H + fu_B \times CLu_{H,int}} \qquad \textbf{Equation 1-2}$$

The hepatic blood flow (Q_H) changes occurring in CHF were incorporated into the model for predicting disposition of carvedilol in patients with CHF.

The oral bioavailability was predicted by using the following equation,

$$F = F_a \times F_g \times F_h \qquad \textbf{Equation 1-3}$$

Where, F_a is the fraction of drug absorbed, F_g is the fraction that escapes metabolism in the gastrointestinal tract and F_h is the fraction that escapes the hepatic metabolism.

1.2.3. Model scaling to children

Only when the adult CHF models have shown to predict carvedilol pharmacokinetics adequately, they were scaled to the children by using pediatric module of Simcyp®. This module of the program incorporates a wide variety of age-specific physiological and anatomical parameters, which facilitates the pediatric scaling of drug clearance on physiological basis. Due to the use of oral suspension of carvedilol in both pediatric clinical trials (Behn, 2001), an optimized value of P_{eff} was used in all pediatric predictions, as in the adults, who were administered oral suspension of carvedilol. The pediatric module of the program also accounts for the age related changes occurring in the total body composition, when predicting distribution of drugs (Johnson and Rostami-Hodjegan, 2011). The key determinants for predicting drug clearance in the pediatric module are, the age specific changes occurring in, plasma protein binding, blood volume, organ blood flows, organ sizes and ontogeny and abundance of hepatic CYP-enzymes (Johnson and Rostami-Hodjegan, 2011). In model-2 the ontogeny profiles of CYP-enzymes were incorporated by default within the program but in model-1, in order to create similar ontogeny profile as model-2, a customized ontogeny profile was created by addition of the fractional contributions of the CYP-enzymes with their respective ontogenies (Oldham and Clarke, 1997; Sehrt et al., 2011; Salem et al., 2013). All the pediatric patients were diagnosed with CHF and the reductions in hepatic and renal blood flows were incorporated in the pediatric models by categorizing the patients into different CHF categories, according to modified Ross score (Laer et al., 2002).

1.2.4.   Blood flow changes to eliminating organs in heart failure

The liver and kidney are the main organs of drug elimination from the human body, and therefore, changes in the blood flows to these organs are of pharmacokinetic importance. In adult heart failure patients, the reduction in hepatic blood flow is known to increase with increased severity of the disease (Leithe et al., 1984). In brief, these organ blood flow reductions occurring in adult heart failure patients were quantified after measuring the hepatic and renal plasma flows in healthy and heart failure patients by administering doses of iv indocyanine green and iv p-Aminohippurate and measuring their respective clearances (Leithe et al., 1984). The quantified reductions were, 23.5%, 46.2%, and 53.7% of normal hepatic blood flow in mild, moderate, and severe CHF patients, respectively (Leithe et al., 1984) (**Table 1-2**). Moreover, the reduction in renal blood flow were also shown to increase with increased severity of CHF, however, this reduction is not absolutely linear when we move from moderate to severe CHF, as it was reported to be around 22.2%, 45%, and 37.1% of normal blood flow in mild, moderate, and severe CHF patients, respectively (Leithe et al., 1984).

Table 1-2 Percentage decrease in hepatic and renal blood flows in heart failure patients. Presented data adopted from Leithe et al. 1984.

Population	Hepatic blood flow	Renal blood flow
Healthy[a]	100.0	100.0
Mild CHF	76.4	77.7
Moderate CHF	53.7	54.9
Severe CHF	46.2	62.8

[a]blood flows in healthy population were taken as 100 %

CHF: chronic heart failure

In the adult patients, the New York Heart Association (NYHA) functional classification system provides a simple way of classifying the severity of CHF (**Table 1-3**), where for example, NYHA class II reflects a mild CHF, NYHA class III a moderate CHF, whereas NYHA class IV stands for a severe CHF (NYHA, 1994). As a result, the reported reductions in blood flows to the liver and the kidney could be directly correlated in adults with the NYHA classification. In order to predict drug exposure in CHF patients using a PBPK model, these reductions in organ blood flows were assigned to the simulated virtual populations within Simcyp® by reducing the percentage blood flow to the liver and kidney, respectively. When the drug exposure in population comprising of NYHA class III (moderate CHF) and IV (severe CHF) patients has to be predicted, the mean organ blood flow reductions of moderate and severe CHF from the reported values were used (Leithe et al., 1984), i.e. a reduction of 49.9% and 41% of normal hepatic and renal blood flow, respectively.

In the pediatric CHF patients, due to difficulty in assessing the physical activity, the NYHA classification is not used to assess the severity of the CHF, instead, Ross score is the common system that is used in children (Ross et al., 1992). According to Ross score, a score of 0–2 categorizes the patient as asymptomatic, 3–6 as with mild CHF, 7–9 as with moderate CHF, and 10–12 as a patient with severe CHF (Ross et al., 1992; Laer et al., 2002) (**Table1-4**). There was no experimental data available, quantifying the reduction of hepatic and renal blood flows in pediatric CHF patients and correlating them to the pediatric CHF classification system, the proposed changes in the pediatric CHF model were adopted from adults' values previously mentioned (Leithe et al., 1984). The

relative reductions in the organ blood flows with their association to the severity of CHF according to NYHA class and Ross score are shown in **Figure 1-2**.

Table 1-3 New York Heart Association (NYHA) classification of heart failure

Class	Symptoms
Class I (Mild)	No limitation of physical activity. Ordinary physical activity does not cause undue fatigue, palpitations or shortness of breath
Class II (Mild)	Slight limitation of physical activity. Comfortable at rest but ordinary physical activity results in fatigue, palpitations and shortness of breath.
Class III (Moderate)	Marked limitation of physical activity. Comfortable at rest and less than ordinary physical activity causes fatigue, palpitations and shortness of breath.
Class IV (Severe)	Unable to carry out any physical activity without discomfort. Symptoms of fatigue, palpitations and shortness of breath are present at rest. If any physical activity is performed, discomfort increases.

Table 1-4 Ross scoring system for heart failure in children.

Parameter	Score		
	0	*1*	*2*
Feeding History			
Volume consumed per feeding (oz)	>3.5	2.5-3.5	<2.5
Time taken per feeding (min)	<40	>40	-
Physical examination			
Respiratory rate (n/min)	<50	50-60	>60
Heart rate(n/min)	<160	160-170	>170
Respiratory pattern	Normal	Abnormal	-
Peripheral perfusion	Normal	Decreased	-
S_3 or diastolic rumble	Absent	Present	-
Liver edge from right costal margin (cm)	<2	2-3	>3

A score of 0–2 categorizes the patient as asymptomatic, 3–6 as with mild CHF, 7–9 as with moderate CHF, and 10–12 as a patient with severe CHF (Ross et al., 1992; Laer et al., 2002)
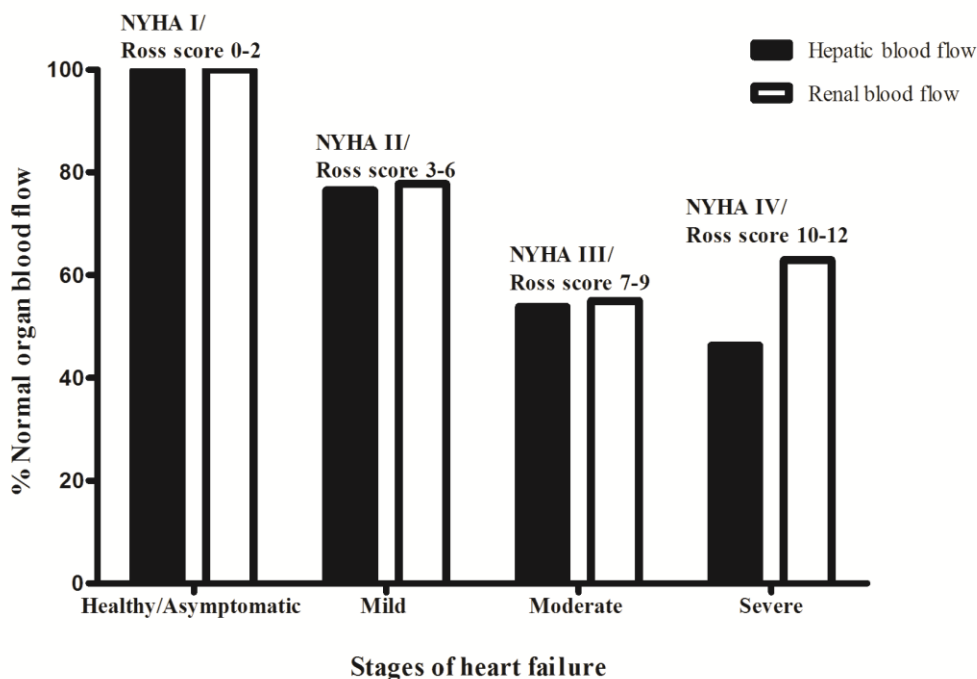
Figure 1-2 Changes in hepatic and renal blood flows in heart failure patients, as incorporated in the developed PBPK heart failure models of carvedilol. Presented data taken from Leithe et al. 1984 (Leithe et al., 1984)

1.2.5. Pharmacokinetic/Clinical data

1.2.5.1. Healthy adult and adult CHF populations

MEDLINE database was screened for pharmacokinetic studies of carvedilol in healthy adults and CHF patients with known age, gender, height or weight, clear dosing information, and reported systemic drug concentration-time profiles. As a result, pharmacokinetic data from four different clinical studies in healthy subjects (3 studies, 41 subjects) and CHF patients (one study, 10 patients with NYHA III and 10 patients with NYHA IV) were used in the adult model development and evaluation (Neugebauer et al., 1987; Tenero et al., 2000; Behn, 2001; Giessmann et al., 2004). These studies provided a total of 9 data sets (5 data sets in healthy,

4 data sets in CHF patients) (**Table 1-5**). Each experimental data set represents a mean or median observed concentration-time profile in an average of 18 subjects who received either iv or oral doses of carvedilol. The average number of observed concentrations in these data sets is 13 (total number is 122). These data sets were either provided by the author (Behn, 2001) or scanned from the publications' figures (Neugebauer et al., 1987; Tenero et al., 2000; Giessmann et al., 2004) using the digitizer tool in the data analysis and graphing software OriginPro® version 9.0 (OriginLab. Northampton, MA). In addition, one study that reported only the pharmacokinetic parameters, but not the concentration-time profiles, after administration of oral suspension in healthy subjects was additionally used in the comparison of the observed and predicted values of the chosen pharmacokinetic parameters (von Mollendorff et al., 1987).

1.2.5.2.   Pediatric CHF patients

Two clinical data sets, including thirty-two pediatric CHF patients of different age groups with known age, gender, height, weight, dosing information, Ross score, and measured plasma profiles were used (**Table 1-6**) (Behn, 2001). The age of the patients ranged from 43 days to 19.3 years (average: 7.3 years) and they received either 0.09 mg/kg single dose or 0.35 mg/kg steady state doses of oral carvedilol for the treatment of CHF. The average number of measured concentrations in each patient is 12 (total number is 197 and 202 for single dose and steady-state sampling). In our paper, no explicit pediatric age groups were used, as the total number of the included pediatric patients was relatively small with an unequal distribution between the different pediatric age subcategories. Whenever the term "children" is used, this refers to the entire pediatric age group

ranging from birth to 18 years old. The 19.3 years old patient has been shown separately in the results, as this patient was out of the pediatric age range according to guidelines set by World Health Organization (WHO).

Table 1-5 Characteristics of the adult data sets used for carvedilol model development

No.	Population	Nr. of subjects	Dose (mg)	Application	Age (years)		Proportion of females	Body Weight (kg)		Ref.
					Mean	Range		Mean	Range	
1	Healthy	12	5	iv infusion[a,b]	-	21-29	0.25	-	59-92	(Giessmann et al., 2004)
2	Healthy	20	12.5	iv infusion[a]	-	19-45	0	-	60-92	(Neugebauer et al., 1987)
3	Healthy	9	6.3[c]	oral	29.6[g]	24-37	0.66	69.8[h]	56-100	(Behn, 2001)
4	Healthy	20	25	oral	-	19-45	0	-	60-92	(Neugebauer et al., 1987)
5	Healthy	20	50	oral	-	19-45	0	-	60-92	(Neugebauer et al., 1987)
6	Healthy	20	50	oral[d]	-	19-45	0	-	60-92	(von Mollendorff et al., 1987)
7	Heart failure[e,f]	20	6.25	oral	55*	39-64*	0	89.5*	60.8-113.1*	(Tenero et al., 2000)
8	Heart failure[e,f]	20	12.5	oral	55*	39-64*	0	89.5*	60.8-113.1*	(Tenero et al., 2000)
9	Heart failure[e,f]	20	25	oral	55*	39-64*	0	89.5*	60.8-113.1*	(Tenero et al., 2000)
10	Heart failure[e,f]	20	50	oral	55*	39-64*	0	89.5*	60.8-113.1*	(Tenero et al., 2000)

[a] Intravenous infusion was given over 1 hour, [b] Mean of individual profiles was used for comparison, [c] Dose administered as 0.09 mg/kg but normalized to total dose by multiplying with the average weight of the participants in the clinical trial, [d] Suspension, [e] The mean results reported in the study were further subdivided into NYHA III and NYHA IV subgroups, [f] The population includes 10 patients with NYHA III and 10 with NYHA IV heart failure, [g] Median age 27 years, SD 5.4 and 25th and 75th percentiles 24.5 and 35 years, [h] Median weight 65 kg, SD 15.04 and 25th and 75th percentiles 58.05 and 80.25 kg, * The presented values for age and weight are the reported values for the initial study population (n=22)

Table 1-6 Characteristics of pediatric data used for model development

No.	Age (years)	Gender	Body Weight (kg)	Single dose (mg/kg)	Steady state dose (mg/kg)	Ross score/ NYHA Class
Patients categorized according to Ross score						
1	0.12	Female	3.1	0.09	0.35	3
2	0.15	Male	3.9	0.09	0.35	3
3*	0.25	Female	4.2	-	0.35	4
4	0.5	Female	5.2	0.09	0.35	8
5**	0.75	Male	8	0.09	-	3
6	1.25	Male	10.1	0.09	0.35	3
7	1.5	Male	9.5	0.09	0.35	10
8	3.5	Female	13.1	0.09	0.35	3
9**	5.5	Male	20.2	0.09	-	3
10	7.5	Male	24.3	0.09	0.35	5
11	8.25	Male	25.8	0.09	0.35	7
12	10.75	Male	25.5	0.09	0.35	4
13	11.6	Female	34.3	0.09	0.35	4
14	11.8	Male	39	0.09	0.35	2
15*	13.5	Male	52	-	0.35	NA
Patients categorized according to NYHA classification						
16	17.0	Male	56	0.09	0.35	NYHA II
17	17.8	Male	61	0.09	0.35	NYHA III
18	19.3[a]	Male	98.2	0.09	0.35	NYHA III
Mean	7.27		27.41	-	-	-
SD	6.72		25.65	-	-	-
Median	6.5		22.25	-	-	-
25th Percentile	0.68		7.3	-	-	-
75th Percentile	12.23		42.25	-	-	-

NA not available, *NYHA* New York heart association classification of heart failure, *SD* standard deviation, All children were diagnosed with heart failure and were participants in the same clinical trial (Behn, 2001), [a]Patient out of the pediatric age range according to guidelines set by World Health Organization, * Measured concentrations available only in steady-state
** Measured concentrations available only after a single dose

1.2.6. Model evaluation

The simulations were performed by creating a virtual population of 100 subjects for every clinical data set with the same age range, proportion of females, fluid intake and fasting/fed states as in the reference clinical studies. The predictions performed with higher number of virtual individuals (500 or 1000) produced no significant difference in comparison to the previous results (100 virtual individuals), so as reported in other model based PBPK studies (Jiang et al., 2013; Jamei et al., 2014; Marsousi et al., 2014), a virtual population of 100 individuals was always used for comparison with the observed profiles. Patient/population specific genotype data was available from two clinical studies (Behn, 2001; Giessmann et al., 2004) and the simulated virtual populations using model-2 were having the same frequency of genotypes as in reported clinical studies.

The evaluation of the developed PBPK models was performed by visual predictive checks and a comparison of the observed and predicted values of various pharmacokinetic parameters. In the visual predictive checks, the complete observed systemic drug concentration-time profile was overlaid on the predicted values so that a direct visual comparison could be made.

For the comparison of pharmacokinetic parameters, a non-compartmental analysis (NCA) was performed for each observed profile and its corresponding predicted value by each model (i.e. using the predicted values at the same time points) using Phoenix WinNonLin® version 6.3 (Pharsight Corporation, CA, USA). The area under the systemic drug concentration-time curve from time 0 to the last

measured concentration (AUC$_{last}$) was calculated via the linear trapezoidal rule. The maximal concentration in a profile was defined as (C$_{max}$) and the clearance (CL for the IV application, CL/F for the oral application) was calculated by dividing the given dose by the calculated AUC$_{last}$.

Following the NCA, the observed/predicted ratios (ratio$_{Obs/Pred}$) of the pharmacokinetic parameters was then calculated and the final results were reported as mean ratios$_{(Obs/Pred)}$ with a 95% confidence interval (95% CI).

To the best of our knowledge, there is no clear guidelines regarding the error range that should be used during the evaluation of predictions obtained by PBPK models. The most commonly used range by researchers in this field is a 2-fold error range (Johnson et al., 2006; Jones et al., 2006; De Buck et al., 2007; Li et al., 2012; Khalil and Laer, 2014). Others have also used a wider (3-fold) (Gertz et al., 2011) or stricter ranges (1.5-fold) (Abduljalil et al., 2014). In our case, and because the models were used to perform predictions in both adults and children, and because of the high variability observed in the reported pharmacokinetic parameters of carvedilol, a 2-fold error range was used and considered to be adequate.

Moreover, goodness to fit plots: population predicted vs. population observed plots, residual vs. population predictions plots and residuals vs. time plots were used for identifying systemic errors in the developed models.

Depending upon the reported values of pharmacokinetic parameters, the predicted mean or median values of pharmacokinetic parameters were used for comparison and calculation of ratios$_{(Obs/Pred)}$.

1.3. Results

1.3.1. Healthy Adults

The observed and predicted systemic drug concentration-time profiles after the administration of iv and oral carvedilol in healthy adults are shown in **Figure 1-3A and B**, **Appendix 1 and 2**, and the residual plots in **Figure 1-4**. The results of both models were in a good agreement with the observed data irrespective of the administered dosages of 5—12.5 mg iv and 6.3—50 mg oral carvedilol. However, model-2 was superior to model-1 in terms of capturing the absorption phase, as the latter tend to slightly over predict early drug concentrations. This was further confirmed when comparing the pharmacokinetic parameters as the resultant mean AUC_{last} ratios$_{(Obs/Pred)}$ after iv application were 1.12 (95% CI: 1.01–1.22) and 0.97 (95% CI: 0.78–1.16) and after oral application were 0.80 (95% CI: 0.51–1.11) and 0.94 (95% CI: 0.65–1.23) using models 1 and 2, respectively. In addition, the calculated mean AUC_{last}, C_{max}, and CL (iv and oral) ratios$_{(Obs/Pred)}$ were within the defined 2-fold error range (**Figure 1-5 *a—c* and Appendix 3**).
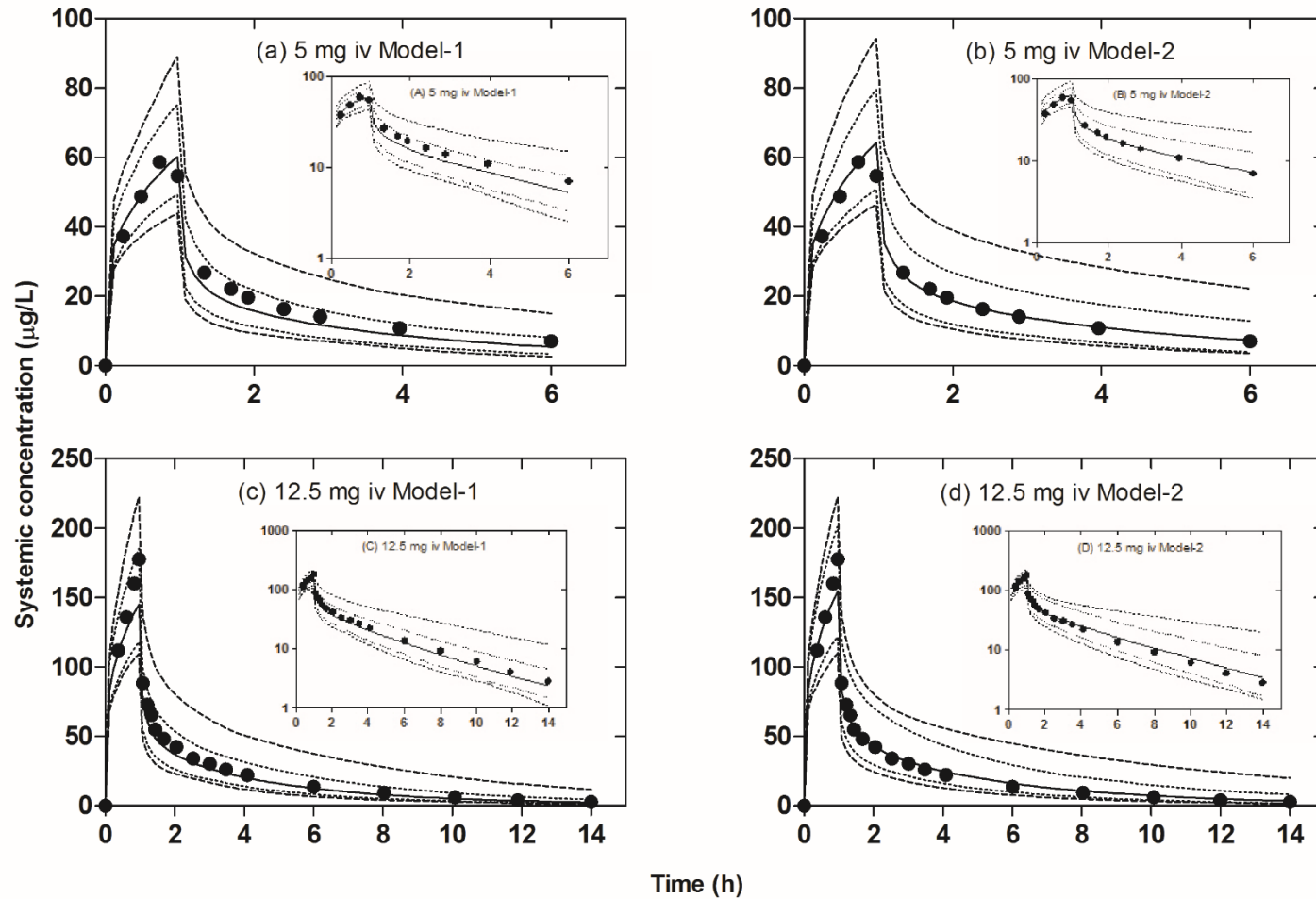
Figure 1-3A Comparison of observed and predicted systemic carvedilol concentration-time profiles in healthy after intravenous drug dosing.

 (a, b) 5 mg*(Giessmann et al., 2004) and (c, d) 12.5 mg (Neugebauer et al., 1987). Prediction results are shown for model 1 or model 2 as median or mean (lines), 5th and 95th percentiles (dotted lines), and minimum/maximum (dashed lines).
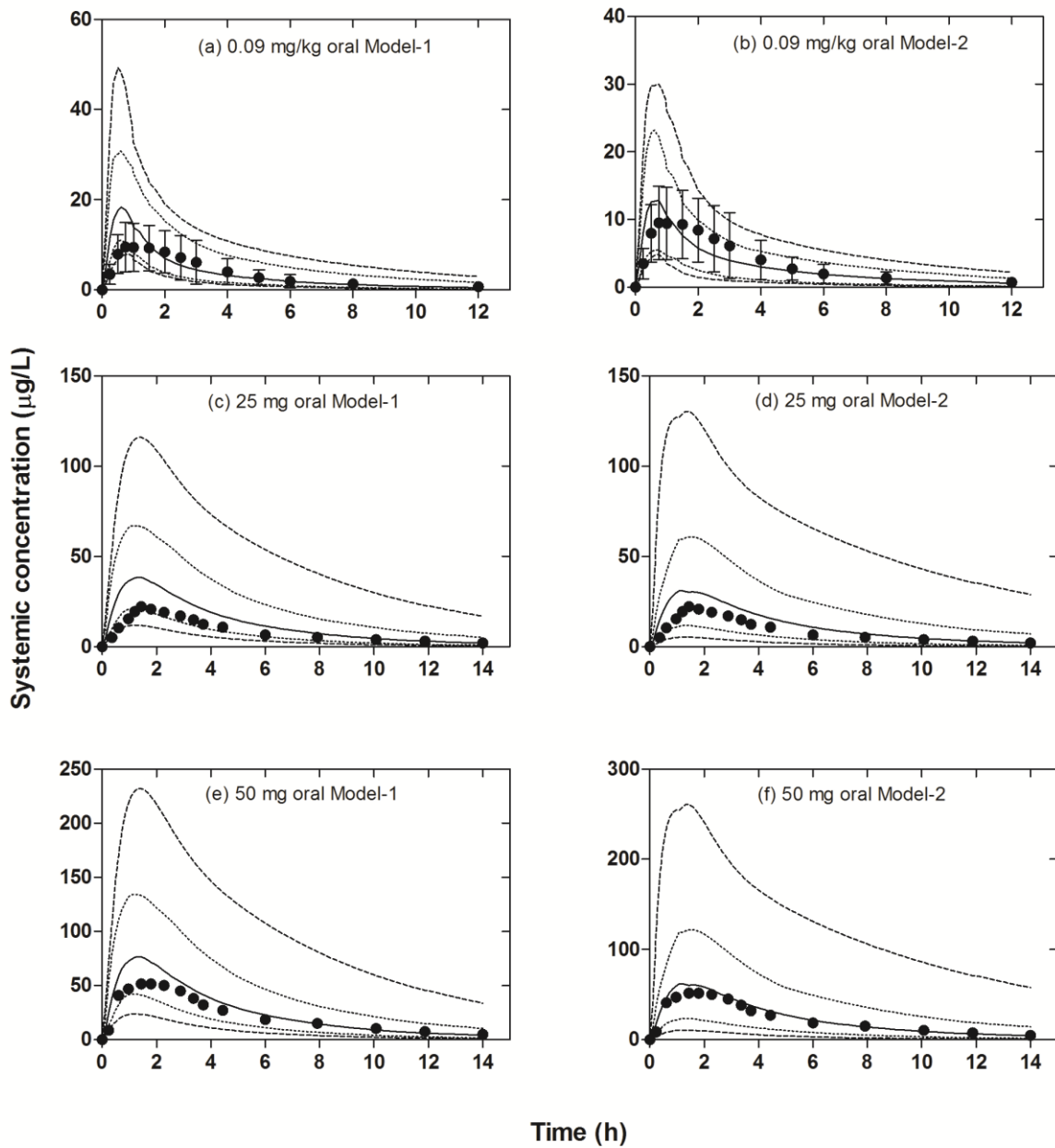
Figure 1-3B Comparison of observed and predicted systemic carvedilol concentration-time profiles in healthy adults after oral drug dosing.

(a, b) 0.09 mg/kg, (Behn, 2001), (c, d) 25 mg (Neugebauer et al., 1987), and (e, f) 50 mg (Neugebauer et al., 1987). Prediction results are shown for model 1 or model 2 as median (lines), 5th and 95th percentiles (dotted lines), and minimum/maximum (dashed lines).
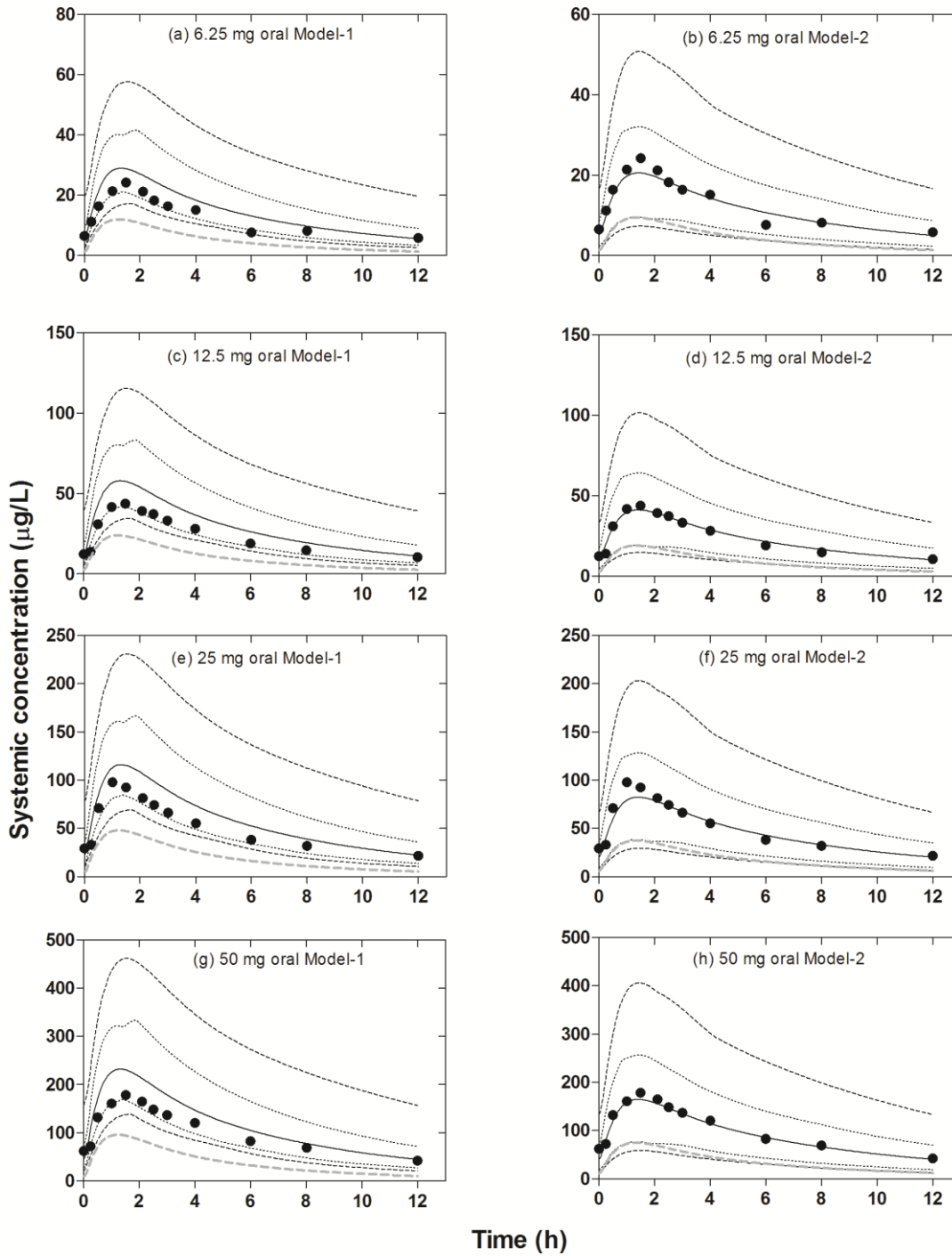
Figure 1-3C Comparison of observed and predicted systemic carvedilol concentration-time profiles in adult chronic heart failure patients after oral drug dosing.

(a, b) 6.25 mg (Tenero et al., 2000), (c, d) 12.5 mg, (e, f) 25 mg, and (g, h) 50 mg oral carvedilol. Prediction results are shown for model 1 or model 2 as mean (lines), 5th and 95th percentiles (dotted lines), and minimum/maximum (dashed lines). The gray dashed line indicates mean model predictions without the incorporation of organ blood flow changes
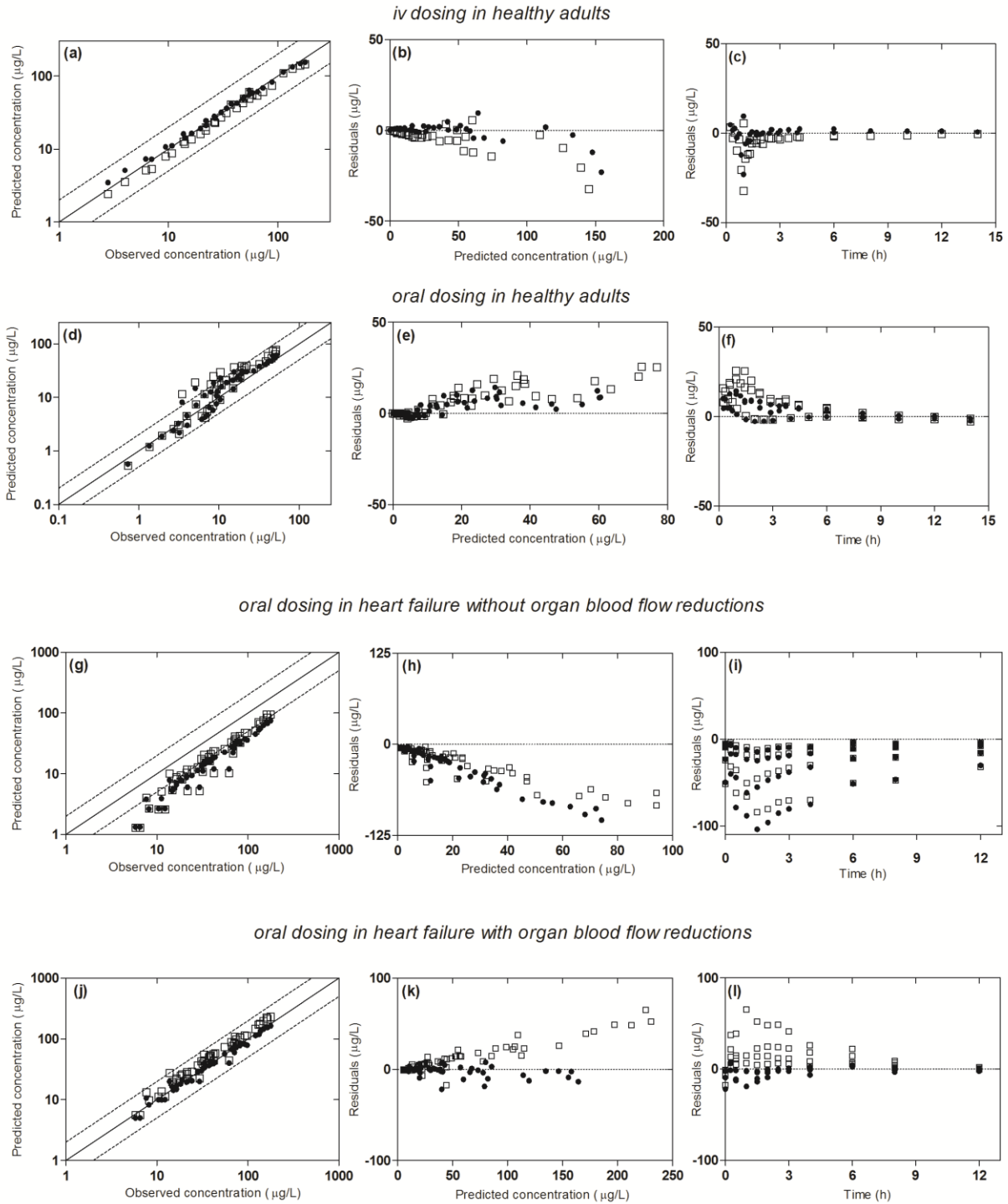
Figure 1- 4 Goodness to fit plots for model predictions in the adult population

presented as predicted vs. observed concentrations plots, residuals vs. predicted concentrations plots, and residuals vs. time plots. (a–c) healthy adults, iv dosing; (d–f) healthy adults, oral dosing; (g–i) *heart failure patients* without renal and hepatic blood flow reductions, and (j–l) heart failure patients with renal and hepatic blood flows reductions. The solid line indicates line of identity, the dashed line a 2-fold error range. (□) results by model-1 and (●) results by model-2

Figure 1-5 Comparison between the observed and predicted values of pharmacokinetic parameters.

Comparison between the observed and predicted values of the area under the plasma concentration-time curve (AUC_{last}), the maximum concentration (C_{max}), and drug clearance in healthy adult and heart failure populations. Results are presented as individual and mean ratios(observed/predicted) with a 95% confidence interval (CI) using model 1 and model-2. *(a—c)* ● In healthy adults, ■ In heart failure without renal and hepatic blood flow reductions, ▼ In heart failure with renal and hepatic blood flows reductions. and *(d—f)* ● In NYHA III and ■ NYHA IV heart failure patients without renal and hepatic blood flow reductions, ▼In NYHA III and ♦ NYHA IV with renal and hepatic blood flows reductions. The shadowed gray area indicates a 2-fold error range. n =number of data sets. Clearance is the calculated oral clearance (CL/F) if the dose is given orally

1.3.2. Adult patients

The observed and predicted systemic drug concentration-time profiles after administering steady state oral doses of carvedilol (6.25 mg to 50 mg) in NYHA III and IV CHF patients are shown in **Figure 1-3C and Appendix 4**. The visual predictive checks show a substantial improvement in predictions after incorporation of reduced organ blood flows in the models. The mean AUC_{last} ratios$_{(Obs/Pred)}$ without adjusting the organ blood flows, were outside the 2-fold error range, i.e. 2.33 (95% CI: 2.02–2.63) and 2.65 (95% CI: 2.29–3.01) by using models 1 and 2 respectively. After incorporating the proposed organ blood flow changes, these ratios improved to 0.79 (95% CI: 0.69–0.90) and 1.03 (95% CI: 0.89–1.16), respectively. The complete comparison of the calculated pharmacokinetic parameters with and without adjusting organ blood flows is shown in **Figure 1-5 (*a—c*)** and in **Appendix 3**. Similar results were seen after further categorizing the CHF patients into NYHA III and IV subgroups. The developed models were capable of predicting carvedilol exposure in NYHA III and NYHA IV patients as can be seen by the mean ratios$_{(Obs/Pred)}$ with their 95% CI (**Figure 1-5 *d—f* and Appendix 5**). Despite the fact that the predicted concentrations by both models were within a 2-fold error range (**Figure 1-4**), it can be noticed that model-1 tends to over-predict drug concentrations in the absorption phase in all dosage levels whereas model-2 predictions were in closer agreement with the observed data.
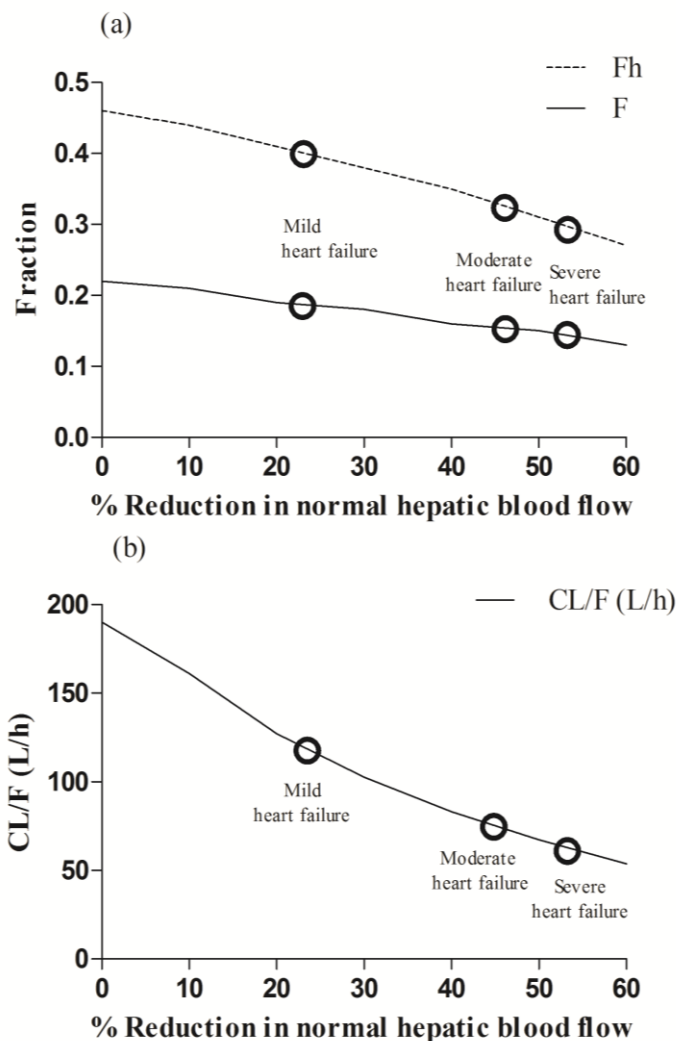
Figure 1-6 The predicted effect of decrease in hepatic blood flow in different stages of heart failure.

The predicted effect of decrease in hepatic blood flow in different stages of heart failure on, *(a)* bioavailability (F) and fraction escaping the hepatic metabolism (F_h) and *(b)* oral clearance (CL/F*)* of carvedilol using model-2 after administering 0.09 mg/kg single oral dose of carvedilol. The data presented is from predictions in 25 years old male virtual population.

Similarly, the mean CL/F ratios$_{(Obs/Pred)}$ without reducing organ blood flows, were outside the 2-fold error range, i.e. 0.34 (95% CI: 0.31–0.37) by using both models and were significantly improved to 1.0 (95% CI: 0.92–1.08) and 0.95 (95% CI: 0.88–1.03), using models 1 and 2, respectively. The predicted bioavailability (F) and the fraction escaping the hepatic metabolism (F_h) decreased with the increase

in hepatic blood flow reduction (increase in severity of CHF). The predicted effect of the decreased hepatic blood flow on carvedilol oral clearance and bioavailability in the different stages of heart failure can be seen in **Figure 1-6**.

1.3.3. Pediatric patients

Carvedilol exposure after single and steady state doses of 0.09 mg/kg and 0.35 mg/kg, respectively, was predicted using both models in the entire pediatric age range (see **Figure 1-7**). It can be seen that both models were able to describe the individual plasma concentration-time points, however, model-2 was again better when compared to model-1 with a higher number of observed plasma concentration-time points within the maximum and minimum prediction range (~93% for model-2 vs. ~86% for model-1).

The individual predictions made by model-2 after administering a single oral dose of 0.09 mg/kg carvedilol to 15 pediatric patients and one young adult are shown for a visual predictive check in **Figure 1-8A–D and Appendix 6**, with and without reducing organ blood flows. In addition, the residual plots are given in **Figure 1-9**. In general, the model was able to predict carvedilol concentrations accurately in all patients above one year of age (12 out of 16). For the one patient with a symptomatic CHF (Ross score of 0-2), no changes in blood flows were incorporated, and therefore, no change to be seen in the visual predictive check. For the ten pediatric patients with mild CHF, the incorporation of blood flow reductions did not improve the predictions in these patients but improvement was seen in one patient classified with NYHA class II. Concerning the four patients with moderate CHF, the model predictions were better without organ blood flow

reductions in those patients classified with Ross scores (n = 2, with scores of 7–9), whereas in the remaining two who were classified as being NYHA class III, the prediction was clearly improved in one patient (19.3-year-old patient) but no improvement was seen in other NYHA III patient (17.8-year-old patient) with reductions in organ blood flows.

.
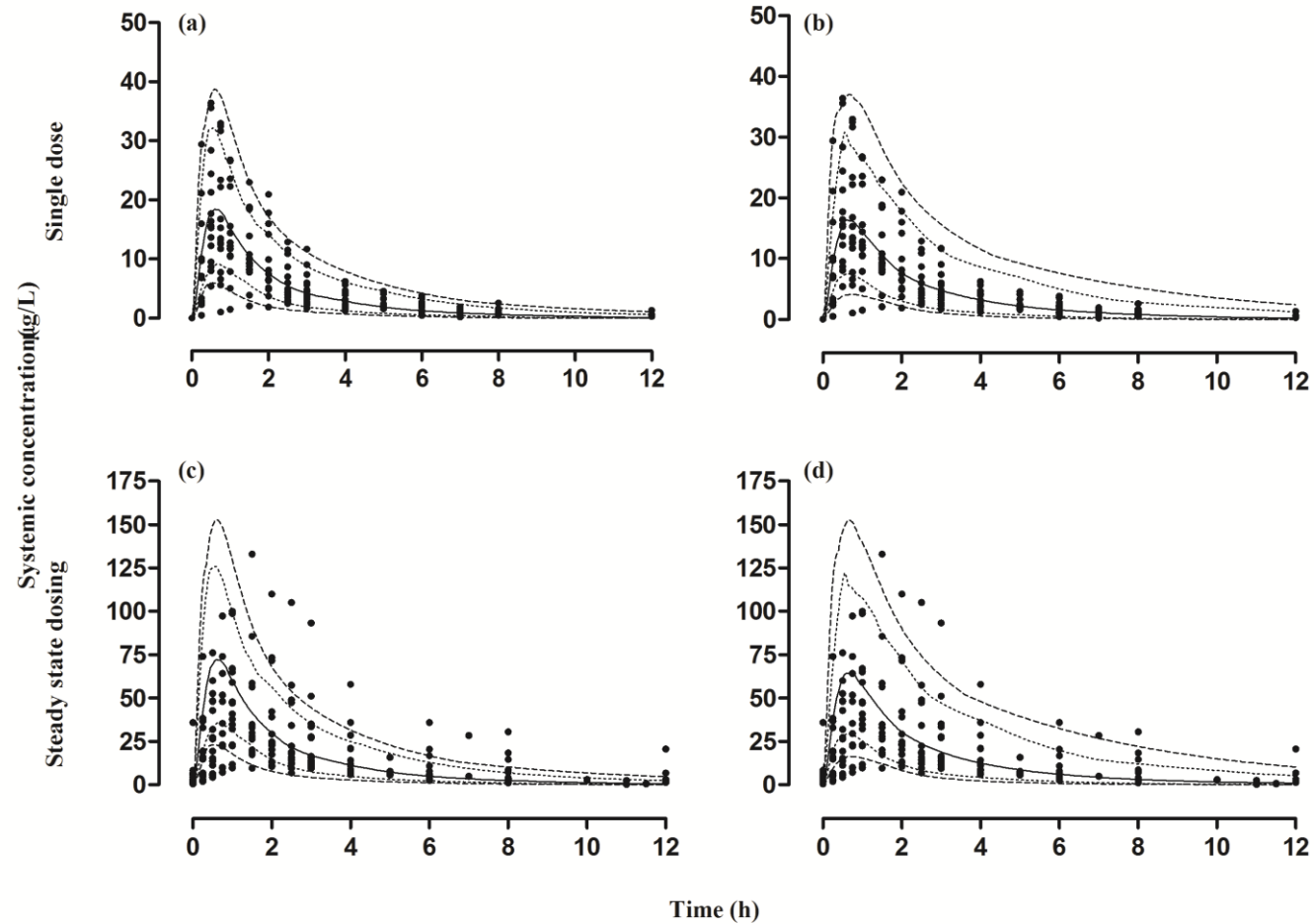
Figure 1-7 Predictions made by using model-1 and model-2 in the entite pediatric age range.

Predictions made by using *(a,c)* model-1 and *(b,d)* model-2 after administering, single 0.09 mg/kg and steady state 0.35 mg/kg oral dosing of carvedilol in the entire pediatric age range (0.12 to 17.8 years), including 19.3 years old patient, (solid line) median prediction, (dashed line) minimum and maximum prediction, (dotted line) 5th and 95th percentiles and ● observed data (Behn, 2001)
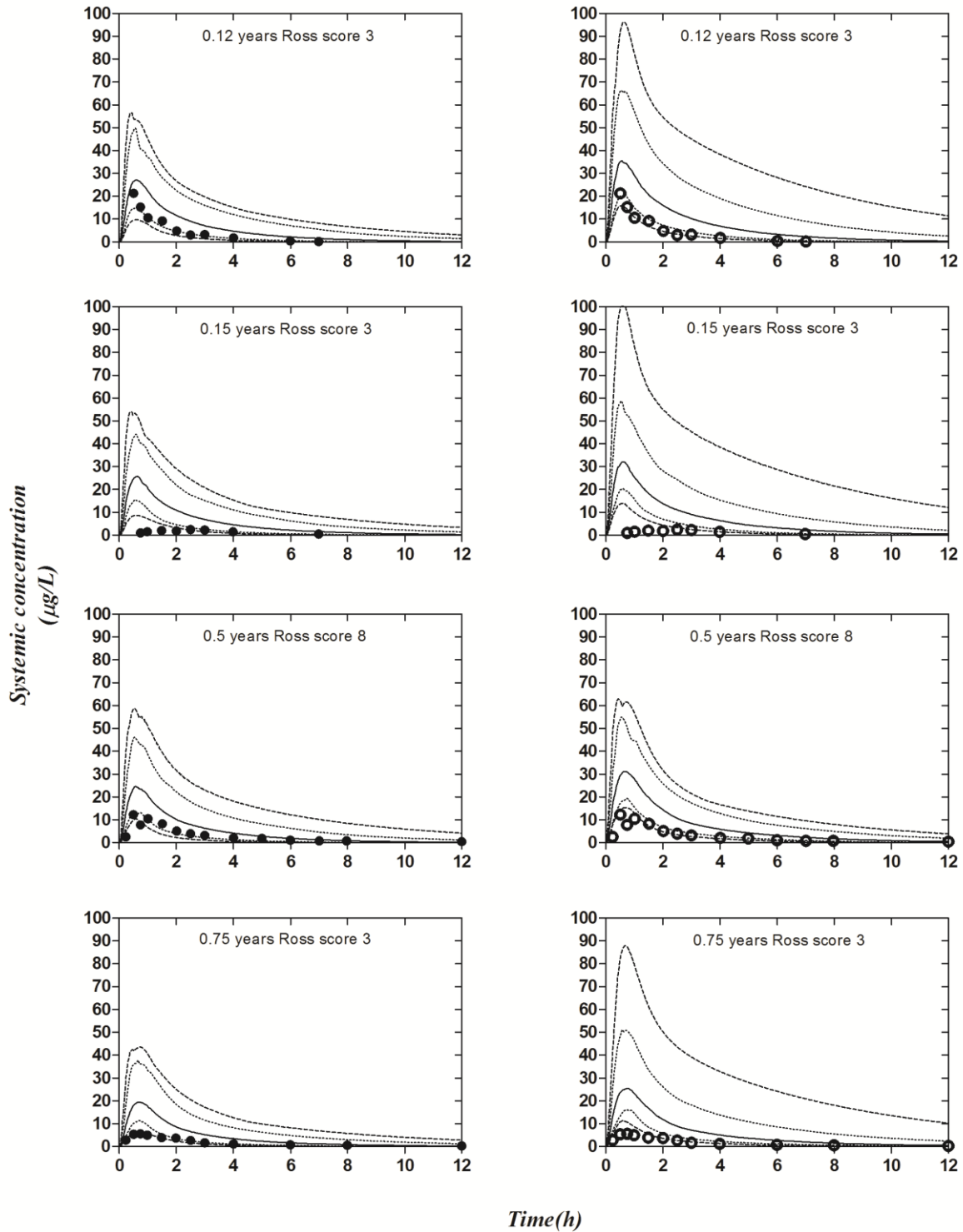
Figure 1-8A The individual predictions made by model-2 after administering single test dose of 0.09 mg/kg oral carvedilol.

The individual predictions made by model-2 after administering single test dose of 0.09 mg/kg oral carvedilol with (○) and without (●) adjusting the organ blood flows, (solid line) median prediction, (dashed line) minimum and maximum prediction, (dotted line) 5th and 95th percentiles and (●,○) observed data (Behn, 2001).
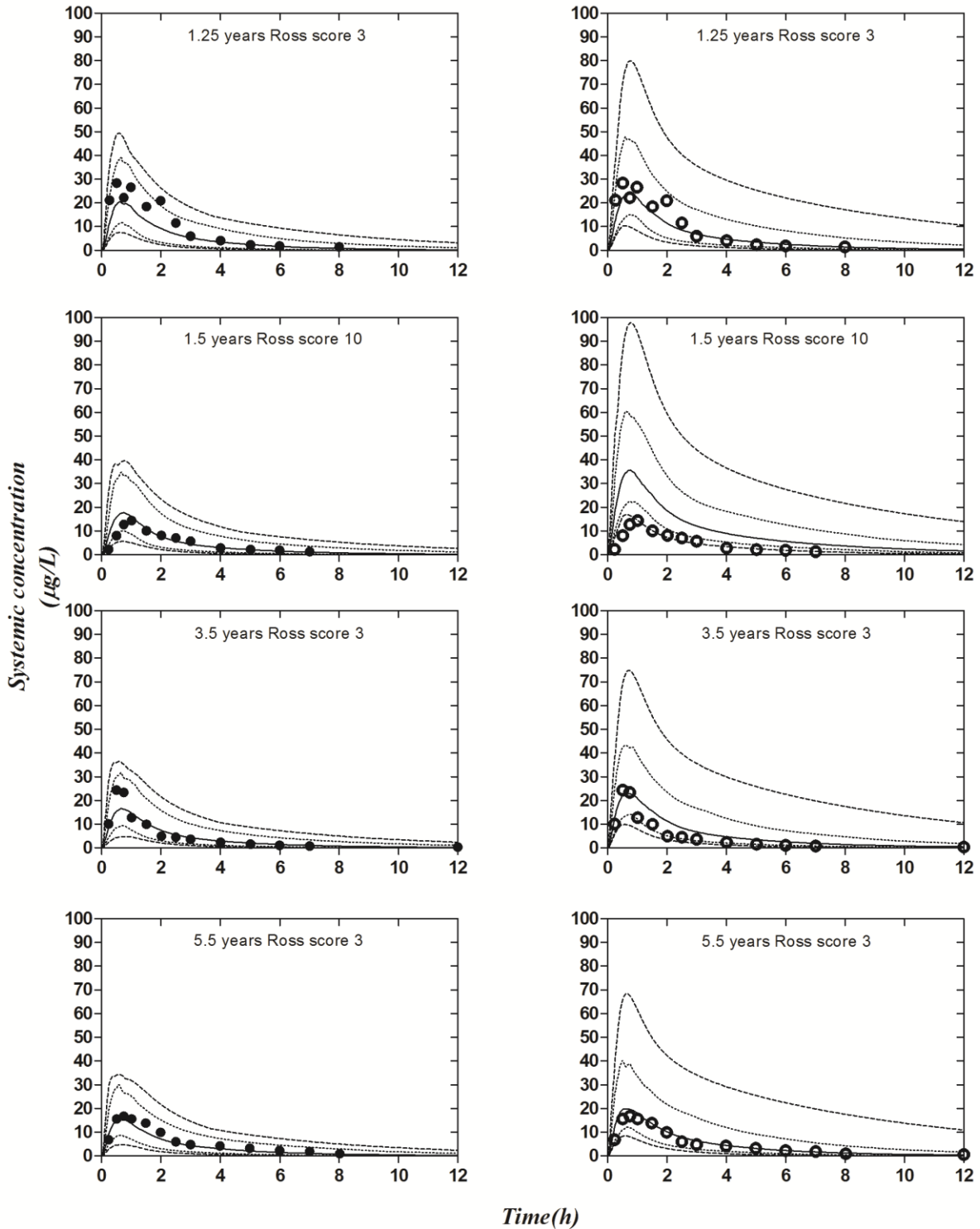
Figure 1-8B The individual predictions made by model-2 after administering single test dose of 0.09 mg/kg oral carvedilol.

The individual predictions made by model-2 after administering single test dose of 0.09 mg/kg oral carvedilol with (○) and without (●) adjusting the organ blood flows, (solid line) median prediction, (dashed line) minimum and maximum prediction, (dotted line) 5th and 95th percentiles and (●, ○) observed data (Behn, 2001)
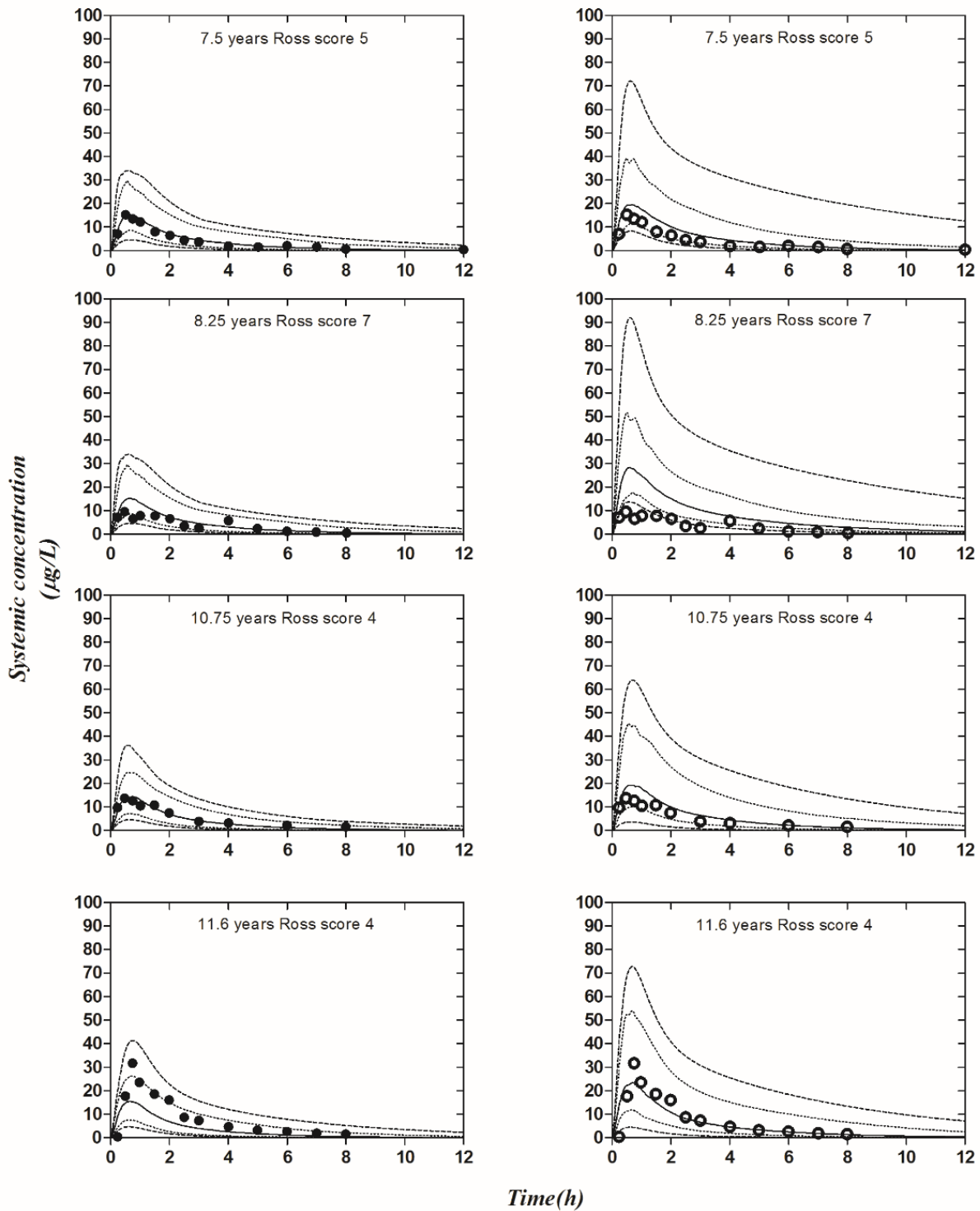
Figure 1-8C The individual predictions made by model-2 after administering single test dose of 0.09 mg/kg oral carvedilol.

The individual predictions made by model-2 after administering single test dose of 0.09 mg/kg oral carvedilol with (○) and without (●) adjusting the organ blood flows, (solid line) median prediction, (dashed line) minimum and maximum prediction, (dotted line) 5th and 95th percentiles and (●, ○) observed data (Behn, 2001)
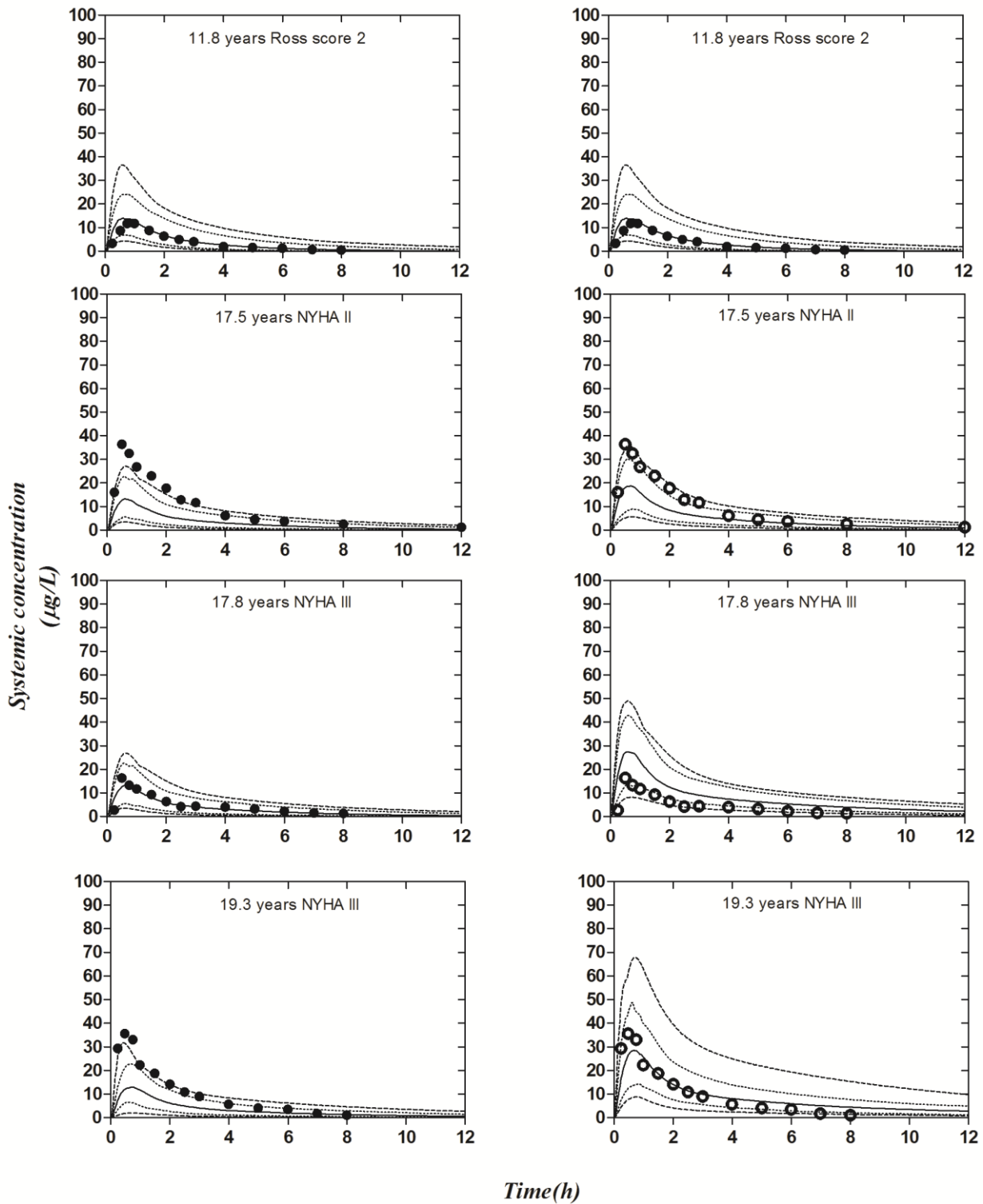
Figure 1-8D The individual predictions made by model-2 after administering single test dose of 0.09 mg/kg oral carvedilol.

The individual predictions made by model-2 after administering single test dose of 0.09 mg/kg oral carvedilol with (○) and without (●) adjusting the organ blood flows, (solid line) median prediction, (dashed line) minimum and maximum prediction, (dotted line) 5th and 95th percentiles and (●, ○) observed data (Behn, 2001)

The mean AUC_{last} ratios$_{(Obs/Pred)}$ with 95% CI after administering single dose (0.09 mg/kg) of carvedilol were 0.98 (95% CI: 0.68–1.28) and 1.0 (95% CI: 0.7–1.30) without incorporation of reduced organ blood flows. There was no improvement seen in the prediction capability of both models by reducing organ blood flows, after administering single and steady state doses of carvedilol as the calculated AUC_{last}, C_{max}, and CL/F ratios$_{(Obs/Pred)}$, were further away from unity (**Figure 1-10 and Appendix 7**). The previous finding that pediatric predictions improved in those patients having a moderate or severe CHF, given by a NYHA classification, after reducing the blood flows can also be seen here.

Without adjusting organ blood flows   *With adjusting organ blood flows*
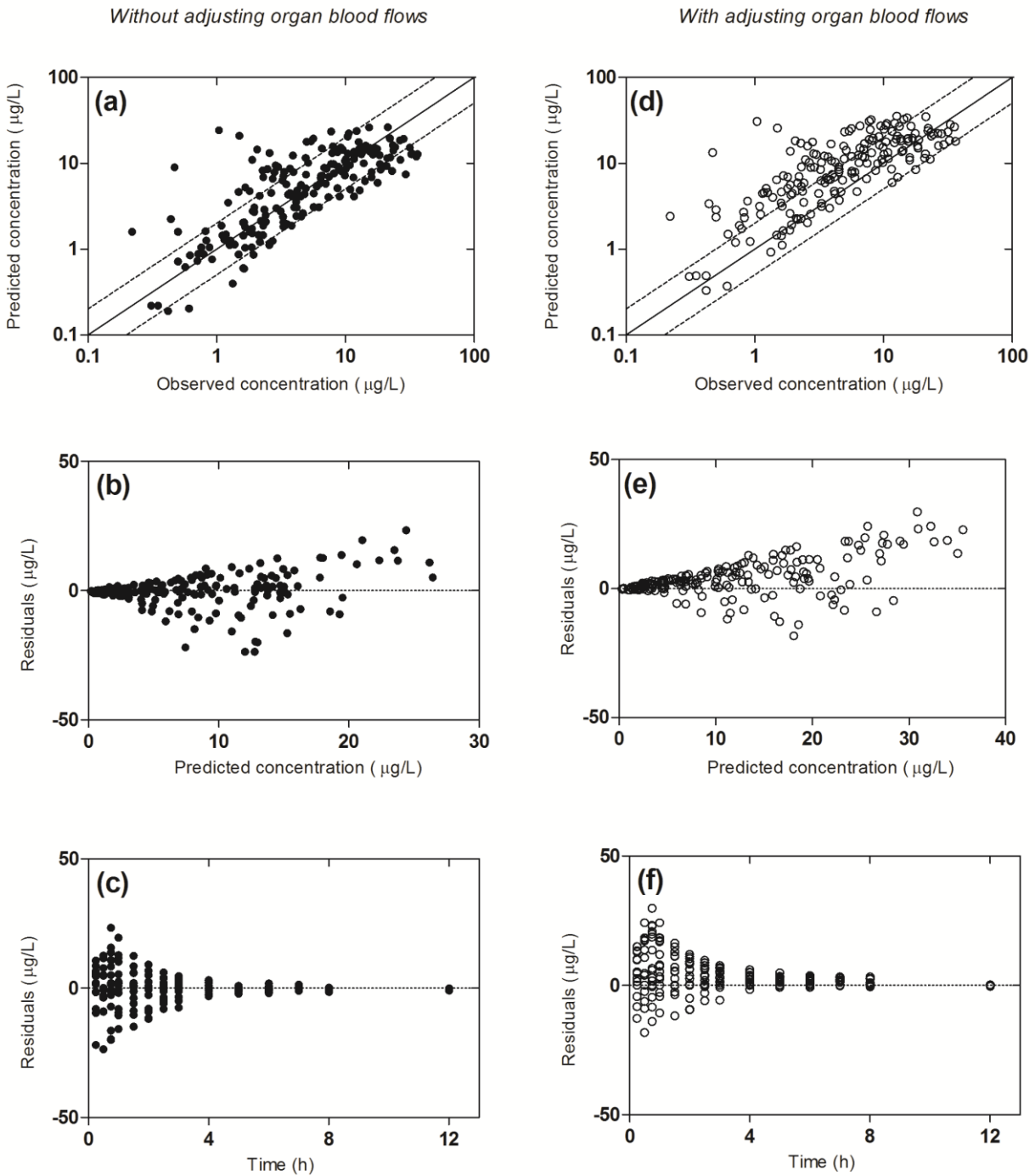
Figure 1-9 Goodness to fit plots for model-2 predictions in the pediatric population.

Goodness to fit plots for model-2 predictions in the pediatric population presented as median predicted vs. individual observed concentrations plots, residuals vs. median predicted concentrations plots, and residuals vs. time plots. (a–c) results without renal and hepatic blood flow reductions and (d–f) results with renal and hepatic blood flows reductions. The solid line indicates line of identity, the dashed line a 2-fold error range. (●) without and (○) with reductions in organ blood flows
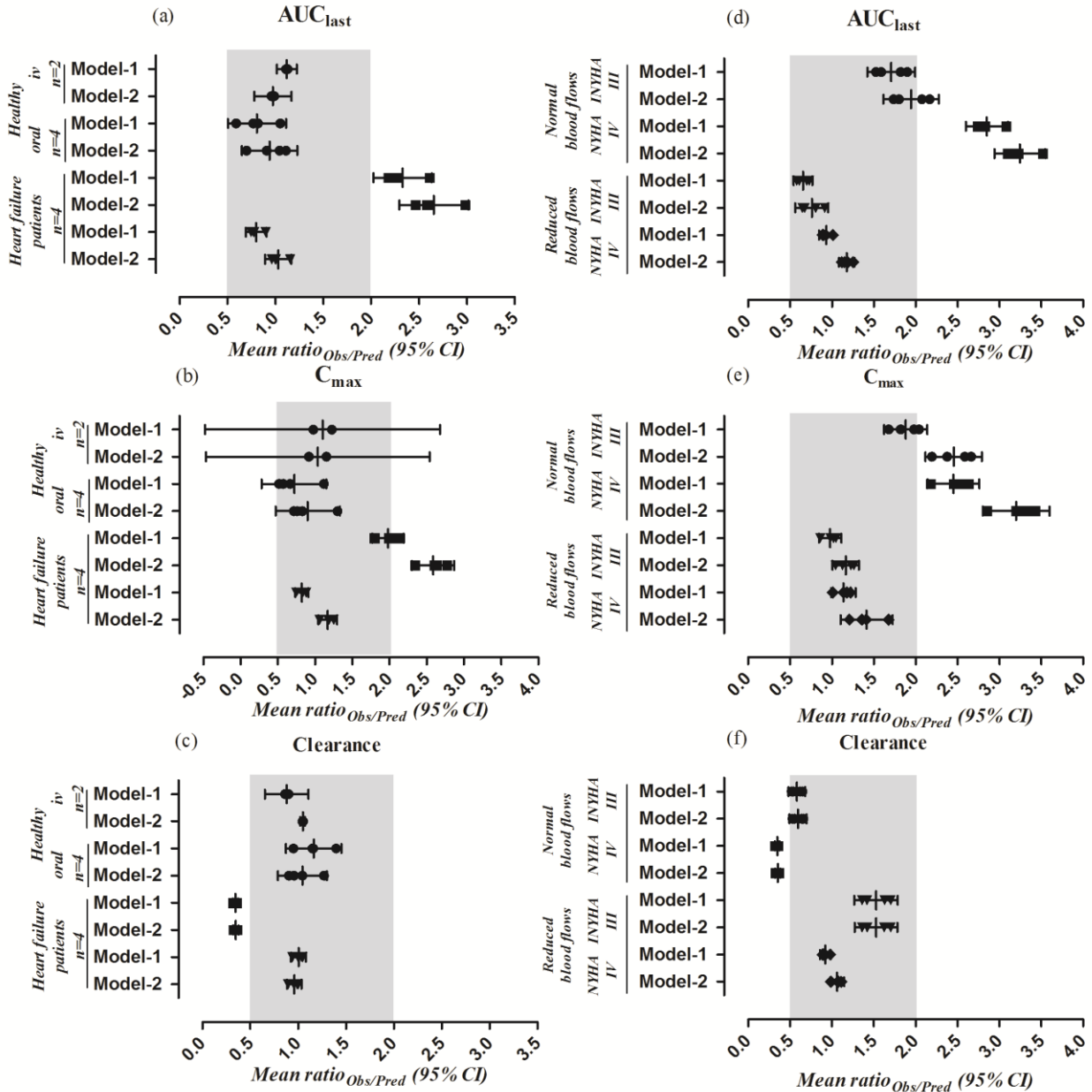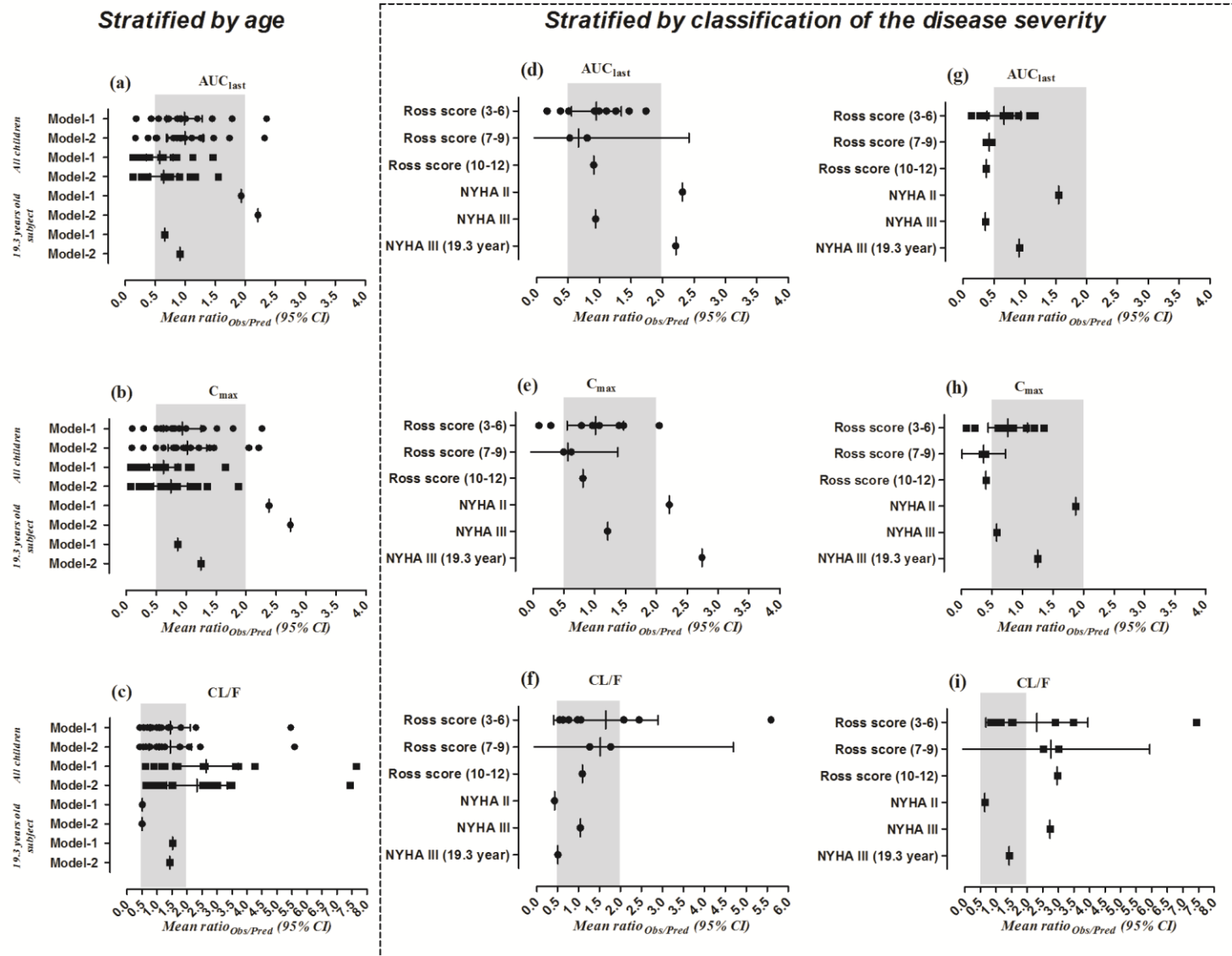
Figure 1-10 Comparison between the observed and predicted values of pharmacokinetic parameters in children

Comparison between the observed and predicted values of the area under the plasma concentration-time curve (AUC_{last}), the maximum concentration (C_{max}), and drug clearance in heart failure pediatric patients after administering single doses of 0.09 mg/kg. Results are presented as individual and mean ratios(observed/predicted) with a 95% confidence interval (CI) without ● or with ■ blood flow reductions. (a–c) results by both models stratified by age, (d–i) results by model-2 stratified by the severity of the disease. The shadowed gray area indicates a 2-fold error range

The observed oral clearance of carvedilol increased with age after administering the single dose of 0.09 mg/kg, starting from 9.20 L/h in a patient with age of 0.12 years and reaching up to 110 L/h in a patient with age of 19.3 years. When the oral clearance was normalized with weight, a decrease was seen with increasing age, as it decreased from 2.94 L/h/kg at the age of 0.12 years to 1.12 L/h/kg until the age of 19.3 years, which is the reflection of the incorporated knowledge enzyme ontogeny in the modeling software. Similar trend was seen after administering steady state target doses of carvedilol. The developed models were capable of capturing the age related changes in oral clearance of carvedilol after single and steady state administration (**see Figure 1-11A and B**).
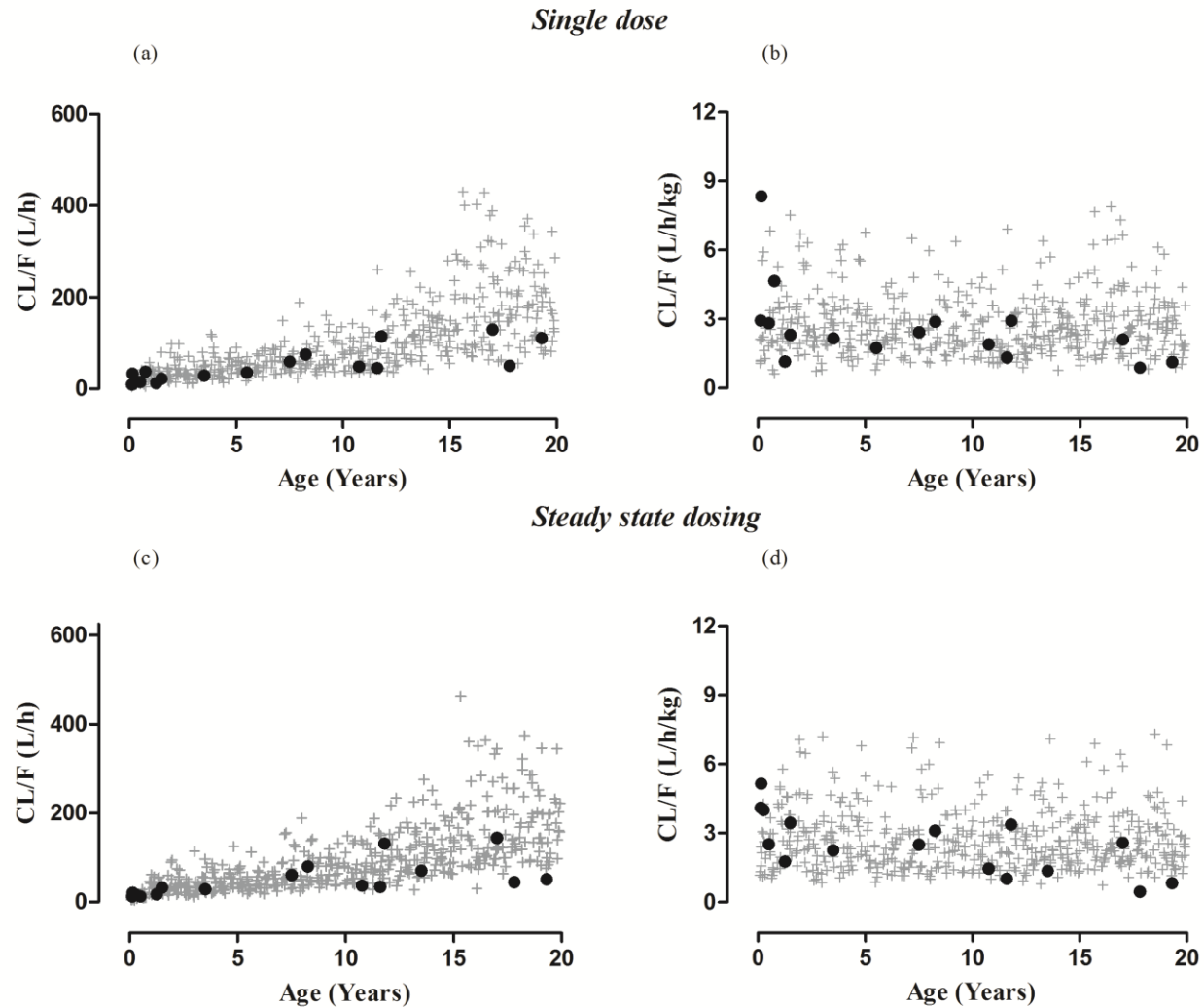
Figure 1-11A The change in carvedilol oral clearance with age.

(a,c) The change in carvedilol oral clearance with age after single (0.09 mg/kg) and steady state (0.35 mg/kg) dosing. *(b,d)* The change in weight normalized oral clearance of carvedilol with age after single dose and steady state dosing. + predicted values by model-1 (n= 500) and ● observed values (Behn, 2001).
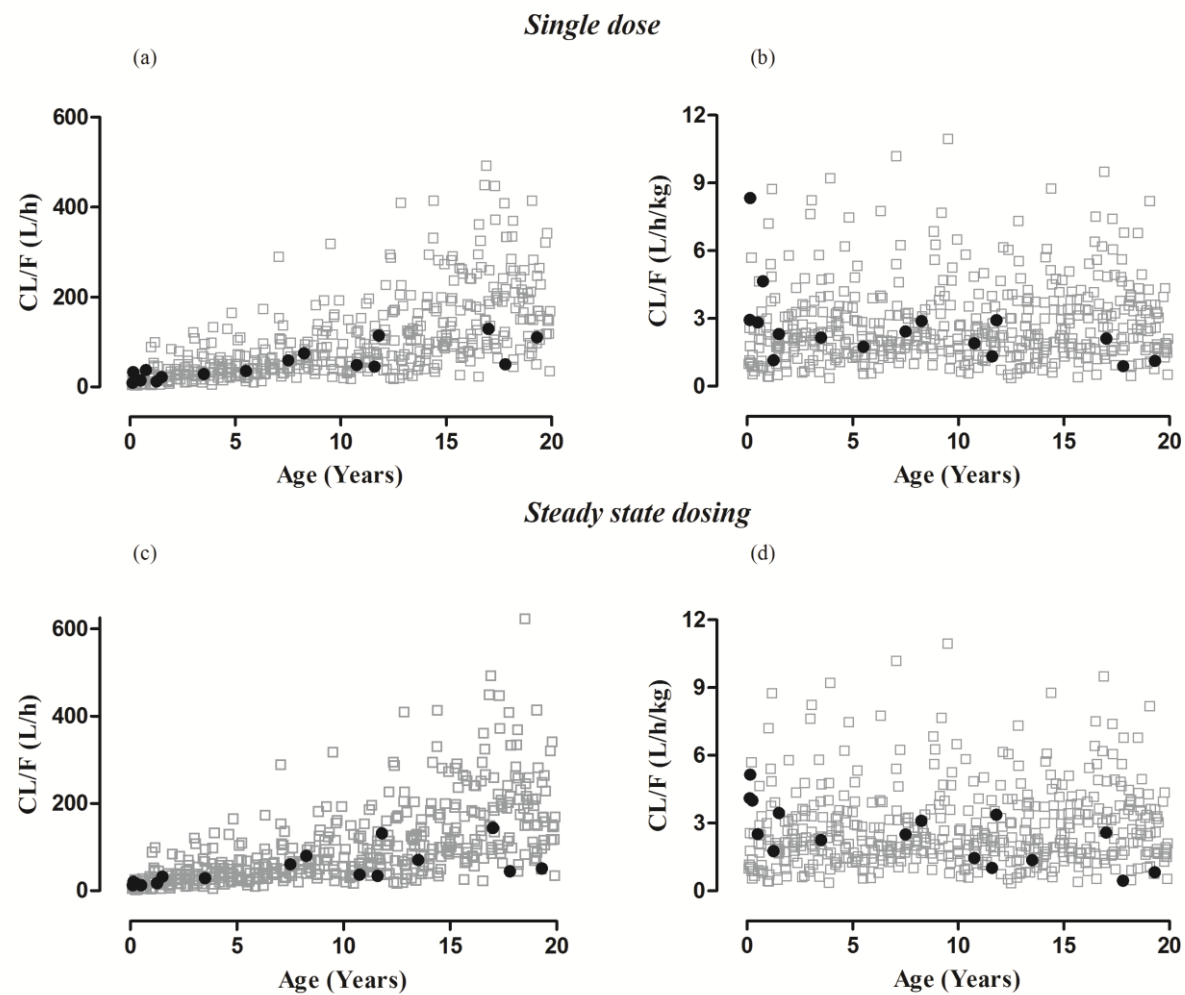
Figure 1-11A The change in carvedilol oral clearance with age.

(a,c) The change in carvedilol oral clearance with age after single (0.09 mg/kg) and steady state (0.35 mg/kg) dosing. *(b,d)* The change in weight normalized oral clearance of carvedilol with age after single dose and steady state dosing. □ predicted values by model-2 (n=500), and ● observed values (Behn, 2001).

1.4.   Discussion

In this study reduced hepatic and renal blood flows were incorporated into whole-body PBPK models to predict carvedilol exposure in CHF patients. Both developed models were able to describe carvedilol pharmacokinetics in adults and pediatrics over 1 year of age, but model-2 was shown to be superior to model-1 in its predictive performance. The incorporation of the reduced hepatic and renal blood flows in the developed CHF models resulted in a significant improvement in predictions of drug exposure in adult patients. Conversely, the incorporated blood flow reductions did not result in any improvements in the pediatric CHF patients, except in those patients having a mild or severe CHF and classified, as in adults, according to NYHA classification system (NYHA III).

Following the implemented strategy of model development, the presented models were first parameterized and evaluated in healthy adults. The results showed accurate prediction of carvedilol exposure over a wide range of administered iv and oral doses (**Figures 1-3A and B, 1-4 and 1-5**), which implicate their ability to account for the various processes governing drug absorption and disposition. The predicted bioavailability in healthy volunteers was in the range of 15–27% by both models, which was quite close to the reported values of 22-24% (von Mollendorff et al., 1987). Furthermore, the mean AUC_{last} ratios$_{(Obs/Pred)}$ in healthy adults were within the 2-fold error range i.e., after iv application: 1.12 (95% CI: 1.01–1.22) and 0.97 (95% CI: 0.78–1.16) and after oral application: 0.80 (95% CI: 0.51–1.11) and 0.94 (95% CI: 0.65–1.23), using models 1 and 2, respectively.

In CHF, hepatic and renal blood flows decrease with increasing severity of the disease (Leithe et al., 1984). Incorporating these reductions improved model predictions significantly, for example, the mean AUC$_{last}$ ratios$_{(Obs/Pred)}$ changed from 2.33 (95% CI: 2.02–2.63) to 0.79 (95% CI: 0.69–0.90) and from 2.65 (95% CI: 2.29–3.01) to 1.03 (95% CI: 0.89–1.16) using models 1 and 2 respectively. The extensive first pass effect and the high hepatic extraction ratio of carvedilol (Neugebauer et al., 1987; von Mollendorff et al., 1987; Abdelaziz et al., 2009) implicate that changes in hepatic blood flow, as seen in CHF, will influence its first-pass and systematic hepatic metabolism and, thus, its bioavailability and total exposure. The reduced hepatic blood flow will lead to an increase of the first-pass metabolism with a subsequent decrease in drug bioavailability (because of a higher hepatic extraction during first pass), and a decrease in the systematic clearance of the drug. The reduction in carvedilol bioavailability and oral clearance with the increased severity of CHF was clearly seen in the predictions (see **Figure 1-6**). On the other hand, the renal clearance of carvedilol is only about 1–2 % (Neugebauer et al., 1987; Gehr et al., 1999) of its total clearance, therefore, the change in the latter is clearly attributed to the decrease in hepatic clearance. The ratios$_{(Obs/Pred)}$ with 95% CI of the pharmacokinetic parameters after further subdividing the adult CHF patients into NYHA III and NYHA IV categories supported out hypothesis that the incorporated reduced hepatic and renal blood flows in the developed models are associated with NYHA classification of CHF (**Figure 1-5**).

The previously presented and evaluated models in adults formed the basis to extrapolate carvedilol pharmacokinetics to children on physiological basis,

using the pediatric module in Simcyp®. The developed pediatric models, that incorporate a wide range of age-specific information, were capable of reflecting carvedilol exposure after single and steady state doses in the pediatric age range (**Figure 1-7**). However, it was noticed that the models tended to generally overpredict the drug concentrations in those patients under one year of age with or without the incorporation of blood flow reductions. An overprediction of drug concentrations in this age was previously reported when child-specific PBPK models were used to predict drug PK when given orally (Khalil and Laer, 2014), with the reason being most probably attributed to age-specific information gaps in the parameterization of the integrated absorption models. Second, in contrast to the adult patients, the improvement in the model predictions by the incorporation of blood flow changes was limited to few cases as will be discussed below.

Ten out of the 14 pediatric CHF patients that were included in the clinical trial were diagnosed with a mild CHF, 9 patients according to the modified Ross score system and 1 patient according to NYHA classification. For patients categorized with Ross score, no substantial improvement was seen, on the other hand prediction was improved in one patient staged NYHA II when reduced organ blood flows were incorporated (**Figure 1-8**). These findings could suggest that the pharmacokinetics of carvedilol may not be affected in mild CHF as in moderate or severe CHF. On the other hand, no improvement was seen when the model was modified to blood flow changes in the only patient with a severe CHF, as indicated by a Ross score of 10, whereas clear improvement was seen only in 19.3 years'

patient staged as NYHA III and the 17.8 years' patient staged as NYHA III was better described without organ blood flow reductions. As a result, an assumption that Ross scoring system is poorly correlated with the reductions in organ blood flows in comparison to NYHA system of grading CHF cannot be completely excluded. In the modified Ross score system, different subjects with different symptoms may end up having same score and CHF category. Amongst the 6 categories used for classification of pediatric patients by the modified Ross score system, 3 are related to breathing, which may result in undermining of the other symptoms associated with CHF in pediatrics (Ross, 2012). In addition, the aetiology and the pathophysiology of CHF is different in adults when compared to children, especially in the first few years after birth. Children have a higher heart rate (Fleming et al., 2011) when compared to adults (Tanaka et al., 2001), which deceases with age after birth and becomes comparable to adults at the age of 18 (Fleming et al., 2011), and therefore, may have a higher capacity to compensate a decrease in cardiac output. Our pediatric disease model is based on the adult heart failure model with its incorporated reductions in organ blood flows because in pediatrics we are not aware of any study that quantified hepatic and renal blood flow reductions with respect to different stages of heart failure in pediatrics. Therefore, these adult quantifications may not be completely true for children. Finally, children also have higher percentage of liver weight to total body weight when compared to adults (Noda et al., 1997), which may lead to a higher drug clearance capacity (by rapidly maturating and abundant metabolizing enzymes), and the influence of a decreased hepatic blood flow may not have the same impact on drug clearance as in adults.

The observed weight normalized oral clearance of carvedilol decreased in pediatric patients with increasing age (43 days to 17.8 years). This was due to the fact that infants have liver weight around 4% of their total body weight, which decreases to about 2% in adults (Noda et al., 1997). Moreover, CYP2D6 is the major enzyme involved in carvedilol metabolism (~60%) and it achieves more than 50% of adult activity within first month of life (Salem et al., 2013). Another enzyme that plays a minor role in carvedilol metabolism is CYP2C9 which also has a fast ontogeny and therefore it was previously reported that significantly higher weight-normalized doses, as compared to adults, are required in young children with drugs that are primarily metabolized with this enzyme (Anderson, 2010). Furthermore, the decrease in oral clearance of carvedilol can also be attributed to decrease in organ blood flows, as improvement in predictions were seen with incorporation of reduced organ blood flows in patients within adolescent age group (**Figure 1-8**). The developed pediatric models were capable of capturing the age specific changes in carvedilol clearance as the mean CL/F ratios$_{(Obs/Pred)}$ after administering single dose of carvedilol, without incorporating reduced organ blood flows, were 1.44 (95% CI: 0.77–2.11) and 1.43 (95% CI: 0.72–2.14) using models 1 and 2, respectively (**Figure 1-10**).

Despite the fact that the already incorporated ontogeny profiles for each of the individual CYP enzymes give model-2 a clear advantage over model-1 through the ability to incorporate enzyme specific genotype data, the predicted results obtained by both models were very similar. One reason could be that, the customized ontogeny profile that was assigned in model-1 is based on the

ontogeny data of each of the individual enzymes used in model-2. A second reason is that; the additional superiority of model-2 could have been clearer if population specific enzyme genotype data were included for all of the used clinical studies. In our study, this was only done in the simulations of two clinical studies (Behn, 2001; Giessmann et al., 2004).

1.5. Limitations

A part of the carvedilol concentration-time profiles observed in adults was scanned from the publications' figures and was not obtained from source. However, the difference seen between the reported PK parameters in the original papers and those calculated by us using the scanned profiles was negligible, and therefore of no significance to the model evaluation results. In addition, the adult CHF model was only evaluated with NYHA III and IV patients, but this was because the availability of only one PK study of carvedilol in CHF patients.

The absorption (ADAM) model used for pediatric simulations was not completely parameterized with age-specific information for all the anatomical and physiological factors that may influence the drug absorption. For example, the model does contain information on the age related changes in intestinal length, diameter, blood flows, and intestinal CYP enzymes but yet no information on changes in gastric and intestinal pH, bile secretion, transporters, and gut fluid dynamics. This reflects the fact that pediatric drug absorption in PBPK modelling software is an area of ongoing research, and therefore, the presented pediatric results must be judged in this context. The fluid intake with dose was not modified according to the age of the pediatric subjects; however, no relevant impact was

seen on the results of the 4 infants under one year of age. The assigned P_{eff} value was not changed with age so that a similar passive diffusion of the substance was assumed in adults and children.

The role of the three different UGTs involved in carvedilol metabolism was assigned collectively as an additional clearance. Since each of these pooled UGT enzyme possess a different ontogeny profile and no clear information about their individual contribution, no specific ontogeny was assigned to this collective value. This can be a limitation in model-2 and an aspect to improve the model in the future.

Finally, in the presented models, we have assumed similar organ blood flow reductions in pediatric heart failure patients as in adults, as no specific clinical information were available for the pediatric population.

The developed PBPK model was successful in describing ADME of carvedilol in adult and pediatric CHF patients. Due to the mechanistic nature of the developed PBPK model it can be extended to predict PK of other high hepatic extraction drugs.

Since, carvedilol is admininstered as a racemic mixture of R and S enantiomers and both enantiomers have different pharmacokinetic and pharmacodynamic properties and therefore, the organ blood flow flow reductions in CHF pateints can effect carvedilol disposition in a stereo-selective fashion. Keeping this in mind, the second chapter of this thesis is focused on development and evaluation of a

PBPK model capable of predicting stereo-selective disposition of carvedilol in healthy and CHF populations.

Chapter 2:

Predicting stereo-selective disposition of carvedilol in adult and pediatric chronic heart failure patients by incorporating pathophysiological changes in organ blood flows–A physiologically based pharmacokinetic approach

2.1. Introduction

Racemic drugs are composed of enantiomers that can differ greatly in their PK and pharmacodynamic (PD) properties (Birkett, 1989). The PK differences between the enantiomers are mainly due to differences in absorption and disposition which can lead to variations in their systemic concentrations and hence can influence the concentration-effect relationship (Tucker and Lennard, 1990). Since, some of the enantiomers show stereo-selective disposition, any pathophysiological condition that can affect their clearance can have a profound impact on their exposure and efficacy. Carvedilol is a racemic mixture of two enantiomers, with S-enantiomer having both α_1-receptor blocking and β-adrenoreceptor blocking activities while R-enantiomer is more selective towards α_1-receptor blocking activity (Neugebauer et al., 1990). Both enantiomers undergo extensive stereo-selective first pass metabolism through CYP enzymes (CYP2D6, CYP1A2, CYP2C9, CYP3A4 and CYP2E1) and UGT enzymes (UGT1A1, UGT2B4 and UGT2B7) (Oldham and Clarke, 1997; Ohno et al., 2004; Takekuma et al., 2012), with reported absolute bioavailability of 31.1 % for R-carvedilol and 15.1 % for S-carvedilol (Neugebauer et al., 1990). Because, CYP2D6 is the main metabolic enzyme that is involved in the metabolism of both enantiomers and is more selective towards the overall disposition of R-carvedilol, the decrease activity of this enzyme in poor metabolizers (PM's) may result in higher systemic

concentration of R-carvedilol and hence an increase in α-blockade, which can cause greater acute blood pressure reduction and increased incidence of orthostatic hypotension in comparison with extensive metabolizers (EM's) of CYP2D6 (Zhou and Wood, 1995). Since, carvedilol is used in the management of CHF and it undergoes extensive stereo-selective first pass metabolism, the organ blood flow reductions occurring in CHF can significantly affect its ADME.

A physiologically based pharmacokinetic (PBPK) model incorporating reduced hepatic and renal blood flows has been used previously to predict PK of racemic carvedilol in adult and pediatric CHF patients (Rasool et al., 2015). However, the reductions in blood flow to limbs, adipose, skin and muscle tissues, which can additionally affect the drug distribution and hence the plasma concentration of the drug, were not yet incorporated in the previously reported carvedilol-CHF model (Rasool et al., 2015). Keeping in mind that carvedilol is administered as a racemic mixture of R and S enantiomers, which have ~2-fold difference in their F, the organ blood flow reductions occurring in CHF can affect the disposition of both in a stereo-selective fashion. The differences in the exposures of R and S carvedilol will influence the expected PD response and may potentially lead to adverse drug reactions. A PBPK model that incorporates all the reported relevant blood flow reductions occurring in CHF can be used to predict stereo-selective disposition of carvedilol in CHF patients. Furthermore, a developed and evaluated PBPK model with clinical data in adult CHF patients can be scaled to pediatrics on physiological basis by using a population based ADME simulator.

2.1.1. Objective

The main objective of this work was to develop a PBPK drug-disease model capable of predicting stereo-selective disposition of carvedilol in CHF patients after incorporating the relevant organ/tissue blood flow changes and to evaluate it with the available clinical data in adult and pediatric CHF patients.

2.2. Methods

2.2.1. Modelling platform

The population based PBPK simulator, Simcyp® version 14.1 (Simcyp Ltd, Sheffield, UK) was used in developing a whole body PBPK model.

2.2.2. Modelling strategy

A PBPK model was developed by adopting a systematic model building strategy (Khalil and Laer, 2014), starting with the literature search for screening of drug specific input parameters and clinical pharmacokinetic data to be used in model development. This was followed by incorporation of these data into the simulator and selection of system parameters for running predictions in virtual populations and the final evaluation of the developed model with the comparison of predicted results with the observed clinical trial data. To avoid the complexity associated with the oral drug absorption, initially predictions were performed after iv drug application and all the drug-specific parameters that can potentially influence drug disposition such as, in-vivo clearance and contributions of various metabolic enzymes (CYP's and UGT's) were optimized. After successful evaluation of the iv predictions with the observed data, the previously selected parameters are kept constant and other additional drug-specific parameters which can affect drug absorption process, such as permeability and fraction unbound of the drug in the enterocyte are selected or optimized. Amongst the seven PK data sets (2 iv and 5 oral) in healthy adults, three data sets (1 iv and 2 oral) were used for model building and remaining data sets were used for model verification and all the data sets were used for model evaluation. After evaluation of developed model in

healthy adults, pathophysiological changes in organ blood flows occurring in CHF were incorporated to predict ADME of carvedilol enantiomers in adult CHF patients. After successful evaluation of developed CHF model with the observed data, it was scaled to pediatrics on physiological basis by using the pediatric module of Simcyp®. In order to see impact of reduced organ blood flows on the model predictions in pediatric CHF patients, simulations were performed in duplicate i.e., with and without incorporating reductions in organ blood flows.

All the predictions were performed by creating a virtual population with same demographics as in the original trial by keeping the age range, proportion of females, fluid intake, fasting/fed states and where applicable same genotypic frequencies. In adults, all the predictions were performed by creating a virtual population of 100 individuals for every PK data set, while in pediatrics, the initial simulations were performed in the entire age range including the young adult, without stratifying them in different age groups, by creating a virtual population of 1000 individuals within the age range of 0.12–19.3 years, followed by simulating pediatric patients in different age groups by creating a virtual population of 100 individuals for every age group. The workflow for the development of PBPK model can be seen in **Figure 2-1**.
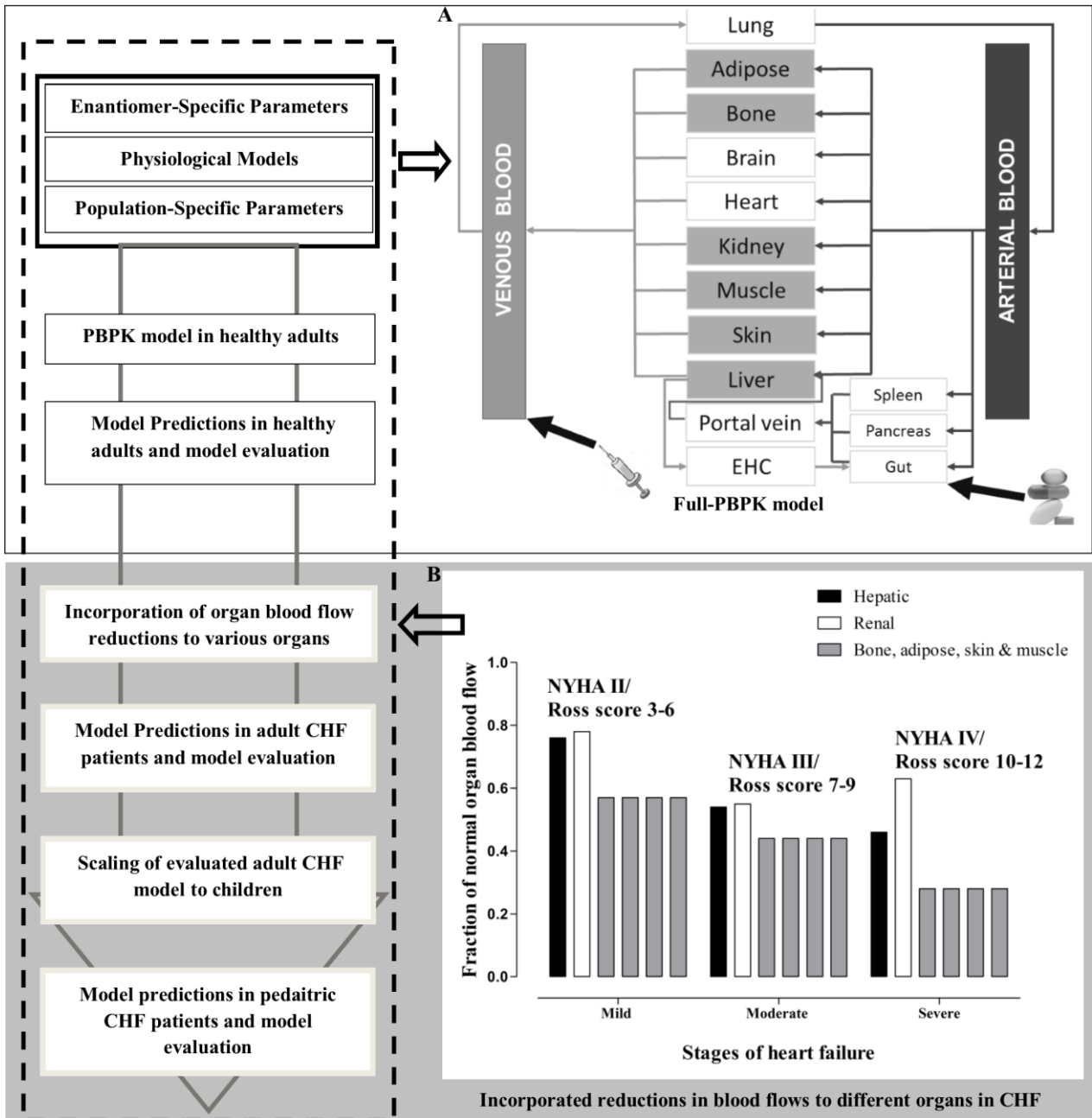
Figure 2-1 Workflow for the development of enantiomeric carvedilol PBPK heart failure model in adult and pediatric populations.

The white area shows model development in healthy adults and the grey shaded area shows stages of model development in chronic heart failure patients. (A) Full PBPK model with different body compartments. The grey compartments show the organs in which blood flow reductions are incorporated. (B) Incorporated organ blood flow reductions in chronic heart failure patients with respect to severity of disease (Adopted from (Leithe et al., 1984). *CHF* chronic heart failure, *NYHA* New York Heart Association functional classification of heart failure *PBPK model* physiologically based pharmacokinetic model.

2.2.3. PBPK Model parameterization

After undergoing through an extensive literature search, relevant in-vivo and in-vitro drug and population-specific data was selected for completing the model parameterization. The final model input parameters are summarized in **Table 2-1**. The detailed parameterization of various drug and disease-specific components used in the final PBPK model is given below.

Table 2-1 The drug dependent parameters and characteristics of the presented PBPK model

Parameter	R-Carvedilol	S-Carvedilol	Source/ Reference
Molecular weight (g/mol)	406.47	406.47	PubChem.
$LogP_{o:w}$	4.19	4.19	PubChem.
pK_a	7.97	7.97	(Caron et al., 1999)
Absorption			
Model	ADAM		
Solubility (mg/mL)[a]	0.01	0.01	(Benet et al., 2011)
$P_{eff,man}$ (cm/s)	3.9×10^{-4}[b]	1.6×10^{-4}	(Tian et al., 2012), Sensitivity analysis and manual optimization
$f_{u,Gut}$	0.00138	0.00124	Simcyp predicted
Q_{Gut} (L/h) [c]	12.2	8.1	Simcyp predicted
Distribution			
Model	Full PBPK		
V_{ss} (L/kg)—predicted	1.57	1.95	Poulin and Theil method
V_{ss} (L/kg)— observed	1.39–3.40	1.42–3.84	(Neugebauer et al., 1990)
Blood to plasma (*B:P*) ratio	0.67	0.74	(Fujimaki et al., 1990)
fu_P	0.0045	0.0063	(Fujimaki et al., 1990)

Parameter	R-Carvedilol	S-Carvedilol	Source/ Reference
Elimination			
CL_{iv} (L/h)—used as input in retrograde model	41	54	(Neugebauer et al., 1990), Optimized
CYP2D6 CL_{int} (µL/min/mg/pmol of isoform)[d]	656.5	702.2	
CYP1A2 CL_{int} (µL/min/mg/pmol of isoform)[d]	2.7	21.6	
CYP2C9 CL_{int} (µL/min/mg/pmol of isoform)[d]	1.9	15.3	
CYP3A4 CL_{int} (µL/min/mg/pmol of isoform)[d]	0.5	4.1	[d,e] Simcyp retrograde model of enzyme kinetics
CYP2E1 CL_{int} (µL/min/mg/pmol of isoform)[d]	1.1	9.2	
UGT1A1 CL_{int} (µL/min/mg/pmol of isoform)[e]	8.8	9.1	
UGT2B4 CL_{int} (µL/min/mg/pmol of isoform)[e]	10.5	10.4	
UGT2B7 CL_{int} (µL/min/mg/pmol of isoform)[e]	8.9	19.6	
CL_R (L/h)[f]	0.25	0.25	(Gehr et al., 1999)

LogP$_{o:w}$ octanal-water partition coefficient, *fu$_P$* fraction of unbound drug in plasma, *pK$_a$* acid dissociation constant, *ADAM* Advanced, Dissolution, Absorption and Metabolism, $f_{u,Gut}$ fraction unbound drug in enterocytes, Q$_{Gut}$ hybrid term derived from villous blood flow and drug permeability through the enterocyte membrane, *CL$_{iv}$* intravenous clearance, *CL$_R$* renal clearance, *CL$_{int}$* intrinsic clearance,

[a]Assumed to be similar for both enantiomers

[b]Human jejunum permeability calculated from *P$_{app}$* value of a Caco-2 assay by calibrating with atenolol and using Simcyp®

[c]Q$_{gut}$ value was adjusted according to decrease in hepatic blood flow in chronic heart failure patients, see method section for details

[d]Values calculated by using retrograde model in Simcyp®

[e]Values calculated manually by predicted additional clearance using retrograde model in Simcyp®

[f]Assumed to be similar in both enantiomers

2.2.3.1.   Absorption

In order to predict oral drug absorption, the advanced, dissolution, absorption and metabolism (ADAM) model was used (Jamei et al., 2009b). The human jejunum permeability ($P_{eff,man}$) of R-carvedilol was predicted using in vitro Caco-2 permeability (P_{app}) input data after calibrating it with reference value of atenolol within Simcyp® (Tian et al., 2012). For S-carvedilol, the $P_{eff,man}$ was optimized and adjusted manually after sensitivity analysis to get a good visual fit with the observed clinical data. The model $P_{eff,man}$ values R for S-carvedilol were 3.9×10^{-4} (cm/s) and 1.6×10^{-4} (cm/s) respectively. The predicted absorbed fractions (f_a) of R and S-carvedilol were 0.98 and 0.85 respectively, which are in accordance with carvedilol having a high permeability and belonging to Biopharmaceutics Classification System (BCS) class II. Additionally, the unbound fractions of R and S-carvedilol within the enterocytes ($f_{u,Gut}$) were predicted using Simcyp®. Although, some reports suggest a possible role of P-glycoprotein (P-gp) in carvedilol disposition (Kaijser et al., 1997; Giessmann et al., 2004), but active transport process is considered to be significant only when carvedilol is given concomitantly with other P-gp substrates (Aiba et al., 2005). Furthermore, carvedilol is considered to be a strong inhibitor and not a good substrate to P-gp (Wessler et al., 2013), taking this information into consideration, no active transport data was incorporated in the developed PBPK model.

2.2.3.2.   Distribution

A perfusion limited whole body, full PBPK model was used for predicting enantiomeric distribution of carvedilol. The volumes of distribution at steady state (V_{ss}) and the tissue to plasma partition coefficients (K_p) for R and S-carvedilol were

predicted by using Poulin and Theil method with the Bierezhkovskiy correction (Berezhkovskiy, 2004).

### 2.2.3.3.	Elimination

Due to absence of relevant metabolic enzyme specific data which can support and predict the reported enantiomer specific carvedilol clearances, the intrinsic clearances of metabolic enzymes involved in R and S-carvedilol clearance were back calculated from their respective iv clearances (CL_{iv}) using the retrograde model for enzyme kinetics in Simcyp® (Neugebauer et al., 1990; Cubitt et al., 2011; Salem et al., 2014). In order to calculate the total hepatic intrinsic clearance (CL_{int}), the adult CL_{iv}, known fractions of hepatic and renal clearance, the fraction of unbound drug (f_u), the blood to plasma drug ratio and the hepatic blood flow were used as input parameters. The predicted hepatic CL_{int} was further divided and assigned to different CYP-enzymes, on the basis of available evidence regarding fractional contributions of these enzymes. The CL_{int} not being assigned to any CYP-enzyme was used as additional drug clearance in the program. The hepatic intrinsic clearance was predicted using the well-stirred liver model:

$$CL_{int} = \frac{Q_H \times CL_H}{fu_B \times (Q_H - CL_H)}$$ **Equation 2-1**

The fractional contributions of CYP-enzymes involved in metabolism of R and S-carvedilol were obtained from available evidences in the published reports (Oldham and Clarke, 1997; Giessmann et al., 2004; Sehrt et al., 2011). It is stated that CYP2D6 is the major metabolic enzyme involved in carvedilol clearance with some minor contributions from CYP1A2, CYP2C9, CYP2E1, and CYP3A4. The 74 % of total R-carvedilol clearance is dependent on CYP2D6 while other CYP-enzymes

have a minor role in its disposition, while 50 % of total S-carvedilol clearance is attributed to CYP2D6 and other metabolic enzymes may have an important role in its overall disposition (Zhou and Wood, 1995; Oldham and Clarke, 1997; Sehrt et al., 2011). In healthy adults, glucuronidation accounts for 20–23 % of total carvedilol clearance (Neugebauer and Neubert, 1991) and three UGT isoforms, UGT1A1, UGT2B4 and UGT2B7 are involved in its metabolism (Ohno et al., 2004). The contributions of UGT1A1, UGT2B4 and UGT2B7 are reported to be around 30 %, 25–40 %, and 30–45 % for R-carvedilol and 12–20 %, 15–26 % and 60–65 % for S-carvedilol respectively (Takekuma et al., 2012).

Taking into account the above mentioned information, 80 % of total carvedilol clearance was assigned to the CYP-enzymes (R-carvedilol: 74 % CYP2D6, 2 % CYP1A2, 2 % CYP2C9, 1 % CYP3A4 and 1 % CYP2E1 and S-carvedilol: 50 % CYP2D6, 10 % CYP1A2, 10 % CYP2C9, 5 % CYP3A4 and 5 % CYP2E1) using retrograde model and remaining 20 % was assigned to UGT-enzymes, which was predicted as additional clearance in the program. The UGT-enzyme contributions were optimized manually to achieve good agreement with the observed clinical data. The final values of different clearance parameters used in the developed PBPK model are shown in **Table 2-1**.

The hepatic clearance (CL_H) was predicted by using well stirred liver model using **equation: 2-2** (Wilkinson and Shand, 1975),

$$CL_H = \frac{Q_H \times fu_B \times CLu_{H,int}}{Q_H + fu_B \times CLu_{H,int}} \qquad \textbf{Equation 2-2}$$

The reductions in hepatic blood flow (Q_H) occurring in CHF were incorporated into the model for predicting clearance of carvedilol enantiomers in CHF patients.

The fraction escaping the gut wall metabolism (F_G) was predicted using **equation: 2-3,**

$$F_G = \frac{Q_{Gut}}{Q_{Gut} + f_{u,Gut} \times CL_{u,int,Gut}}$$ **Equation 2-3**

Where $f_{u,Gut}$ is the unbound fraction of the drug in the enterocyte, $CL_{u,int,Gut}$ intrinsic clearance in the gut, and Q_{Gut} is a hybrid term predicted by using villous blood flow (Q_{villi}) and the permeability clearance (CL_{perm}), which is measured from the effective permeability of the compound. Q_{Gut} is calculated by using **equation: 2-4,**

$$Q_{Gut} = \frac{Q_{villi} \times CL_{perm}}{Q_{villi} + CL_{perm}}$$ **Equation 2-4**

The oral bioavailability was predicted by using **equation: 2-5,**

$$F = f_a \times F_g \times F_h$$ **Equation 2-5**

Where, f_a is the fraction of drug absorbed, F_g is the fraction that escapes metabolism in the gastrointestinal tract and F_h is the fraction that escapes the hepatic metabolism.

2.2.4. Pediatric PBPK model

When the developed PBPK was able to predict ADME of both R and S-carvedilol in adult healthy and CHF patients, it was scaled to pediatrics on physiological basis using the paediatric module of Simcyp®. This module includes

a wide variety of relevant age-specific physiological and anatomical parameters which facilitates the pediatric scaling of drug clearance on physiological basis. These parameters include the age related changes in, total body composition, plasma protein binding, blood volume, organ blood flows and abundance of different metabolic enzymes (Johnson and Rostami-Hodjegan, 2011). In pediatric module, the renal function is described on the basis of glomerular filtration rate (GFR), which is linked with BSA of the simulated individuals (Johnson et al., 2006). In order to simulate the oral drug absorption process in pediatrics, the β-version of the pediatric ADAM model was used with the similar input value of mean gastric emptying time as in the adult model (0.4 hour).

Because, all the pediatric patients included in model evaluation were diagnosed with CHF, the organ blood flow reductions were incorporated in the pediatric model to see the impact of blood flow reductions on ADME of R and S-carvedilol.

2.2.5. Blood flow changes to different organs/tissues in heart failure

Previously explained changes in hepatic and renal blood flows were incorporated in the developed PBPK model (see **Chapter 1** for details). Additionally, the changes in blood flow to limbs can affect the drug distribution, as the blood flow to the limbs also supplies skin, adipose, muscle and bone (Lee et al., 1993). The reported fractional reduction in limb blood flow was, 0.57, 0.44 and 0.28 of normal limb blood flow in mild, moderate and severe CHF patients (Leithe et al., 1984).

In CHF patients there is hepato-splanchic congestion, affecting the passive drug diffusion, that results in decreased migration of drug from the intestinal lumen into systemic circulation, which is depicted as decrease in f_a of the drug (Sica, 2003). Furthermore, the gastrointestinal absorption of drugs having low solubility like carvedilol (0.01 mg/mL, BCS II) are more sensitive to CHF associated changes occurring in gut blood flow (Ogawa et al., 2014). Since, in the developed model the reduction in blood flow to gut was accounted by reducing the Q_H (both arterial and portal) and in order to account for decrease in Q_{villi} with severity of CHF, the predicted Q_{Gut} (equation: 4) value due to its dependence on Q_{villi} was reduced in accordance with the reduction in hepatic blood flow.

The incorporated organ blood flow reductions with respect to severity of CHF in adults (NYHA class) and in pediatric patients (Ross score) are described in detail in **Chapter 1** and are shown graphically in **Figure 2-1**.

2.2.6. Pharmacokinetic/Clinical data

2.2.6.1.   Healthy and Adult patients with CHF

MEDLINE database was searched for screening and identification of pharmacokinetic studies of R and S-carvedilol in healthy adults and CHF patients with known demographic information and reported systemic drug concentration-time profiles. As a result of the search, systemic drug concentration-time data from five different clinical studies in healthy adults (4 studies, and 36 subjects) and CHF patients (one study, 10 patients with NYHA III and 10 patients with NYHA IV, 4 PK data sets) were used in the adult model development and evaluation (Neugebauer et al., 1990; Spahn et al., 1990; Zhou and Wood, 1995; Tenero et al.,

2000; Behn, 2001). These studies provided a total of 11 data sets (7 data sets in healthy and 4 data sets in CHF patients) (**Table 2-2**). Each PK data set used for model development and evaluation represents a mean or median observed concentration-time profile after iv or oral doses of R and S-carvedilol. Amongst the data sets used, one was provided by the author (Behn, 2001) and rest were scanned from the publications' figures (Neugebauer et al., 1990; Spahn et al., 1990; Zhou and Wood, 1995; Tenero et al., 2000) using the "digitizer" tool in software OriginPro® version 9.0 (OriginLab. Northampton, MA). CYP2D6 specific genotype data was available in two clinical studies (Zhou and Wood, 1995; Behn, 2001).

Table 2-2 Characteristics of the adult data sets used for carvedilol model development

No.	Population	Nr. of subjects	Dose (mg)	Application	Age (years)		Body Weight (kg)		Ref.
					Mean	Range	Mean	Range	
1	Healthy	10[a]	12.5	iv infusion[b]	29.5	21-39	73.9	56.5-98	(Neugebauer et al., 1990)
2	Healthy	3	12.5	iv infusion[b]	-	-	-	-	(Spahn et al., 1990)
3	Healthy	10[a]	50	oral	29.5	21-39	73.9	56.5-98	(Neugebauer et al., 1990)
4	Healthy	3	50	oral	-	-	-	-	(Spahn et al., 1990)
5	Healthy	9	25	oral	28.4[c]	-	82.1[c]	-	(Zhou and Wood, 1995)
6	Healthy	7	25	oral	32[d]	-	89.0[d]	-	(Zhou and Wood, 1995)
7	Healthy	7	6.4[e]	oral	29.7	24-37	71	56-100	(Behn, 2001)
8	Heart failure[f,g]	20	6.25	oral	55	39-64	89.5	60.8-113.1	
9	Heart failure[f,g]	20	12.5	oral	55	39-64	89.5	60.8-113.1	(Tenero et al., 2000)
10	Heart failure[f,g]	20	25	oral	55	39-64	89.5	60.8-113.1	
11	Heart failure[,f,g]	20	50	oral	55	39-64	89.5	60.8-113.1	

[a] The number of patients included in pharmacokinetic analysis of S-carvedilol after iv and oral application were 6 and 7 respectively, [b] Intravenous infusion was given over 1 hour, [c] SEM for age ± 1.3 years and for weight ± 3.2 kg, [d] SEM for age ± 2.4 years and for weight ± 6.9 kg, [e] Dose administered as 0.09 mg/kg but normalized to total dose by multiplying with the average weight of the participants in the clinical trial, [f] 20 patients completed the study (10 patients with NYHA III and 10 with NYHA IV heart failure), [g] The presented values for age and weight are the reported values for the initial study population (n=22)

2.2.6.2.   Paediatric patients with CHF

One clinical PK data set, including 15 pediatric CHF patients and one young adult with known age, gender, height, weight, CYP2D6 genotype, dose, Ross score, and measured systemic drug concentration-time profiles was used (**Table 2-3**) (Behn, 2001). The age of the patients ranged from 43 days to 19.3 years (average: 6.7 years) and they received a 0.09 mg/kg dose of oral R and S-carvedilol. Fifteen of these patients were similar to that included in the previous chapter for model evaluation. The pediatric patients were divided in different age groups i.e., infant (1 month–1 year), young child (2–6 year), children (6–12 year) and adolescents (12–18 year) according to guidelines set by World Health Organization (WHO).

Table 2-3 Characteristics of pediatric data used for model development

No.	Age (years)	Gender	Body Weight (kg)	Dose (mg/kg)	Ross score/ NYHA Class
1	0.12	Female	3.1	0.09	3
2	0.13	Male	4	0.09	6
3	0.15	Male	3.9	0.09	3
4	0.5	Female	5.2	0.09	8
5	0.75	Male	8	0.09	3
6	1.25	Male	10.1	0.09	3
7	1.5	Male	9.5	0.09	10
8	3.5	Female	13.1	0.09	3
9	5.5	Male	20.2	0.09	3
10	7.5	Male	24.3	0.09	5
11	8.25	Male	25.8	0.09	7
12	11.6	Female	34.3	0.09	4
13	11.8	Male	39	0.09	2
14	17.5	Male	56	0.09	NYHA II
15	17.8	Male	61	0.09	NYHA III
16	19.3[a]	Male	98.2	0.09	NYHA III
Mean	6.7		26	-	-
SD	6.72		25.6	-	-

NYHA New York heart association classification of heart failure, *SD* standard deviation
All patients were diagnosed with heart failure and were participants in the same clinical trial (Behn, 2001)

[a] Patient out of the pediatric age range according to guidelines set by World Health Organization (WHO).

2.2.7. Model evaluation

Please refer to **Chapter 1**.

2.3.   Results

2.3.1. Healthy Adults

The model predictions after iv and oral application in healthy adults were in a good agreement with the observed data at all administered dosages of 12.5 mg iv and 6.4—50 mg oral racemic carvedilol (**Figure 2-2, Appendix 8, 9 and 10**). The ratios$_{(Obs/Pred)}$ for AUC$_{0-\infty}$, C$_{max}$ and CL after iv and oral administration of R and S-carvedilol were within 2-fold error range (**Figure 2-3**). After iv administration, the systemic concentration of R-carvedilol was slightly higher than that of S-carvedilol which was evident from a mean R/S AUC$_{0-\infty}$ ratio of 1.2 and 1.4 for observed and predicted data, respectively. An increase in the mean observed and predicted R/S AUC$_{0-\infty}$ ratios was seen after oral administration of carvedilol as it was increased to 2.5 and 2.4 respectively, suggesting that stereo-selective disposition is more pronounced after oral administration.

The visual predictive checks in extensive and poor metabolizers (EM's and PM's) of CYP2D6 show that the model has slightly over-predicted the absorption phase (C$_{max}$) for S-carvedilol but for R-carvedilol, the C$_{max}$ predictions were in agreement with the observed data (**Figure 2-2 and Appendix 11**). The ratios$_{(Obs/Pred)}$ for all the PK-parameters in EM's and PM's of CYP2D6 were within 2-fold error range (**Figure 2-3**). Furthermore, the predicted vs. observed systemic drug concentration plots after iv and oral application of R and S-carvedilol showed that the model has successfully predicted the observed data at high and low systemic drug concentrations (**Figure 2-4**).

The predicted V_{ss} were 1.57 and 1.95 L/kg for R and S-carvedilol, which are in line with reported values (range) of 1.39–3.40 and 1.42–3.84 L/kg respectively. Additionally, the predicted bioavailability of R and S-carvedilol in healthy adults was 0.34 and 0.17 respectively, which is in agreement with the reported absolute bioavailability of these enantiomers (**Table 2-4**).
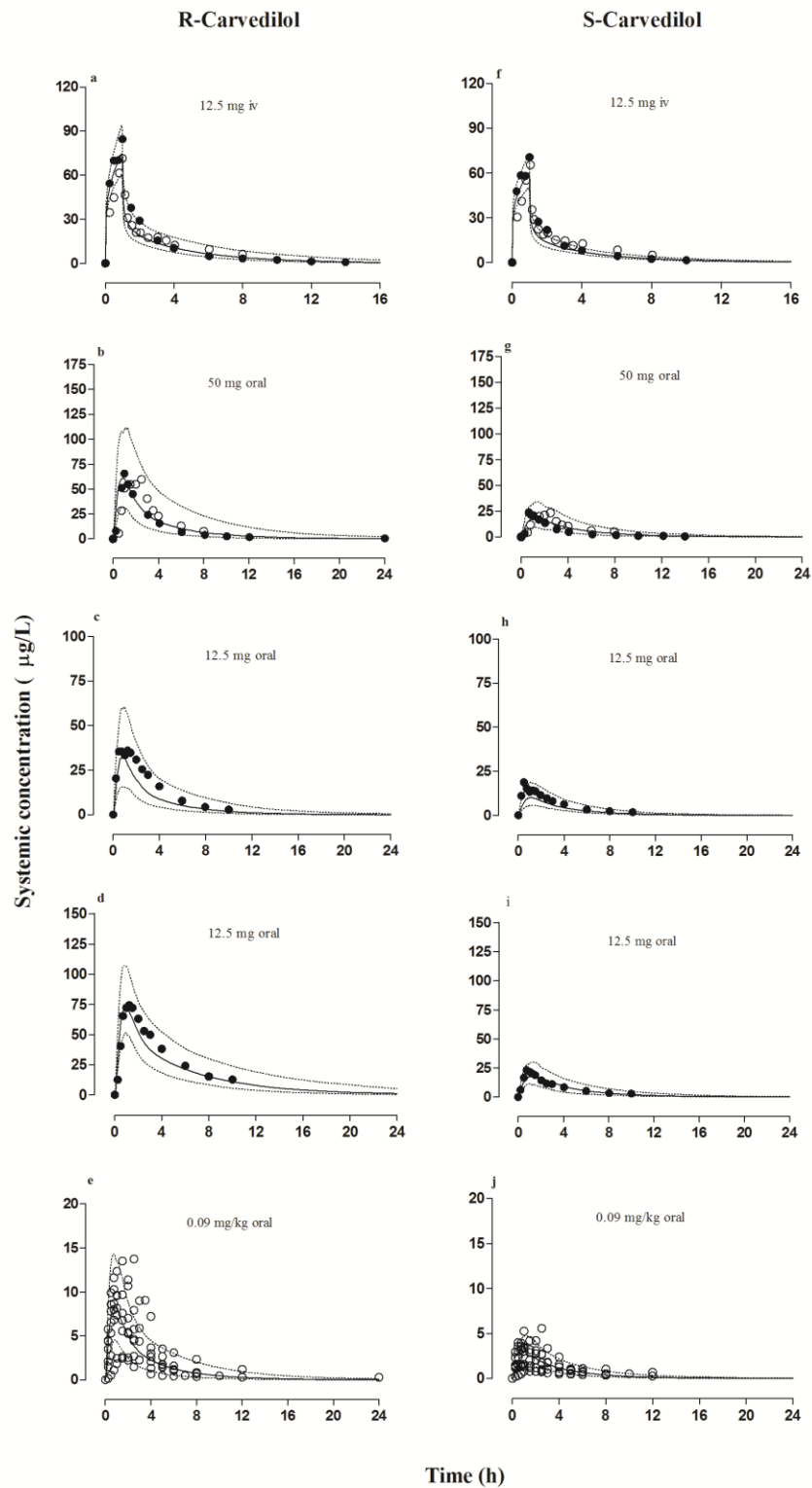
Figure 2-2 Comparison of observed and predicted systemic R and S-carvedilol concentration-time profiles in healthy adults after intravenous or oral drug dosing

Comparison of observed and predicted systemic R and S-carvedilol concentration-time profiles in healthy adults after intravenous or oral drug dosing. *Healthy adults, iv application* (a, f) 12.5 mg, ● (Neugebauer et al., 1990), ○ (Spahn et al., 1990). *Oral application*, (b, g) 50 mg, ● (Neugebauer et al., 1990), ○ (Spahn et al., 1990), 25 mg, (Zhou and Wood, 1995), (c, h) extensive metabolizers, (d, i) poor metabolizers, (E, J) 0.09 mg/kg, n = 7, (Behn, 2001). Prediction results are shown as median (lines), 5th and 95th percentiles (dotted lines), and minimum/maximum (dashed lines). The observed data is shown as filled and empty circles.
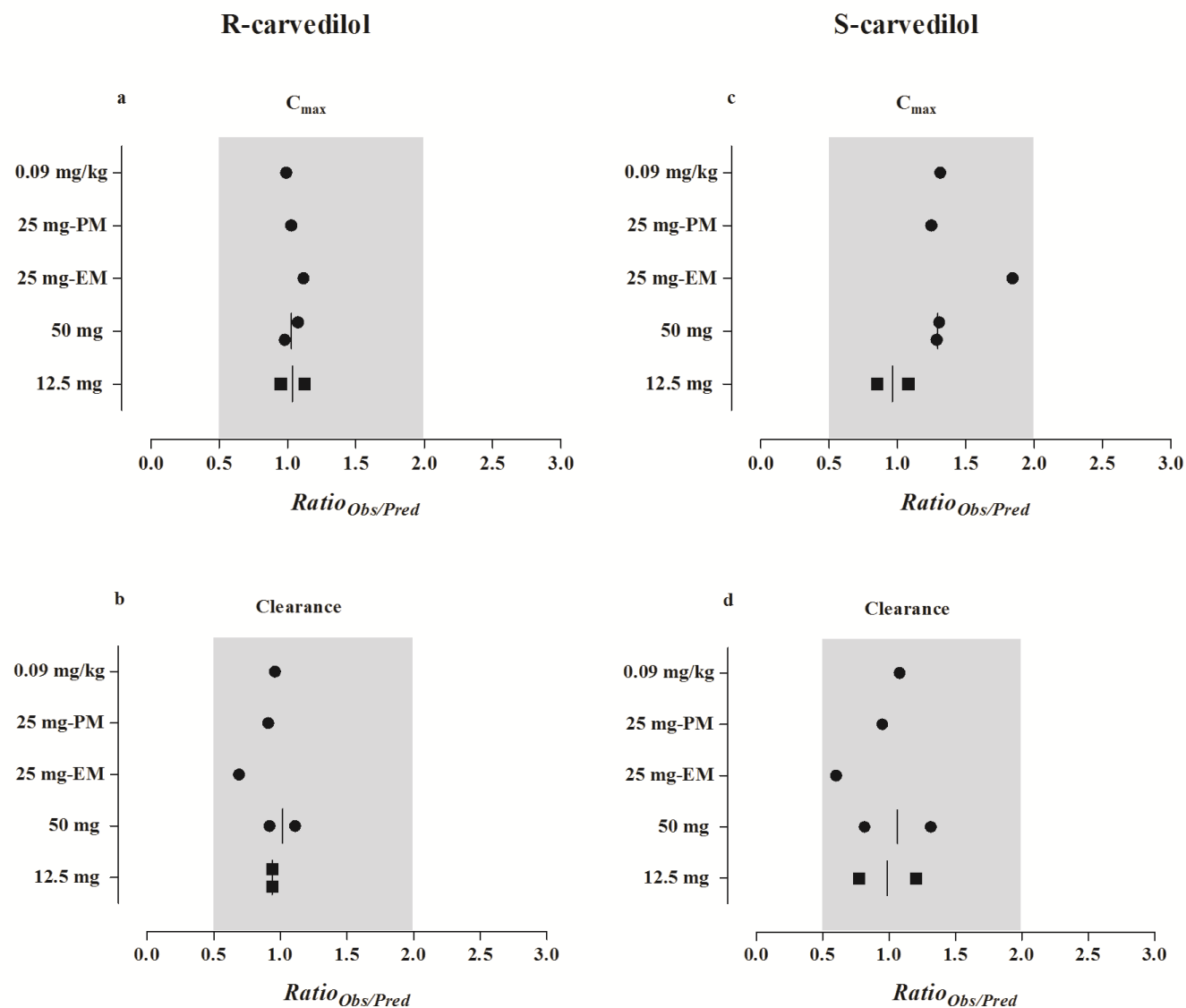
Figure 2-3 Comparison between the observed and predicted values of pharmacokinetic parameters.

Comparison between the observed and predicted values of the maximum concentration (C_{max}), and drug clearance in healthy adults. Results are presented as ratios(observed/predicted) (a, b) R-carvedilol and (c, d) S-carvedilol ● oral application, ■ intravenous application. EM: extensive metabolizers and PM: poor metabolizers. The shadowed gray area indicates a 2-fold error range. When more than one clinical observed data was available at the same dose level, a line was used to show the mean of the ratio(observed/predicted). Clearance is the calculated oral clearance (CL/F) if the dose is given orally.

R-Carvedilol

S-Carvedilol

In healthy adults after iv application

In healthy adults after oral application

In adult CHFpatients after oral application
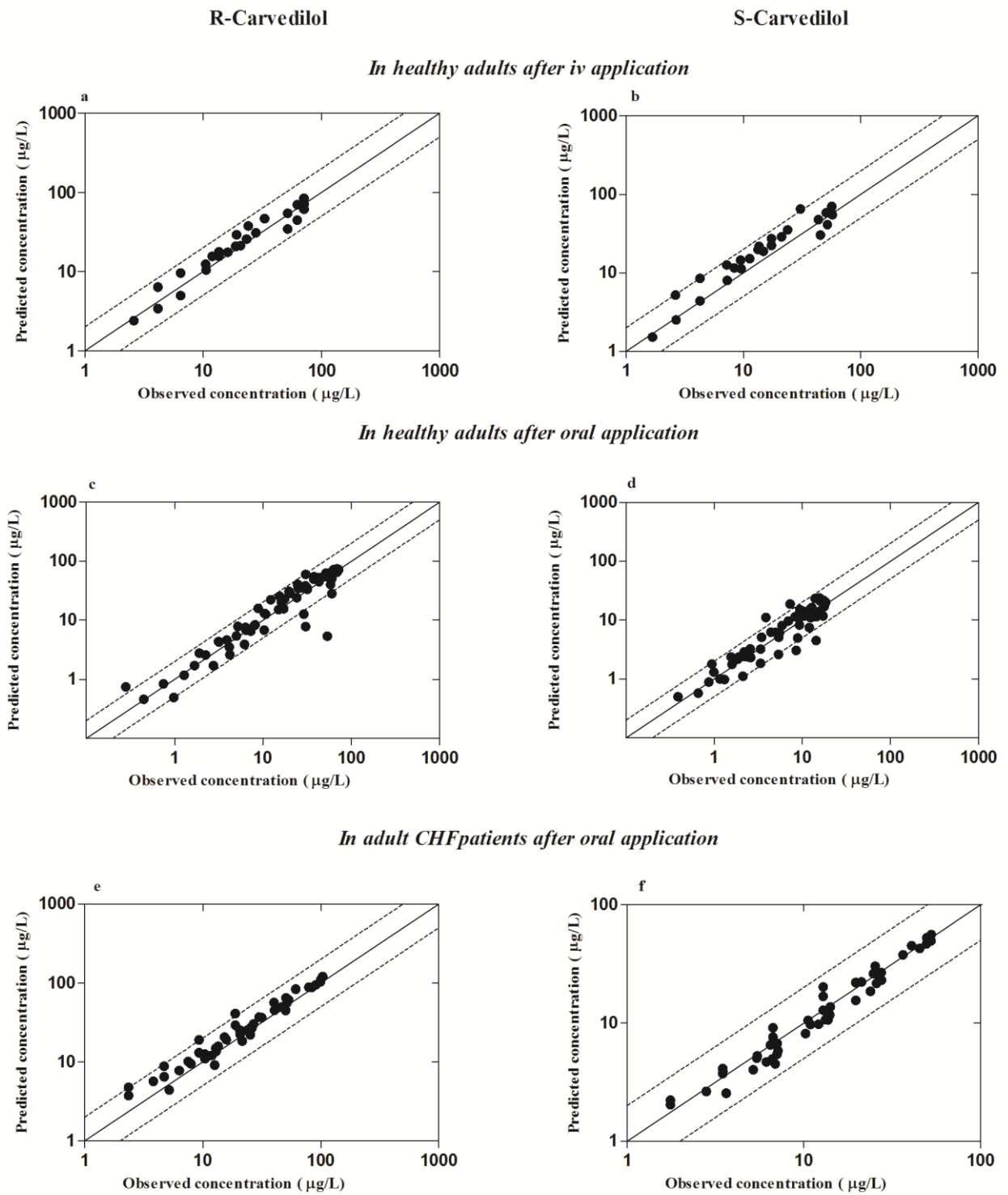
Figure 2-4 Observed vs. predicted concentrations plots in adults.

Observed vs. predicted concentrations plots in healthy adults after intravenous (a, b), oral (c, d) R and S-carvedilol application and in chronic heart failure patients after oral application of R and S-carvedilol (e, f). The solid line indicates line of identity and the dashed line show a 2-fold error range.

Table 2-4 Predicted bioavailability of carvedilol enantiomers in different populations

Simulated population	R-Carvedilol				S-Carvedilol			
	F_g	F_h	f_a	F	F_g	F_h	f_a	F
Healthy adults	0.98	0.35	0.99	0.34	0.96	0.21	0.88	0.17
Extensive metabolizers	0.99	0.35	0.99	0.34	0.96	0.20	0.89	0.17
Poor metabolizers	1.00	0.65	0.99	0.64	0.98	0.34	0.89	0.30
Adults with heart failure	0.97	0.19	0.74	0.14	0.92	0.11	0.55	0.05
Pediatrics with heart failure[a]	0.98	0.42	0.99	0.41	0.96	0.27	0.93	0.23

f_a fraction of drug absorbed, F_g fraction of drug escaping metabolism in the gut, F_h fraction of drug escaping the hepatic metabolism and F is the bioavailability. [a] simulation performed without reducing organ blood flows, number of virtual patients included in predictions; n=100.

2.3.2. Adult CHF patients

The developed adult CHF model was successful in predicting stereo-selective disposition of R and S-carvedilol after administering steady state oral doses of racemic carvedilol (6.25–50 mg) in CHF patients (**Figure 2-5 and Appendix 13**). The mean ratios(Obs/Pred) of the PK parameters for both enantiomers were within 2-fold error range and close to unity. The mean ratios(Obs/Pred) for $AUC_{0-\infty}$ and CL/F were 1.2 and 0.8 for R-carvedilol and 1.1 and 0.9 for S-carvedilol (**Figure 2-6 and Appendix 14**). Moreover, the predicted vs. observed systemic drug concentration plots in CHF showed that the model has successfully predicted steady state systemic concentrations of R and S-carvedilol at all dosage levels (**Figure 2-4**). In adult with CHF, the mean R/S $AUC_{0-\infty}$ ratios were reduced to 1.8 and 1.6 for observed and predicted data, respectively, showing a relative increase in S-carvedilol concentration in CHF patients.

A decrease in predicted bioavailability (F) of both R and S-carvedilol was seen in CHF patients, which was associated with decrease in f_a and F_h. The

predicted f_a, F_h and F in adult CHF patients were reduced to 0.74, 0.19 and 0.14 for

R-carvedilol and to 0.55, 0.11 and 0.05 for S-carvedilol (**Table 2-4**).
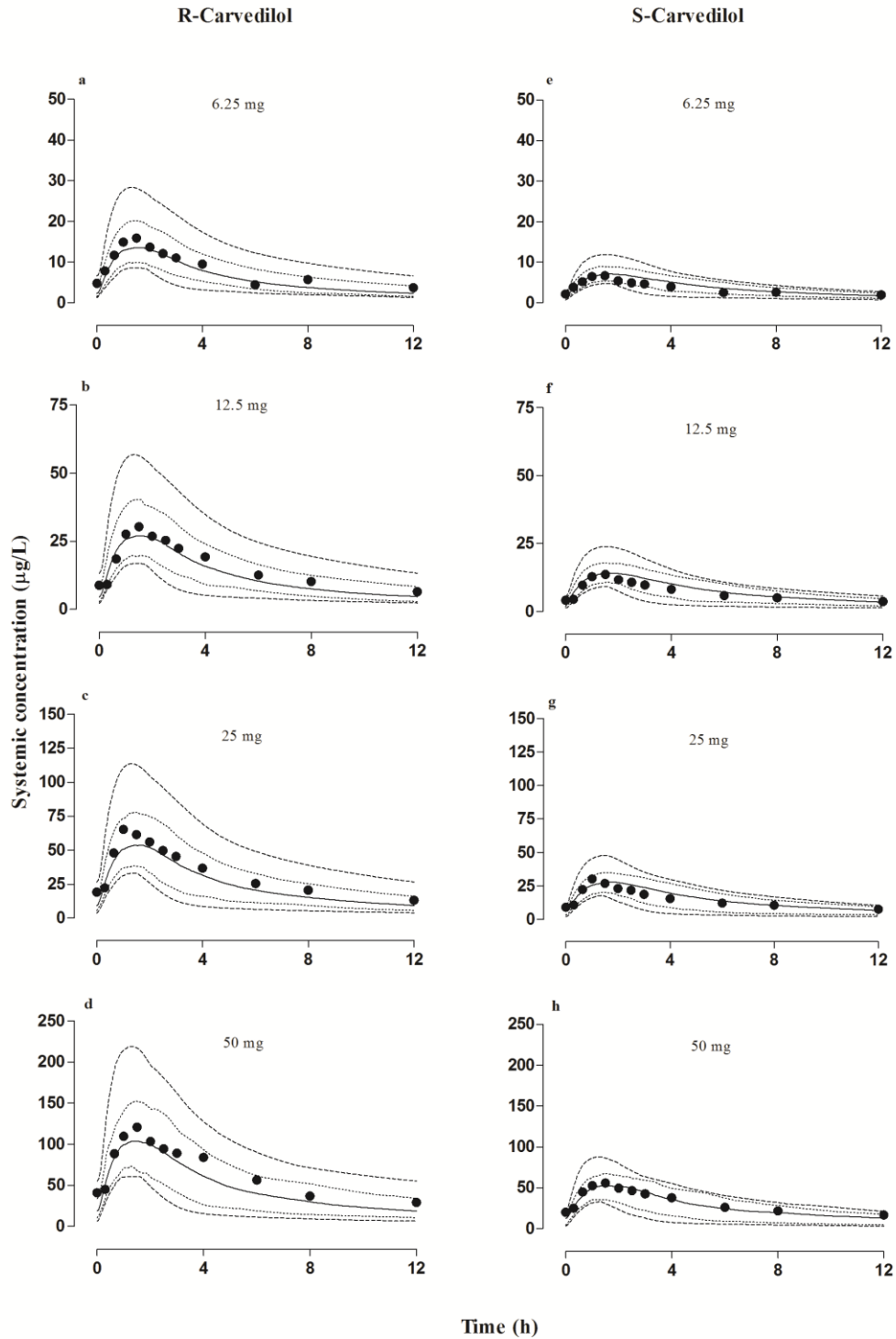
Figure 2-5 Comparison of observed and predicted systemic R and S-carvedilol concentration-time profiles after steady state oral drug dosing in Heart failure patients

Comparison of observed and predicted systemic R and S-carvedilol concentration-time profiles after steady state oral drug dosing in *Heart failure patients:* (a, e) 6.25 mg, (b, f) 12.5 mg, (c, g) 25 mg, and (d, h) 50 mg oral carvedilol. Observed data are shown as dark circles (Tenero et al., 2000). Prediction results are shown as median (lines), 5th and 95th percentiles (dotted lines), and minimum/maximum (dashed lines).
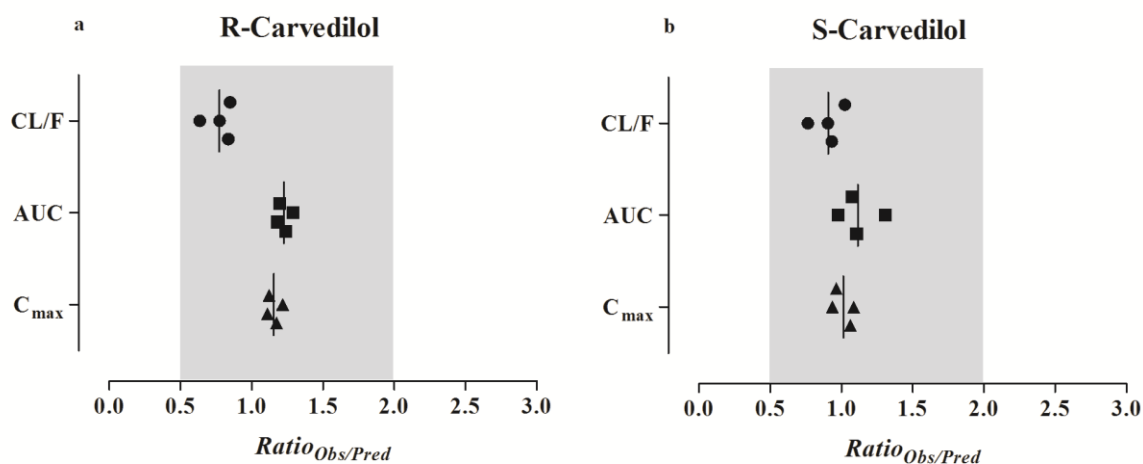
Figure 2-6 Comparison between the observed and predicted values of pharmacokinetic parameters in adult chronic heart failure patients.

Comparison between the observed and predicted values of the area under the plasma concentration-time curve (AUC) ■, the maximum concentration (C_{max}) ▲ , and drug clearance (CL/F) ● in adult heart failure population. Results are presented as mean ratios(observed/predicted) for R-carvedilol (a) and S-carvedilol (b).

2.3.3. Pediatric CHF patients

The systemic concentration-time profiles of R and S-carvedilol after administering an oral dose of 0.09 mg/kg racemic carvedilol in the entire age range (0.12–19.3 years) without incorporating any pathophysiological changes show that the developed model was capable of predicting the age specific changes in systemic concentrations of both enantiomers, since, most of the observed systemic concentration-time were within predicted 5th and 95th percentiles (**Figure 2-7**). Moreover, the age related changes occurring in CL/F of R and S-carvedilol was captured by the model, as the observed values were within the predicted CL/F range, except in two patients with age of 17.5 and 19.3 years, where the observed CL/F was lower than the predicted values (**Figure 2-7**).
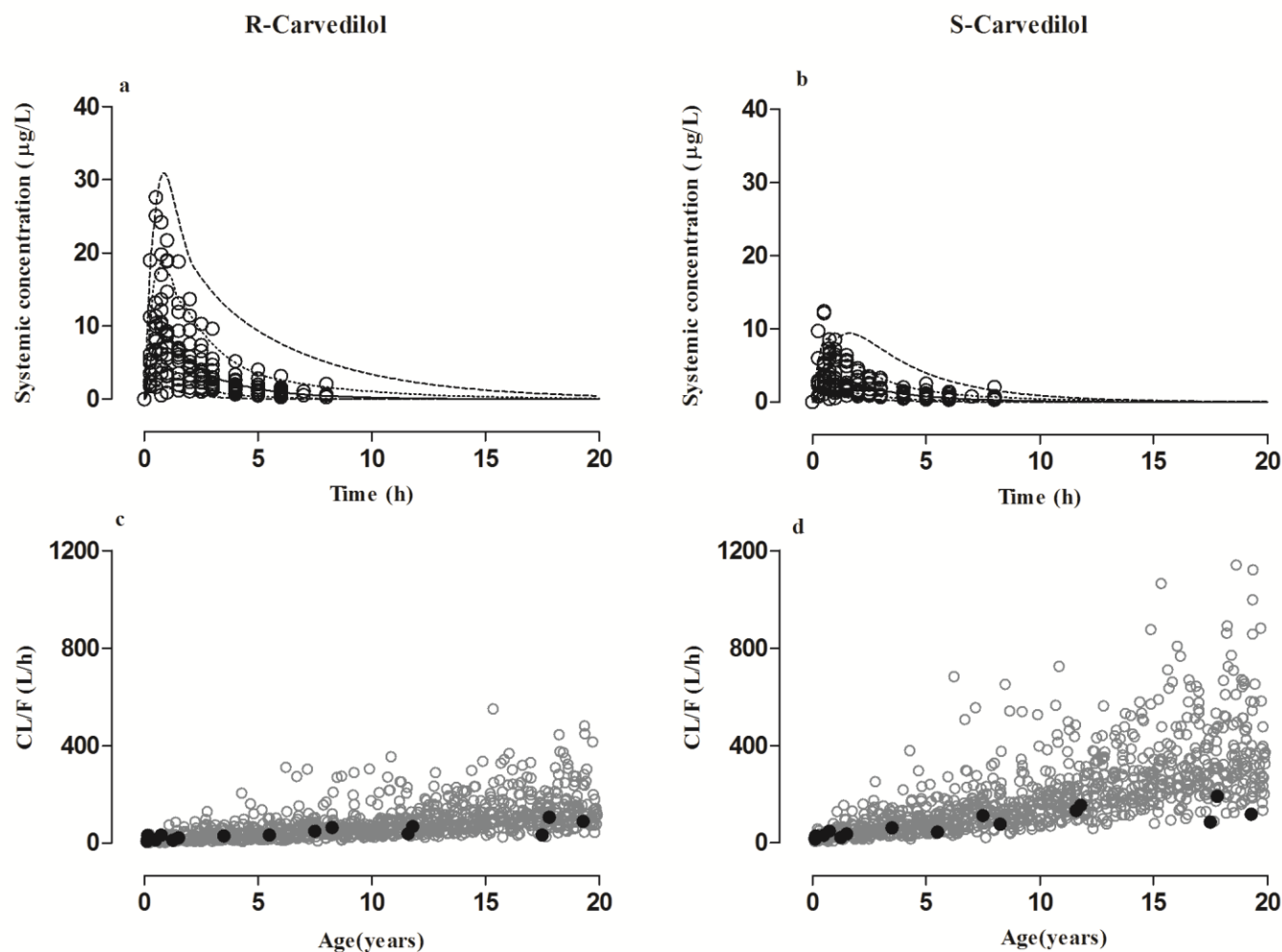
Figure 2-7 Model predictions in the entire pediatric age range.

Model predictions in the entire pediatric age range n=15 (0.12 to 17.8 year) including the young adult n=1 (19.3 year) after administering 0.09 mg/kg R and S-carvedilol, (a, b) systemic concentration-time plots, ○ observed data ― median prediction, ---- minimum and maximum prediction, ⋯ 5th and 95th percentiles and (c, d) Change in oral clearance of R and S-carvedilol with age ○ Predicted CL/F, ● observed CL/F (Behn, 2001). Simulations performed by creating a virtual population of 1000 individuals.

The predicted systemic concentration-time profiles and the ratios$_{(Obs/Pred)}$ of the PK parameters in different pediatric age groups after administering an oral dose of 0.09 mg/kg racemic carvedilol are shown in **Figures 2-8 and 2-9, Appendix 15 and 16)**. The infants, young children and children who were classified with respect to Ross score were better described without incorporating pathophysiological changes in the model, as the AUC$_{0-\infty}$ and CL/F ratios$_{(Obs/Pred)}$ were always within 2-fold error range and the results in these age groups are as follows: In infants, the model has slightly over-predicted systemic concentration of both enantiomers, that can be seen in the ratios$_{(Obs/Pred)}$ for C$_{max}$ and AUC$_{0-\infty}$ which were 0.8 for R-carvedilol and 0.7 for S-carvedilol. The predictions in young children for R-carvedilol were in close agreement with the observed data but the C$_{max}$ for S-carvedilol was over predicted in this age group and the AUC$_{0-\infty}$ ratios$_{(Obs/Pred)}$ for R and S-carvedilol were 1.2 and 1.7 respectively. In children, the predictions for both enantiomers were in agreement with the observed data and the CL/F and C$_{max}$ ratios$_{(Obs/Pred)}$ for R and S carvedilol were, 1.1 and 1.2 respectively. (**Figures 2-8 and 2-9**).
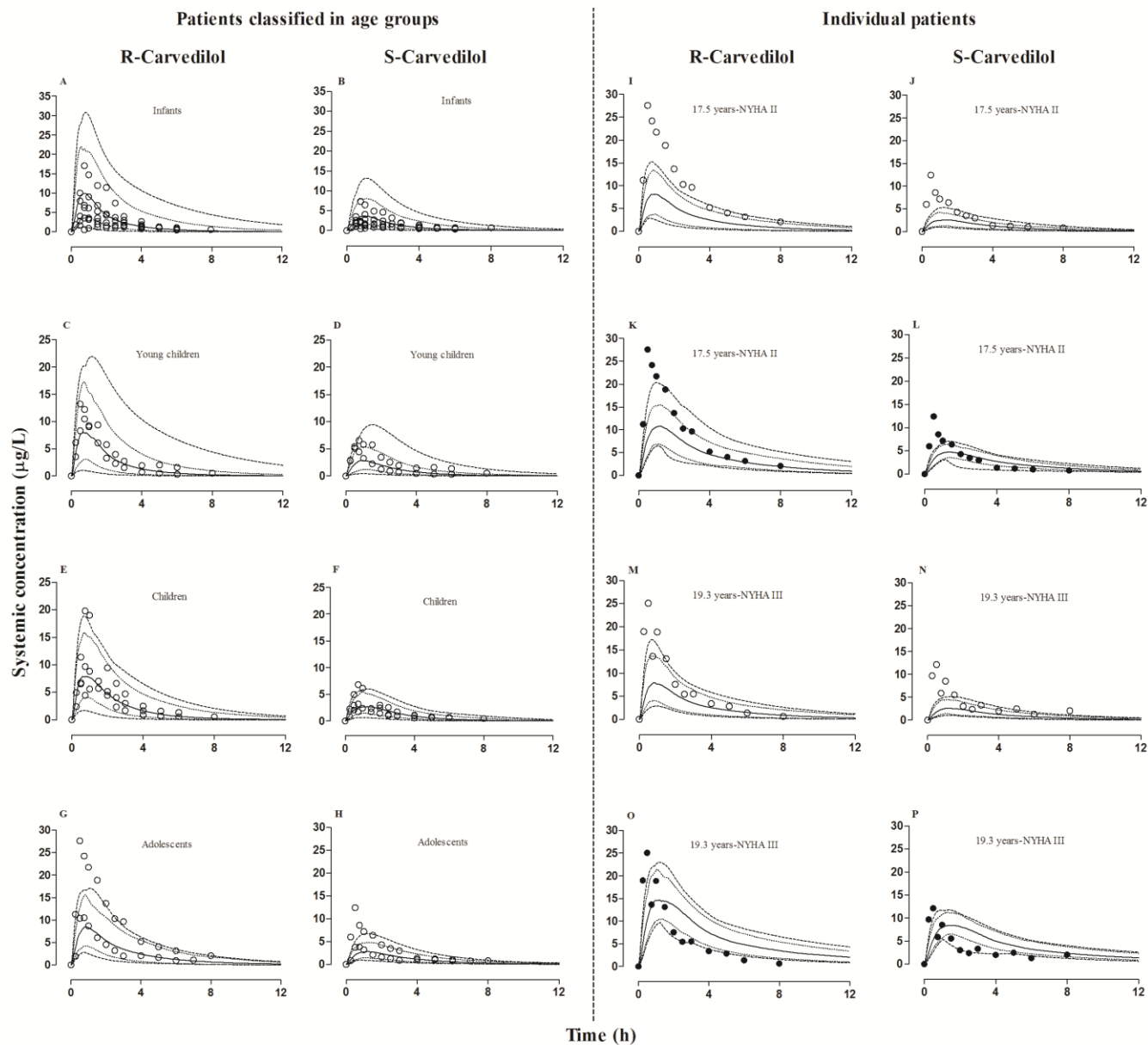
Figure 2-8 Model predictions in different pediatric age groups.

Model predictions in different pediatric age groups for R and S-carvedilol (a, b) infants, (c, d) young children, (e, f) children and (g, h) adolescents. Model predictions in individual patients (i–p) after administering 0.09 mg/kg oral dose of R and S-carvedilol, without (○) and with (●) adjusting the organ blood flows, — median prediction, ---- minimum and maximum prediction, ⋯ 5th and 95th percentiles and ●, ○ observed data (Behn, 2001)

R-Carvedilol

S-Carvedilol
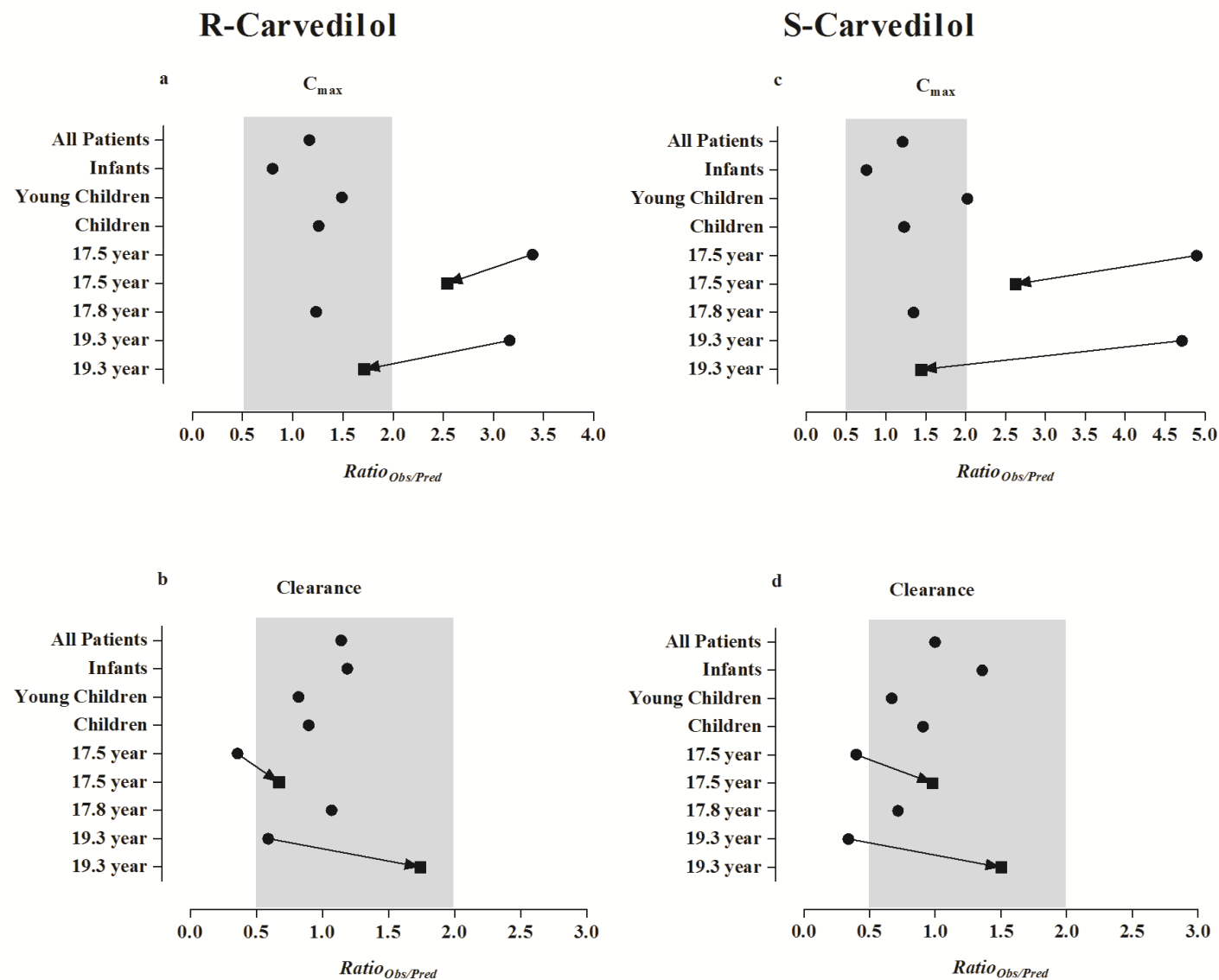
Figure 2-9 Comparison between the observed and predicted values of pharmacokinetic parameters in pediatrics

Comparison between the observed and predicted values of the maximum concentration (C_{max}), and drug clearance (CL/F) in pediatric chronic heart failure patients. Results are presented as individual and ratios(observed/predicted) (a, b) R-carvedilol and (c, d) S-carvedilol ● predictions without organ blood flow reductions and ■ predictions with incorporation of organ blood flow reductions. The arrow head of the line points from ratio(observed/predicted) without reduction in organ blood flow to ratio(observed/predicted) with reduction in organ blood flow in the same patient. The shadowed gray area indicates a 2-fold error range.

Amongst the three patients (2 adolescents and 1 young adult) who were classified as adults, according to NYHA functional classification, two (17.5 and 19.3 years) were better described with incorporation of the pathophysiological changes, as in adults with CHF and are presented individually in the visual predictive checks and comparison of PK parameters (**Figures 2-8 and 2-9**). The 17.5-year-old patient classified as NYHA class II was better described with organ blood flow reductions as the ratios$_{(Obs/Pred)}$ for $AUC_{0-\infty}$ and CL/F without reduction in organ blood flows were outside the 2-fold error range, but with incorporation of adult organ blood flow reductions they were improved and were within 2-fold error range (**Figure 2-9**). The 17.8-year patient classified as NYHA class III was better described without reductions in organ blood flows. The organ blood flow reductions in 19.3-year young adult classified as NYHA class III significantly improved the predictions as the ratios$_{(Obs/Pred)}$ for CL/F and C_{max} without reductions in blood flow were, 0.6 and 3.2 for R-carvedilol and 0.3 and 4.7 for S-carvedilol and were improved to 1.7 for R-carvedilol and 1.5 and 1.4 for S-carvedilol respectively (**Figure 2-9**).

Lastly, the predicted vs. observed systemic drug concentration plots in pediatrics show that with few exceptions, particularly with R-carvedilol, where model has under-predicted the systemic concentrations, in general the model was capable of predicting the individual concentrations of both enantiomers, as most of the concentrations were within 2-fold error range (**Figure 2-10**).
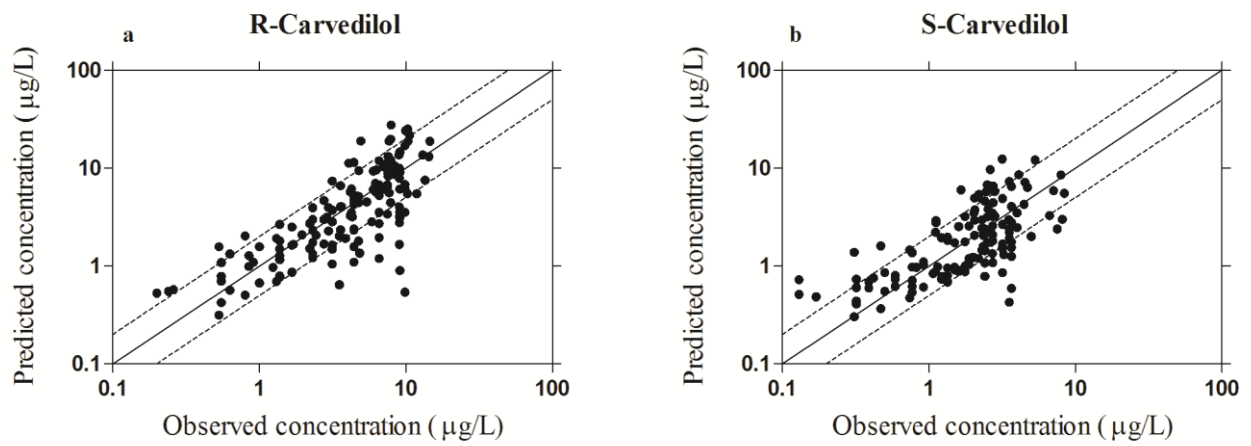
Figure 2-10 Observed vs. predicted concentrations plots in pediatric CHF patients.

Observed vs. predicted concentrations plots in pediatric CHF patients after administering 0.09 mg/kg R and S-carvedilol (a, b). The solid line indicates line of identity and the dashed line show a 2-fold error range.

2.4.   Discussion

In the presented work, the pathophysiological organ blood flow changes occurring in CHF were incorporated into whole body PBPK model to predict stereo-selective disposition of carvedilol in CHF patients. When the developed PBPK model has successfully described PK of R and S-carvedilol in healthy adults and after incorporation of reduced organ blood flows in adult CHF patients, it was scaled to pediatric CHF patients. In contrast to adults, pediatric patients up to 12 years of age were better described without the reductions in organ blood flow, whereas older pediatric patients were better described after incorporating organ blood flow reductions.

The model development was initiated by parameterization of various drug-specific parameters after iv application in healthy adults, which was followed by predictions of R and S-carvedilol after oral administration. The predicted bioavailability of R and S-carvedilol was in very close agreement with the reported absolute bioavailability of these enantiomers (Neugebauer et al., 1990) (**Table 2-4**). The additional success in predicting the disposition of R and S-carvedilol in EM's and PM's of CYP2D6 provided additional confidence in the CYP2D6 CL_{int} values used in the developed model, as this enzyme is the most relevant for the drug metabolism. Moreover, in comparison to R-carvedilol, the slight over-prediction of C_{max} with S-carvedilol highlights the equally important role of other cyp-enzymes involved in its metabolism, as in the developed model only 50 % clearance of S-carvedilol is attributed to CYP2D6 and remaining 30 % to other cyp-enzymes while with R-carvedilol 74 % clearance is associated with CYP2D6 and

remaining 6 % is attributed to other cyp-enzymes. Therefore, suggesting that, in addition to CYP2D6-gentotype, the incorporation of genotype-specific data for other cyp-enzymes involved in clearance of S-carvedilol is equally important for predicting its ADME

The developed model was successful in predicting the ~2-fold difference in *F* of both enantiomers (**Table 2-4**). It was seen that carvedilol undergoes extensive stereo-selective first pass metabolism which is more sensitive towards S-carvedilol. Furthermore, the resulted R/S $AUC_{0-\infty \text{ ratios}}$ suggest that stereo-selective clearance of carvedilol is more distinct after oral administration, since the predicted R/S $AUC_{0-\infty}$ ratio in healthy adults after iv administration was 1.4 and it was increased to 2.4 after oral administration of carvedilol. The predicted R/S $AUC_{0-\infty}$ ratio was decreased to 1.6 in adult CHF patients after administering steady state oral application of carvedilol. This decrease in R/S $AUC_{0-\infty}$ ratio was associated with differences in CL_{int} of both enantiomers, as the reduction of Q_H in CHF resulted in a differential effect on clearance of both enantiomers. Therefore, in CHF compared to R-carvedilol there will be a relative increase in S-carvedilol systemic concentration and hence its $AUC_{0-\infty}$. This relative increase in S-carvedilol exposure is expected to expand with increased severity of disease.

The incorporation of reduced blood flows to liver and kidney in adult CHF patients resulted in decrease CL/F of R and S-carvedilol, because, both carvedilol enantiomers undergo extensive first pass metabolism (Neugebauer et al., 1990), this decrease in CL/F was primarily attributed to reduction in Q_H. The reduced Q_H lead to an increased first-pass metabolism (decrease in F_h) which in turn, resulted

in reduced F of both enantiomers. The decrease in carvedilol CL/F and F was successfully predicted by the developed model in CHF patients (**Figures 2-5, 2-6 and Table 2-4**). Because, the adult patients were having decompensated CHF (NYHA class III and IV) (Tenero et al., 2000) and reduction in CL (~50 %) of various drugs has been reported previously in these patients (Ogawa et al., 2013) which suggests that the incorporated reduced organ blood flows can be correlated with the NYHA functional classification of heart failure. Furthermore, the predicted f_a of both enantiomers was reduced in adult CHF patients (**Table 2-4**), which is consistent with the reports stating reduction in passive drug diffusion due to reduction in Q_{villi} in CHF (Berkowitz et al., 1963; Sica, 2003). Moreover, in CHF, the absorption of drugs with low solubility are more susceptible to changes in intestinal blood flow, therefore, for drug like carvedilol (BCS class II) having low solubility and high permeability, any change in blood flow to intestine can have an impact on its f_a (Ogawa et al., 2014). In the developed model due to absence of any clear information on the intestinal blood flow in relation to severity of CHF, intestinal blood flow was not reduced with severity of CHF, instead reduction in Q_H was used as a surrogate, therefore, to account decrease in Q_{villi} and its impact on absorption of both enantiomers, the Q_{Gut} was reduced in relation to reduction to Q_H.

The pediatric simulations showed that in contrast to the adults, the patients up to 12 years of age, all categorized with Ross scoring system, were better described without the reductions in organ blood flow. On the other hand, one from the two adolescent' patients as well as the young adult patient (17.5 and 19.3 years, all classified according to NYHA classification), were better described

after incorporating organ blood flow reductions. One of the possible reasons for such a difference may be the use of the same organ blood flow reductions in pediatric population as in adults. Since, the incorporated blood flow reductions in pediatrics simulations were based on adult values, it is likely that these values might be close to what is happening in the late adolescence but not be true for young children, as improvement in predictions with incorporation of reduced organ blood flows was only seen in old adolescents (the young adults). Moreover, the pathophysiology of CHF is different between adult and pediatric patients, with congenital heart disease being the main cause of CHF in the vast majority of pediatric patients (Hsu and Pearson, 2009). When compared with adults, children have higher frequency of heart rate (Tanaka et al., 2001; Fleming et al., 2011) and a higher drug CL due to higher percentage of liver weight in relation to body weight (Noda et al., 1997). This can lead to differences in the total impact of these changes on drug CL between both populations. In addition to that, it is not clear if the different grading system that was used is related, in any way, to this finding, as both grading systems are based on different criteria. In order to draw conclusions about the validity of this finding as well as the possible reasons for it, more data is needed specially to confirm if this difference is true. However, the presented findings indicate that the incorporated blood flow reductions in the adult model cannot be directly adopted in pediatrics, at least for the young ones.

The ontogeny of the metabolic cyp-enzymes seems to have a minor impact on the overall disposition of carvedilol enantiomers in the pediatric CHF patients that were included in the model evaluation (Behn, 2001). This is, because, all of these pediatric patients were above one month of age and the two major cyp-

enzymes for carvedilol metabolism (i.e. CYP2D6 and CYP2C9) have a fast ontogeny profile, as they achieve more than ~50 % of adult activity by the age of 0.1 year (Salem et al., 2013). Nevertheless, in the developed model about 20 % of the total assigned metabolism of S-carvedilol is due to cyp-enzymes with slow enzyme-ontogeny and a later maturation time point, i.e. CYP1A2: 10 %, CYP2E1: 5 % and CYP3A4: 5 %. The latter enzymes contribute only to about 4 % in the case of R-carvedilol, i.e. CYP1A2: 2 %, CYP2E1: 1 % and CYP3A4: 1 %. As a result, the impact of the slow maturation of these enzymes will be more profound on the clearance of S- rather than the R-carvedilol. Moreover, if pediatric patients less than one month of age would have been included, the effect of enzyme ontogeny on the predicted drug clearance would have been more pronounced.

The predicted systemic drug concentration profiles for R and S-carvedilol in different pediatric age groups have successfully captured the observed data, with few exceptions, where model has over-predicted the systemic concentrations of R and S-carvedilol, particularly in infants. These over-predictions in infants may be associated with the knowledge gaps with respect to intestinal permeability and perfusion within CHF patients of this age group, as low drug absorption in comparison to adults has been previously reported in pediatric CHF due to congenital heart defects (Nakamura et al., 1994). Since, changes in intestinal morphology, permeability and absorption are affected in adult CHF patients, the possibility of such changes in pediatric CHF patients cannot be completely ruled out (Sica, 2003; Sandek et al., 2007).

The age related changes in CL/F for R and S-carvedilol have been successfully captured by the developed PBPK model (**Figure 2-7**). The observed CL/F values were within the predicted values, except in 17.5 and 19.3 year patients, where the observed CL/F for both enantiomers were low, which can be attributed to reduced blood supply to eliminating organs in these patients as only in these 2 patients, the predicted PK parameters were improved with incorporation of reduced organ blood flows (**Figure 2-9**). Additionally, due to the higher hepatic extraction of S-carvedilol, the impact of reduction in Q_H on its CL/F was more significant when compared to R-carvedilol. However, it seems that the role of reduced organ blood flows becomes important only in adolescent age group who are categorized according to NYHA classification of CHF. Since, the number of participants in the clinical study used for model evaluation in pediatrics was small, therefore, these results cannot be generalized for all the pediatric CHF patients.

Even though in comparison to R-carvedilol, the developed model has slightly over-predicted the S-carvedilol systemic concentration, the ratios$_{(Obs/Pred)}$ for the PK parameters for both enantiomers were within the 2-fold error range. Keeping in view the fact that in disposition of S-carvedilol, contrary to R-carvedilol, CYP2D6 is not the only responsible enzyme, since minor differences were seen in systemic concentrations of S-carvedilol between PM's and EM's of CYP2D6 (Zhou and Wood, 1995). Because, genotype-specific data was only available for CYP2D6 in two clinical studies (Zhou and Wood, 1995; Behn, 2001), the differences seen in observed and predicted values for S-carvedilol highlights the equally important role of other enzymes involved in metabolism of S-carvedilol.

Since, the developed model has successfully predicted the stereo-selective disposition of carvedilol in healthy and diseased populations, it can be linked with the PD data (Blood pressure and heart rate). The incorporation of PD data in the developed model can help in improving safety profile of carvedilol by reducing the adverse drug reactions associated with it, particularly, the ones associated with higher systemic concentrations of R-carvedilol (orthostatic hypotension), that can lead to serious consequences in geriatric population.

2.5. Limitations

Some of the observed pharmacokinetic data used for model evaluation was extracted from the publication figures, as original data was not accessible. In order to identify any error arising from scanning of data from the figures, the calculated values of pharmacokinetic parameters from the scanned and reported data were compared. It was seen that there were no significant differences between the reported and calculated values for different pharmacokinetic parameters that could potentially impair the model evaluation process.

The first two chapters of the thesis were focused on predicting carvedilol ADME in adult and pediatric CHF patients. Because, carvedilol is clinically used for the management of portal hypertension in liver cirrhosis patients and there are no clear dosing recommendations available for its use in patients with different Child-Pugh score (disease severity). Therefore, in the next chapter previously developed PBPK model for carvedilol in chapter 1 will be extrapolated to liver cirrhosis patients for optimizing clinical use of carvedilol in management of portal hypertension..

Chapter 3:

Optimizing the clinical use of carvedilol in liver cirrhosis: a physiologically based pharmacokinetic approach

3.1.   Introduction

Liver cirrhosis is a complex pathophysiological condition that can affect the pharmacokinetics (PK) of many therapeutic agents with a potential to alter the intensity of their desired and undesired effects (Verbeeck, 2008). In liver cirrhosis, both hepatic blood flow (Q_H) and hepatic drug extraction ratio (ER) are reduced, which can lead to impaired metabolism of drugs having high and low hepatic clearance (Morgan and McLean, 1995). The dysfunction of the liver is not merely associated with a reduction in the capacity of the hepatic metabolism and biliary clearance, but is also accompanied with alterations in the production of drug binding proteins (Verbeeck, 2008). As a result, drug dosing in liver cirrhosis patients' needs to be adjusted to the severity of the disease state. The drug regulatory agencies in the US, Food and Drug Administration (FDA), and Europe, the European Medicines Agency (EMA), expect sponsors to conduct pharmacokinetic studies in patients with impaired hepatic function for disease specific dosing recommendations, particularly when the PK of the drug are likely to be affected in this condition (FDA, 2003; EMA, 2005).

In this context, the inherent ability of physiologically based pharmacokinetic (PBPK) models to incorporate the pathophysiological changes that occur in liver cirrhosis make it a very valuable tool. By using a PBPK approach, population specific (system) parameters can be separated from the drug related parameters and the likely impact of the disease-associated changes on the kinetics

of administered drugs can be studied. In fact, reports about the use of PBPK models to predict drug absorption, distribution, metabolism and elimination (ADME) and drug dosing in healthy and diseased populations (liver cirrhosis, renal failure and chronic heart failure, etc.) have been previously published (Edginton and Willmann, 2008; Johnson et al., 2010; Li et al., 2012; Jones et al., 2013; Rasool et al., 2015). Among these are two PBPK-cirrhosis models that were modified with relevant pathophysiological changes with respect to the severity of liver cirrhosis (classified with a Child-Pugh [CP] score A–C) to predict the PK profiles of various drugs (Edginton and Willmann, 2008; Johnson et al., 2010).

The non-selective β-blockers (NSBB) have been successfully used for the treatment of portal hypertension, a condition for which liver cirrhosis is a main cause (Bosch et al., 2008; de Franchis, 2010; Giannelli et al., 2014). Carvedilol is an NSBB with an additional anti-α-1 adrenergic activity and proven efficacy in the management of portal hypertension (Bosch, 2013; Reiberger et al., 2013; Giannelli et al., 2014; Sinagra et al., 2014). However, the clinical benefits that are associated with its use in cirrhosis patients for the management of portal hypertension are overshadowed by the associated reports of adverse drug reactions (ADR's), particularly at higher dosing (i.e. 25 mg/day) (Forrest et al., 1996; Stanley et al., 1999; Hemstreet, 2004). Because carvedilol undergoes an extensive first pass metabolism with a high hepatic extraction, the pathophysiological changes in Q_H and cyp-enzyme expression/activity due to liver cirrhosis can have a profound impact on its disposition (Neugebauer et al., 1987; Neugebauer et al., 1990; Neugebauer and Neubert, 1991; Abdelaziz et al., 2009). Furthermore, carvedilol is a highly protein bound drug and the decrease in blood albumin levels in liver

cirrhosis when compounded with the potential decrease in the metabolic capacity may affect its unbound systemic concentration and hence, its associated pharmacodynamic (PD) effect. As a result, administering similar carvedilol doses in different cirrhosis populations (CP-A–C) may lead to different drug exposures and/or different effects.

Looking in the literature, there are plenty of available PK data for carvedilol in healthy subjects (Neugebauer et al., 1987; Tenero et al., 2000; Behn, 2001; Giessmann et al., 2004). In contrast, there are only limited PK data for carvedilol in liver cirrhosis patients (only CP–C) (Neugebauer et al., 1988). Up to date, there is no report of a PBPK model to predict carvedilol ADME in patients with liver cirrhosis.

3.1.1. Objective

The objective of this study was to develop and evaluate a PBPK-carvedilol-cirrhosis model with the available clinical data in liver cirrhosis CP–C population and to extrapolate the evaluated PBPK model to CP–A and CP–B cirrhosis populations, where no clinical PK data are available. The ultimate aim was to generate data that may substantiate a safer drug therapy by recommending model based drug dosing in liver cirrhosis after exploring the underlying differences in drug disposition as well as drug unbound and total (bound and unbound) exposure with the different disease stages.

3.2.   Methods

3.2.1. Modelling Platform

A whole body PBPK model was developed using the population based PBPK simulator, Simcyp® (version 14 release 1, Simcyp Ltd, Sheffield, UK).

3.2.2. Model Structure

Refer to **chapter 1** for details.

3.2.3. Modeling strategy, simulation conditions, and drug-specific parameters

The PBPK model presented here is a modified and extended version of the model developed and evaluated previously in healthy adults (Rasool et al., 2015); however, after modifications with regard to the assigned clearance due to glucuronidation. In the previous report (Rasool et al., 2015), clearance due to glucuronidation was assigned collectively as 20% of the total drug clearance that was calculated using the retrograde model of enzyme kinetics within Simcyp®. There are, however, reports stating the involvement of UGT1A1, UGT2B4 and UGT2B7 enzymes in the glucuronidation of carvedilol (Ohno et al., 2004; Takekuma et al., 2012), along with their relative contributions (Takekuma et al., 2012). Therefore, in this model, the previously assigned intrinsic clearance due to glucuronidation was divided by the respective contributions of UGT-enzymes (Takekuma et al., 2012) and then by their abundances in the liver to get individual intrinsic clearance values (CL_{int}) for each enzyme. The calculated UGT-CL_{int} values were refined by using the parameter estimation (PE) module within Simcyp® utilizing the iv plasma concentration vs. time data in healthy adults as a reference

(Neugebauer et al., 1988). This modified model was then further evaluated in healthy adults after oral application. The final list of drug-specific parameters is presented in **Table 3-1**.

Table 3-1 Drug-specific parameters incorporated in the developed PBPK model

Parameter	Value/Model	Reference
Molecular weight (g/mol)	406.47	PubChem.
Log$P_{o:w}$	4.19	PubChem.
pKa	7.97	(Caron et al., 1999)
Absorption		
Model	ADAM	
$P_{eff,man}$ (cm/s)	1.94×10^{-4}	(Bachmakov et al., 2006)
		Predicted after calibrating with metoprolol and propranolol using Simcyp®
Distribution		
Model	Full PBPK	
Prediction method	Poulin and Theil method with the Bierezhkovskiy correction	
Blood to plasma (B:P) ratio	0.69	(Fujimaki et al., 1990)
fu_P	0.0054	(Fujimaki et al., 1990)
Elimination		
CL_{iv} (L/h)	38	(von Mollendorff et al., 1987)
CYP2D6 CL_{int} (µL/min/mg/pmol of isoform)[a]	339.7	
CYP1A2 CL_{int} (µL/min/mg/pmol of isoform)[a]	8.71	
CYP2C9 CL_{int} (µL/min/mg/pmol of isoform)[a]	3.1	[a]Simcyp® retrograde model of enzyme kinetics
CYP2E1 CL_{int} (µL/min/mg/pmol of isoform)[a]	3.71	
UGT1A1 CL_{int} (µL/min/mg/pmol of isoform)[b]	4.04	
UGT2B4 CL_{int} (µL/min/mg/pmol of isoform)[b]	3.43	[b]Simcyp® parameter estimation module, (Takekuma et al., 2012)
UGT2B7 CL_{int} (µL/min/mg/pmol of isoform)[b]	5.75	
CL_R (L/h)	0.25	(Gehr et al., 1999)

LogP$_{o:w}$ octonal-water partition coefficient, fu$_P$ fraction of unbound drug in plasma, pK$_a$ acid dissociation constant, ADAM Advanced, Dissolution, Absorption and Metabolism, CL$_{iv}$ intravenous clearance, CL$_R$ renal clearance, CL$_{int}$ intrinsic clearance

In order to run simulations in cirrhotic patients, some of the system parameters were modified according to the reported changes in liver cirrhosis (see "System parameters" for details). Simulations in liver cirrhosis population were performed after iv and oral application of carvedilol using the Simcyp® CP –C population and were compared to available experimental data. Only when the developed PBPK model was able to predict carvedilol ADME in liver cirrhosis CP–C population, simulations were extended to cirrhosis CP–A and CP–B populations were no experimental data are available. At this stage, the developed PBPK model was used to predict carvedilol unbound and total (bound and unbound) AUC's in healthy and cirrhosis populations (CP-A–C) in order to explore the need of dose adjustments. The simulations in healthy and cirrhosis populations were performed by creating a virtual population of 100 subjects for every clinical data set with the same age range (same in healthy adults but in cirrhosis patients the age range for created virtual population was 40–70 years), proportion of females and fluid intake as in the reference clinical study (**Table 3-2**). An overview of the workflow for the development of this PBPK-carvedilol-cirrhosis model is shown in **Figure 3-1**.

3.2.4. System parameters

The "Sim-Healthy Volunteer" population library in Simcyp® was used for simulating carvedilol ADME in healthy volunteers, whereas "Sim-Cirrhosis-CP (A, B, or C)" population libraries were used for simulating carvedilol PK in liver cirrhosis patients as categorized with respect to CP score. The "Sim-Healthy Volunteer" population library comprises of demographic, genetic, anatomical and

physiological parameters obtained from an extensive literature search (Simcyp®

version 14 release 1). The "Sim-Cirrhosis-CP (A–C)" population libraries categorize

the cirrhosis patients based on the disease severity based on the CP scoring system

into CP–A (well compensated disease), CP–B (significant functional compromise),

or CP–C (decompensated disease) (Pugh et al., 1973). These population libraries

incorporate demographic and physiological information specific to liver cirrhosis

that were reported previously (Johnson et al., 2010), such as changes in liver

weight, CYP-enzyme expression/activity, cardiac output, liver blood flow,

intestinal blood flow, renal function, hematocrit and plasma protein

concentrations (data summarized in Fig. 2). These factors can influence carvedilol

PK, for example, equation 4, implemented in simcyp® shows how changes in the

concentration of plasma albumin can affect the unbound fraction of carvedilol in

cirrhosis patients,

$$fu_{cirr} = \frac{1}{1+\left[\frac{[P]_{cirr}}{[P]_{HV*}} \times \frac{(1-fu_{HV*})}{fu_{HV*}}\right]} \quad (4)$$

Where, Cirr is cirrhosis, P is for plasma protein (albumin) and HV* is the typical

value in a healthy subject (25 years old).
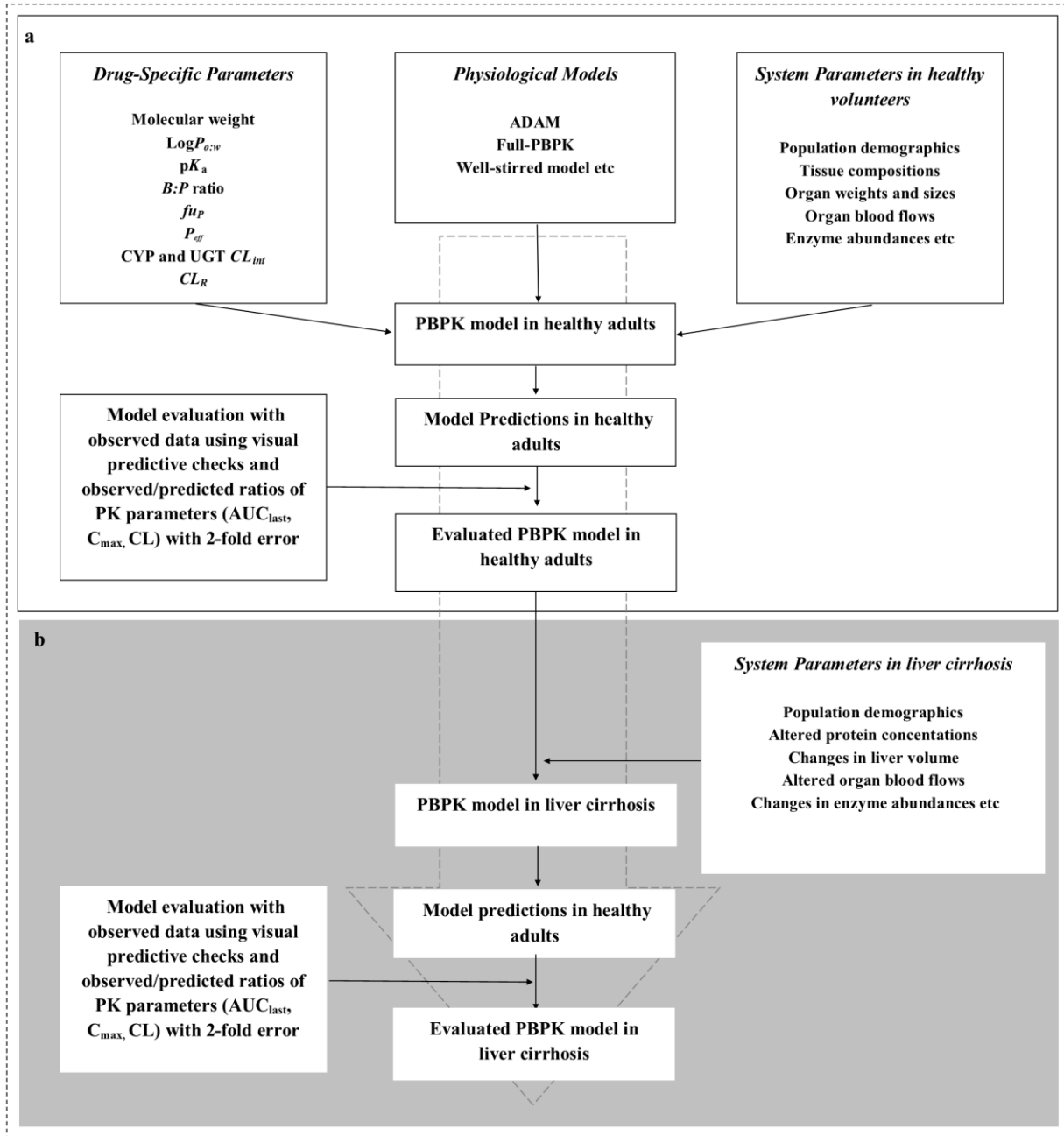
Figure 3-1 Schematic workflow for the development of PBPK model of carvedilol in cirrhosis population.

white area (a) healthy adults and grey area (b) liver cirrhosis patients. $LogP_{o:w}$= octonal-water partition coefficient, pK_a= acid dissociation constant, $B:P$= blood to plasma, fu_P= fraction of unbound drug in plasma, $P_{eff,man}$= human jejunum permeability, CL_{int}= intrinsic clearance, CL_R= renal clearance, $ADAM$= Advanced Dissolution Absorption and Metabolism Model.
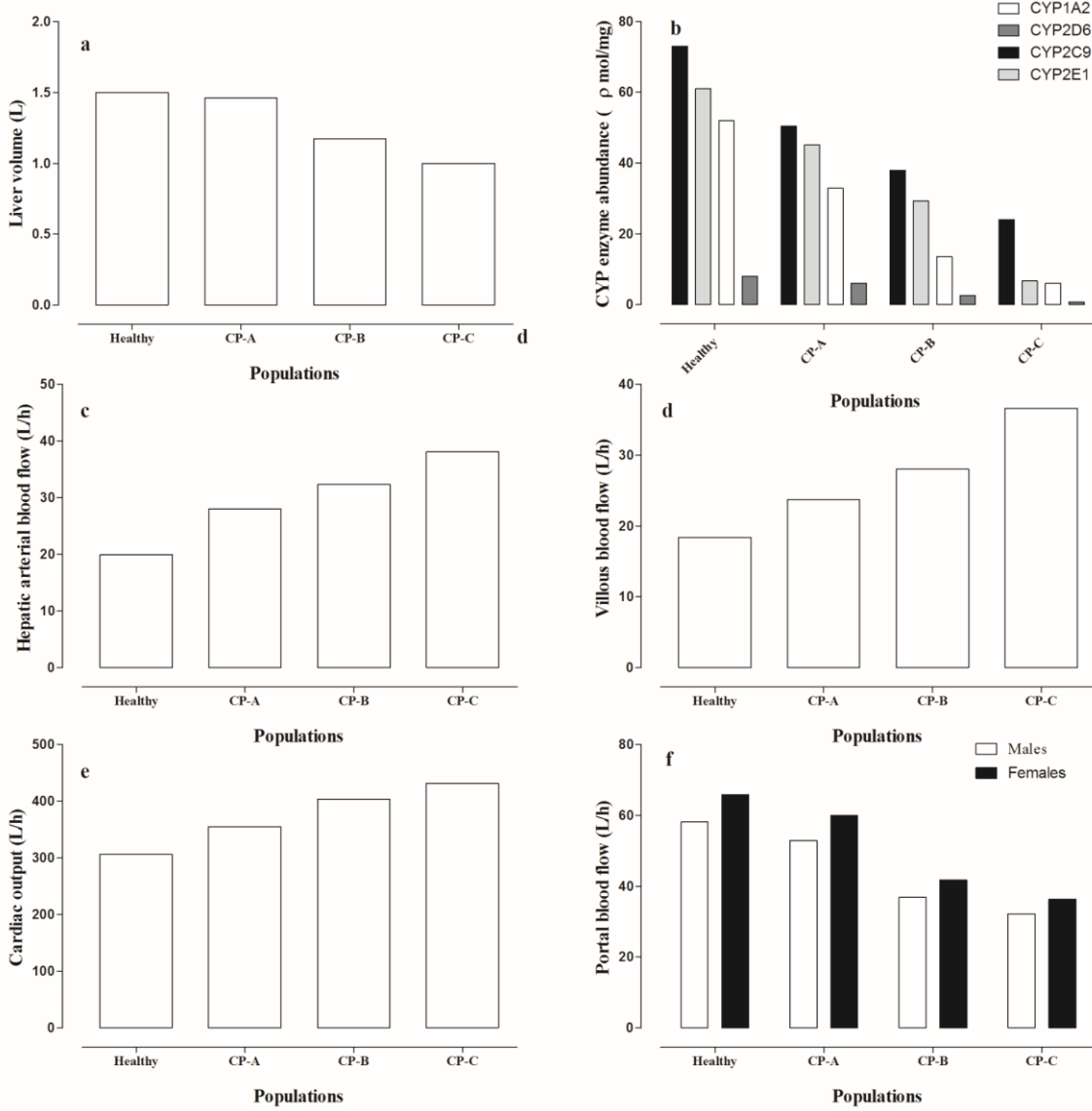
Figure3-2A Pathophysiological changes in different cirrhosis populations.

(a) Liver volume (b) CYP-enzyme abundance (c) Hepatic arterial blood flow (d) Villous blood flow (e) Cardiac output (f) Portal blood flow. *CP-A–C*: Child-Pugh class A–C. Presented data were extracted from Johnson et al (Johnson et al., 2010) and Simcyp® version 14 release 1.
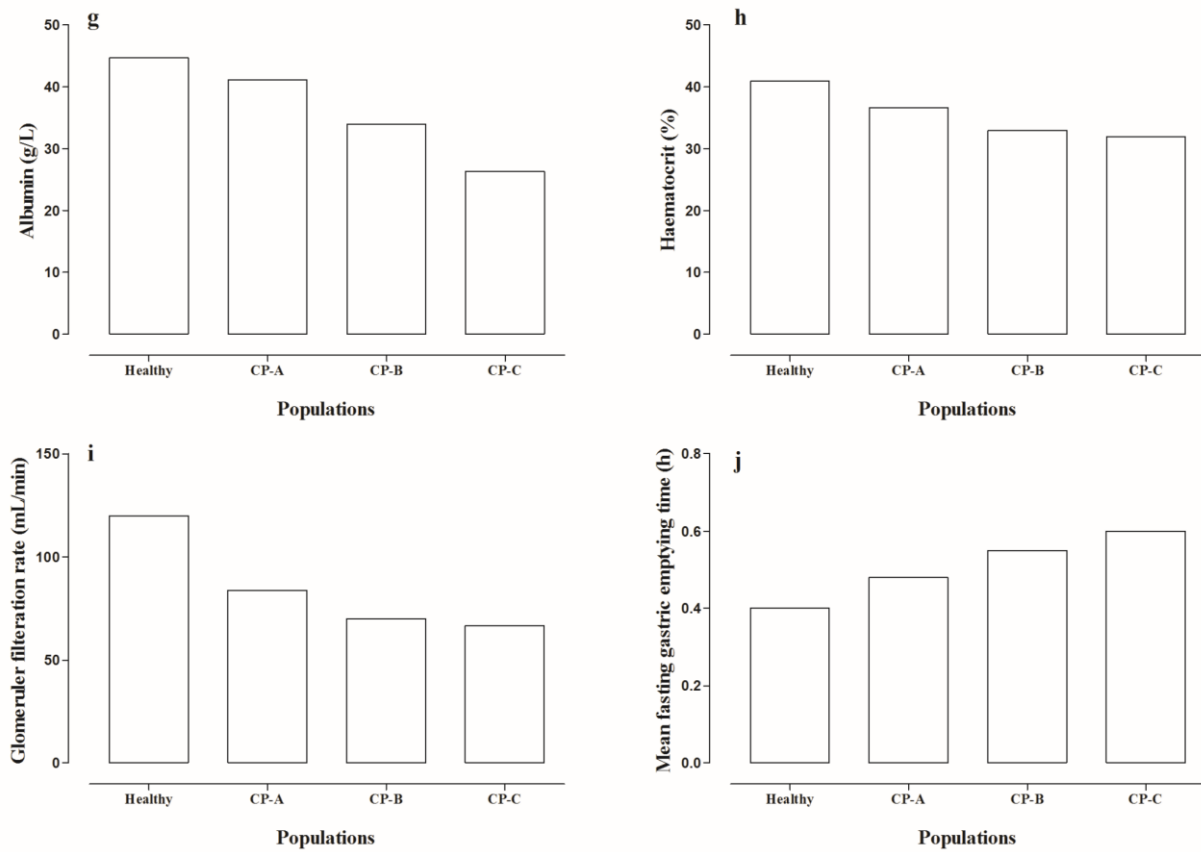
Figure3-2B Pathophysiological changes in different cirrhosis populations.

(g) Albumin (h) Haematocrit (i) Glomerular filtration rate and (j) Mean fasting gastric emptying time. *CP-A–C*: Child-Pugh class A–C. Presented data were extracted from Johnson et al (Johnson et al., 2010) and Simcyp® version 14 release 1.

3.2.5. Clinical data

Pharmacokinetic data in healthy volunteers and liver cirrhosis patients after iv and oral administration of carvedilol (Neugebauer et al., 1988) were extracted using the digitizer tool in the software OriginPro® version 9.0 (OriginLab. Northampton, MA). The reference clinical study provided four median systemic drug concentration vs. time profiles (2 in healthy adults and 2 in cirrhosis patients) after administering 12.5 mg iv infusion and 25 mg of oral carvedilol (**Table 3-2**). In short, twenty healthy adults included in the reference study served as historical controls and received the same dose under similar conditions as the cirrhosis patients (Neugebauer et al., 1988). Six liver cirrhosis patients (5 males and 1 female) included in this study were diagnosed by a decreased serum cholinesterase (less than 1800 U/L) and Quick test vales (less than 70%). The cirrhosis patients included in this study were not stratified by the authors with respect to CP score; therefore, on the basis of the available information, the decreased serum cholinesterase levels (less than 1800U/L) served as a surrogate for categorizing these patients into CP–C class (Meng et al., 2013).

3.2.6. Model evaluation

Refer to **Chapter 1** for details.

Table 3-2 Characteristics of the clinical data used in model development

No.	Population	Nr. of subjects	Dose (mg)	Route	Age (years) (Range)	Proportion of females	Body weight (kg) (Range)	Height (cm) (Range)	Reference
1	Healthy	20	12.5	iv infusion[a]	19-45	0	60-92	160-197	(Neugebauer et al., 1988)
2	Cirrhosis-CP–C[b]	6	12.5	iv infusion[a]	40-76	0.16	65.5-96	163-174	(Neugebauer et al., 1988)
3	Healthy[c]	20	25	oral	19-45	0	60-92	160-197	(Neugebauer et al., 1988)
4	Cirrhosis-CP–C	6	25	oral	40-76	0.16	65.5-96	163-174	(Neugebauer et al., 1988)

CP–C: Child-Pugh class C

[a] Intravenous infusion was given over 1 hour

[b] only 5 subjects were included in PK analysis

[c] only 19 subjects were included in PK analysis

3.3.   Results

3.3.1. Model evaluation in healthy adults

The here presented PBPK model was first checked for the ability to reflect carvedilol PK behavior in healthy adults before extending it to liver cirrhosis. **Figure 3-3 and Appendix 17** shows the median observed and predicted systemic drug concentration-time profiles after iv and oral drug application in healthy adults for a visual check. As can be seen in **Figure 3-3**, there is a good agreement between the observed and predicted systemic carvedilol concentration-time profiles indicating that the drug ADME were well captured by the model. This was further supported by the predicted V_{ss} and k_e values, as the observed and predicted values for V_{ss} were 1.4 L/kg and 1.6 L/kg and for k_e were 0.2 1/h and 0.18 1/h after iv drug iv application, respectively. In addition, the ratios$_{(Obs/Pred)}$ for the calculated $AUC_{0-\infty}$, C_{max}, and CL matched well and were all within a 1.5-fold range (**Table 3-3**). For example, the predicted iv and oral carvedilol clearance values were 35 L/h and 150 L/h, which were very close to the observed values of 36 L/h and 174 L/h, respectively. Finally, the drug absolute bioavailability (F) after oral administration of carvedilol was also well predicted when compared to the observed value (23% vs. of 21%, see **Figure 3-4**).
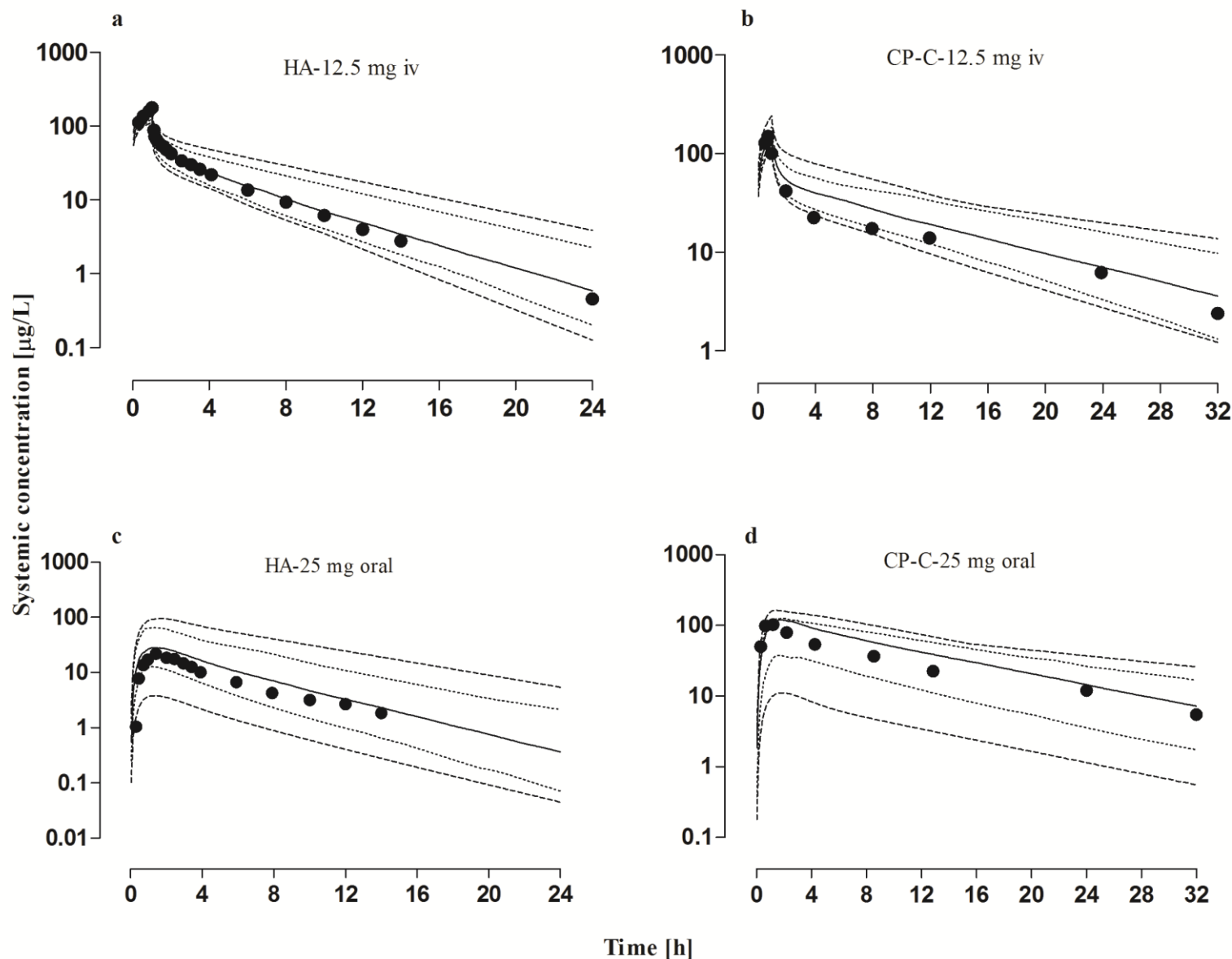
Figure 3-3 Visual predictive checks of the observed and predicted carvedilol systemic concentration-time profiles in healthy adults and liver cirrhosis Child Pugh Class C patients.

(a) *Healthy adults*, 12.5 mg iv infusion (b) *Liver cirrhosis patients,* 12.5 mg iv infusion; (c) *Healthy adults,* 25 mg oral; (d) *Liver cirrhosis patients,* 25 mg oral. Observed data (solid circles) are median measured concentration of the study population (Neugebauer et al., 1988). Prediction results are shown as median (lines), 5th and 95th percentiles (dotted lines), and minimum/maximum (dashed lines).

Table 3-3 Comparison of median observed and predicted pharmacokinetic parameters along with their ratio$_{(Obs/Pred)}$ in healthy and cirrhosis populations after iv and oral administration of carvedilol

PK-parameter	Healthy adults			Liver cirrhosis		
	Observed	Predicted	ratio$_{(Obs/Pred)}$	Observed	Predicted	ratio$_{(Obs/Pred)}$
Intravenous application						
C_{max} (µg/L)	177.50	149.54	1.19	149.22	151.59	0.98
$AUC_{0-\infty}$ (µg.h/L)	342.06	354.15	0.97	556.48	726.48	0.77
Oral application						
C_{max} (µg/L)	21.90	28.23	0.78	103.32	117.42	0.88
$AUC_{0-\infty}$ (µg.h/L)	167	163.8	1.02	981.66	1278.35	0.77

$AUC_{0-\infty}$; area under the systemic drug concentration-time curve from time zero to infinity, C_{max}; the maximum concentration. n=20 for healthy adults and n=6 for cirrhosis patients (Neugebauer et al., 1988).

.
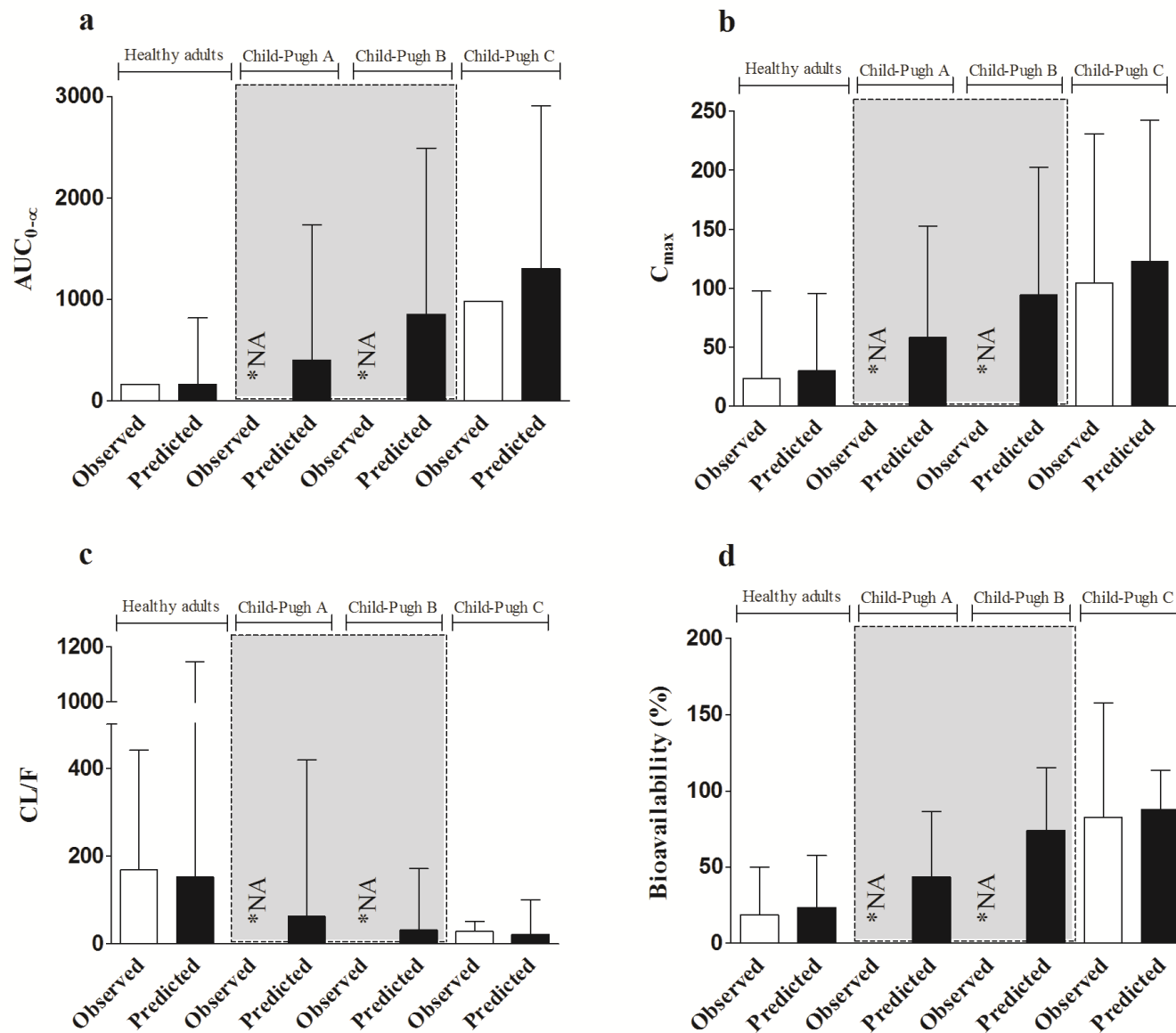
Figure 3-4 Comparison between the observed and predicted values of pharmacokinetic parameters.

(a) the area under the plasma concentration-time curve ($AUC_{0-\infty}$), (b) the maximum concentration (C_{max}), (c) the oral drug clearance (CL/F), and (d) the absolute bioavailability. The columns represent the median values of a parameter (white for observed data and black for predicted data), the bars represent the upper limit of the range (where available), while the shadowed gray area indicate the median predicted values of the pharmacokinetic parameter in CP-A and B populations (Neugebauer et al., 1988). HA= healthy adult; *CP-A*= Child-Pugh Class A; *CP-B*= Child-Pugh Class B; and *CP-C*= Child-Pugh Class C and *NA*= where no observed clinical data is available.

3.3.2. Model evaluation in cirrhosis CP–C patients

After incorporating the main physiological changes that accompany liver cirrhosis in a disease modified model, model predictions were compared with experimental PK data obtained from decompensated liver cirrhosis CP–C patients (**Figure 3-3**). The visual predictive checks showed that all the observed systemic drug concentration-time points were within the maximum and minimum prediction range indicating that the presented model has also successfully captured carvedilol PK in these patients after oral and iv drug application. The increase in V_{ss} and the decrease in k_e in cirrhosis population CP–C when compared with healthy subjects were also well predicted by the model. Whereas the observed and predicted values of V_{ss} in cirrhosis patients after administering iv carvedilol were increased from 1.4 L/kg and 1.6 L/kg in healthy subjects to 3.1 L/kg and 2.5 L/kg respectively, the observed and predicted values for k_e were decreased from 0.2 1/h and 0.18 1/h to 0.08 1/h and 0.08 1/h, respectively.

In addition, the model predictions captured the ~4-fold increase in C_{max}, the ~3-fold increase in F, ~6-fold increase in $AUC_{0-\infty}$ and the ~8-fold decrease in CL/F between observed healthy and cirrhosis CP–C population after oral drug application. The predicted increase in F from 23% to 88% was comparable with the increase in observed F from 24% to 88% (**Figure 3-4**). Finally, the calculated ratios$_{(Obs/Pred)}$ of the main PK parameters of interest is presented in **Table 3-3**. These results confirm again that the modified model was able to capture the drug disposition in patients also, and therefore, is a strong basis to perform simulations of drug application to CP–A and CP–B diseased populations.

3.3.3. Model simulations in virtual cirrhosis CP–A and B patients

In liver cirrhosis populations CP–A and CP–B, no clinical PK data were available, and therefore, model simulations were intended to fill some of the information gap. First, a comparative analysis of $AUC_{0-\infty}$, C_{max}, CL, and F in these cirrhosis populations when compared to healthy and CP-C patients was presented in **Figure 3-4**. Here, a periodic increase was seen in predicted values of $AUC_{0-\infty}$, C_{max} and F between CP–A to CP–C populations. Second, the fractional contribution of the metabolizing enzymes in the cirrhosis populations was investigated (**Figure 3-5**). The results showed changes in the predicted percentage contribution of CYP and UGT contributions to the overall carvedilol clearance between healthy and cirrhosis populations. Whereas the CYP enzymes were dominating the overall drug clearance in healthy adults by 76%, their contribution decreased to 72% in CP–A, to 56% in CP–B, and to 32% in CP–C populations. In contrast, UGT-enzyme contributions gradually raised from 23% in healthy adults to 66 % in cirrhosis (CP–C) population. This finding can have important implications, particularly in the investigations of drug-drug interactions (DDI's).
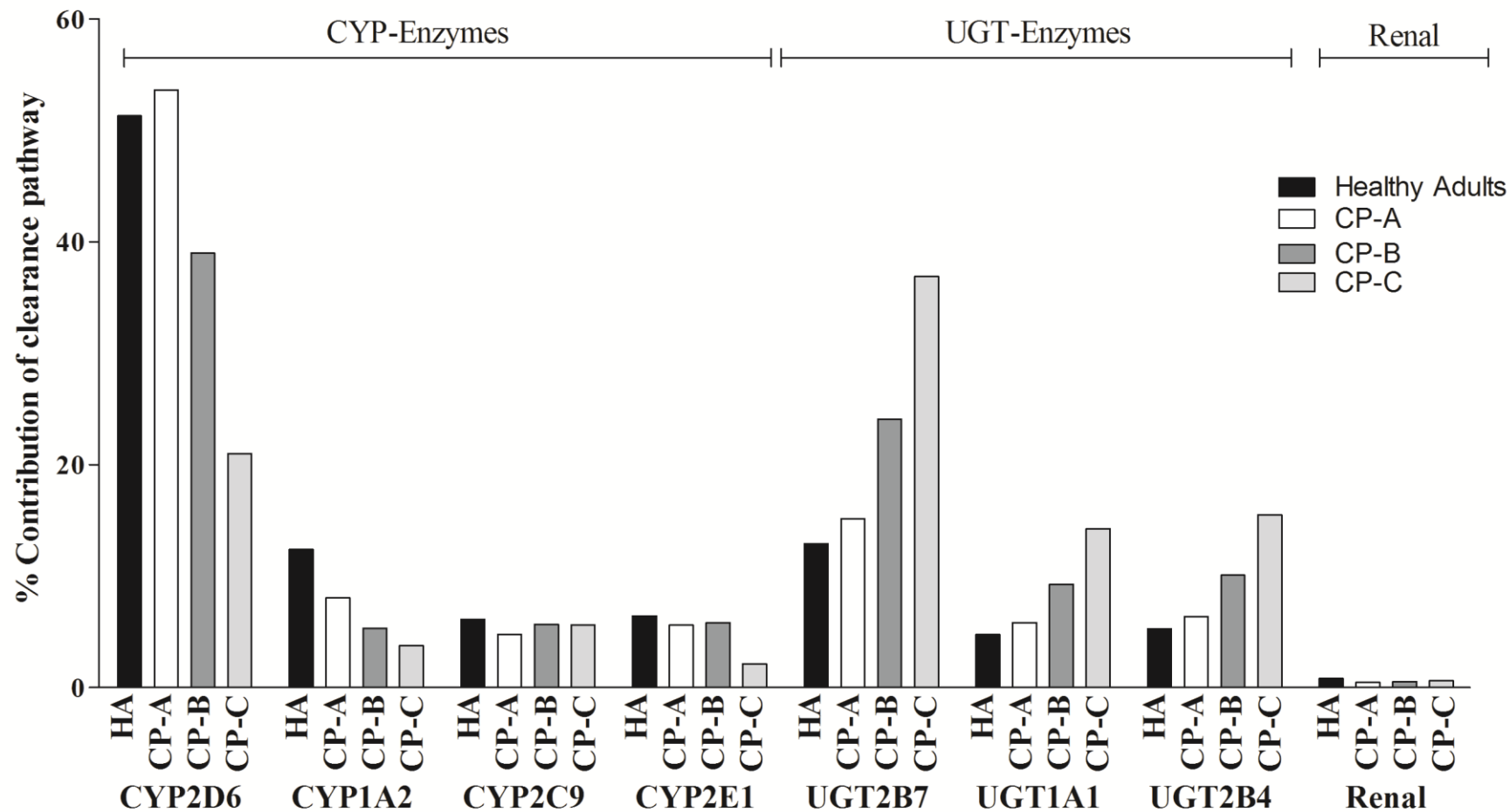
Figure 3-5 The model predicted contributions of the various metabolic enzymes and the renal clearance in the overall carvedilol metabolism in healthy adult and in liver cirrhosis populations.

CP-A= Child-Pugh Class A; *CP-B*= Child-Pugh Class B; and *CP-C*= Child-Pugh Class C

3.3.4. Predicted drug exposure in virtual cirrhosis populations

Further simulations were performed to predict the relative drug exposure from healthy subjects to cirrhosis patients of different severity of the disease. The predicted mean total (bound and unbound) drug exposure (AUC_{total} [µg.h/L]) after administering 25 mg oral carvedilol increased significantly between the healthy and the cirrhosis populations (CP-A–C) populations, i.e. from 204.0 (95 % CI 175.2–232.7) in healthy adults to 1397 (95% CI 1289–1505) in CP–C population. In order to have a similar total carvedilol exposure between healthy and cirrhosis populations, the first dosing modification suggested to reduce the administered carvedilol doses to 12.5 mg in CP–A, 6.25 mg in CP–B and 3.125 mg in CP–C population. As a result of this dosing modification, the mean total exposure was predicted to be 233.3 (95 % CI: 206.5–260.1) in CP–A, 186.1 (95 % CI: 169.4–202.9) in CP–B, and 174.6 (95% CI: 161.1–188.2) in CP–C population (**Figure 3-6 and Appendix 18**).

Looking at the unbound systemic concentrations of carvedilol, an increase was also seen as the mean unbound drug exposure ($AUC_{unbound}$ [µg.h/L]) changed from 1.06 (95 % CI 0.91–1.21) in healthy adults to 13.8 (95 % CI 12.8–14.8) in CP-C population (**Figure 3-6**). The trend of increase was similar to that seen with the total exposure, however, it was more pronounced as here the magnitude of change was ~13-folds in comparison to a ~7-fold increase for the total carvedilol exposure between healthy and the CP–C population. Applying the previously mentioned dose modification, the upper 95 % CI of mean unbound carvedilol exposure in CP-A–C populations were still higher than that in healthy adults

(**Figure 3-6 and Appendix 19**). As a result, a further 25% reduction doses to be administered was suggested so that the required carvedilol doses were adjusted to 9.375 mg in CP–A, 4.68 mg in CP–B and 2.34 mg in CP–C population. This model based final dosing proposal resulted in a comparable mean unbound drug exposure in all patient subgroups, i.e. 1.03 (95 % CI: 0.91–1.14) in CP–A, 1.34 (95 % CI: 1.22–1.45) in CP–B and 1.3 (95% CI: 1.2–1.4) in CP–C population as well as in the total drug exposure (**Figure 3-6 and Appendix 20**).
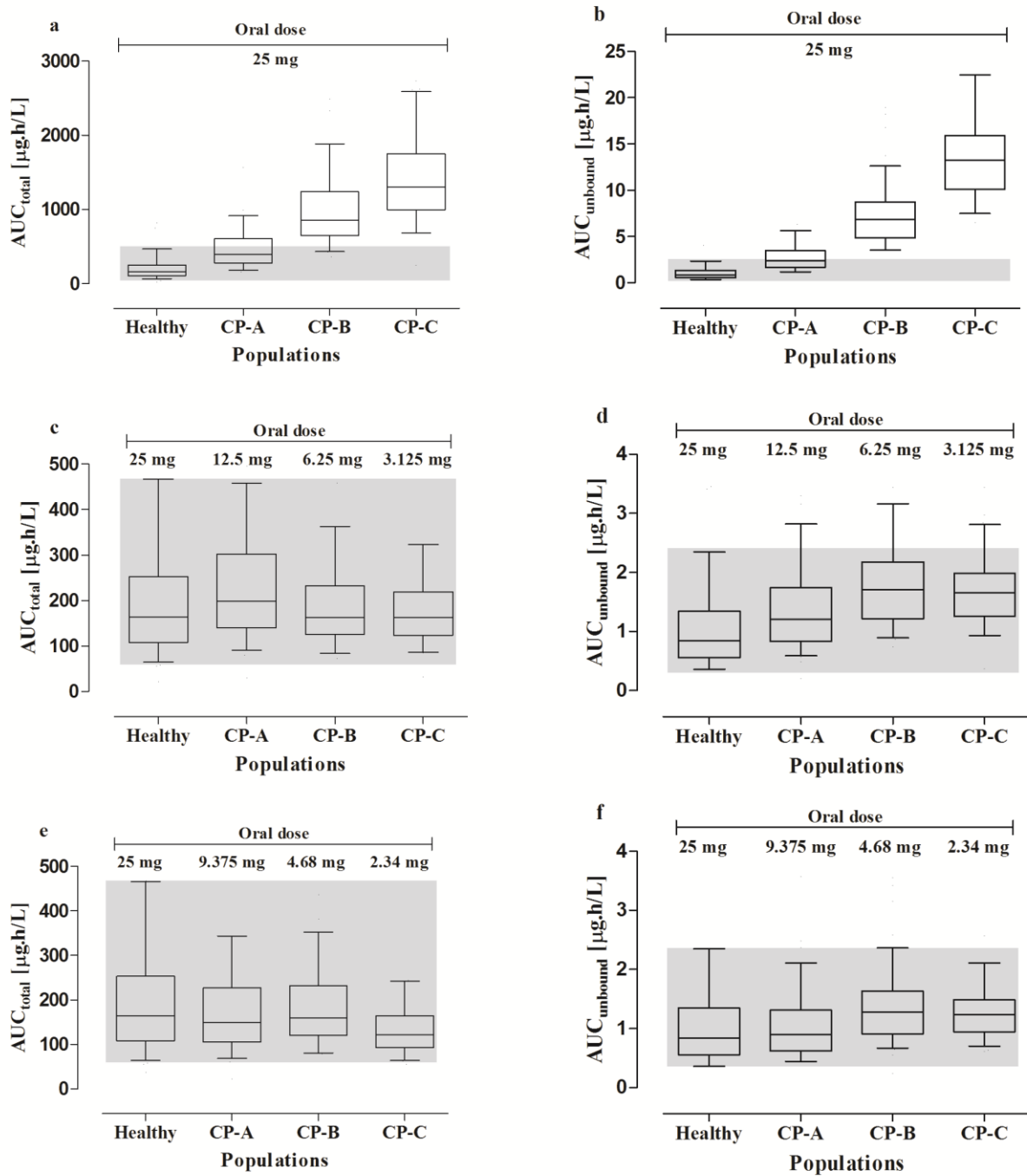
Figure 3-6 Box plots showing predicted area under the curve with 5th–95th percentiles in healthy and cirrhosis populations.

(a) Predicted AUCtotal after administering 25 mg dose of carvedilol in healthy and cirrhosis populations. (b) Predicted AUCunbound after administering 25 mg dose of carvedilol in healthy and cirrhosis populations. (c) Predicted AUCtotal after reduction in administered carvedilol doses in different cirrhosis populations (CP-A–C). (d) Predicted AUCunbound after reduction in administered carvedilol doses in different cirrhosis populations (CP-A–C). (e) Predicted AUCtotal after further 25% reduction in administered carvedilol doses in different cirrhosis populations (CP-A–C). (f) Predicted AUCunbound after further 25% reduction in administered carvedilol doses in different cirrhosis populations (CP-A–C). The grey shaded area shows the exposure after administering 25 mg oral dose of carvedilol in healthy adults. HA= healthy adult; *CP-A*= Child-Pugh Class A; *CP-B*= Child-Pugh Class B; and *CP-C*= Child-Pugh Class C

3.4. Discussion

Due to recent reports on comparative clinical evaluation of non-selective beta-blockers in cirrhosis patients with portal hypertension, there is a renewed interest in the clinical use of carvedilol. However, the therapeutic benefits associated with its use in cirrhosis patients with portal hypertension are often overshadowed by the associated reports of ADR's, particularly at higher doses of 25 mg/day. Keeping this in mind, a PBPK model of carvedilol was developed to predict drug exposure and recommend dosing in order to optimize its clinical use in liver cirrhosis populations of different disease severity. The final model simulations quantified a significant increase in the unbound and total (bound and unbound) systemic exposure of carvedilol with the increased severity of the disease, with the increase of the former being more pronounced. Based on these predicted drug exposures, suggestions for dose selection/optimization were given in order to enhance a safer carvedilol therapy in cirrhotic patients.

The developed model has successfully captured the ADME processes in healthy adults after iv and oral administration of carvedilol, as the predicted C_{max}, $AUC_{0-\infty}$, and clearance in healthy adults were in close agreement with the observed values with ratios$_{(Obs/Pred)}$ within 1.5-fold range (**Table 3-3**). Keeping in mind that carvedilol undergoes extensive first pass metabolism (Neugebauer et al., 1987; Neugebauer et al., 1990; Neugebauer and Neubert, 1991; Abdelaziz et al., 2009) through different CYP P450 enzymes (~80 %) and UGT-enzymes (~20 %) (Oldham and Clarke, 1997; Giessmann et al., 2004; Ohno et al., 2004; Sehrt et al., 2011; Takekuma et al., 2012), any change in enzyme expression/activity and in

liver size and volume in cirrhosis can have a significant impact on its metabolic clearance.

In liver cirrhosis, there is a gradual decrease in liver volume and in the abundance of the CYP enzymes with increased severity of the disease. The liver volume decreases from 1.5 L in healthy adults to 1.0 L in cirrhotic patients (CP–C), whereas the abundances of the CYP-enzymes that are involved in carvedilol metabolism, i.e. CYP2D6, CYP1A2, CYP2C9 and CYP2E1, are reduced from 8, 52, 73 and 61 pmol/mg microsomal protein in healthy adults to 0.84, 6.1, 24.4 and 6.71 pmol/mg microsomal protein in cirrhosis CP–C patients, respectively (Johnson et al., 2010). On the other hand, the activity of UGT-enzymes is believed to be preserved (Johnson et al., 2010). Therefore, in comparison to healthy individuals, the relative contributions of CYP and UGT-enzymes to the total carvedilol metabolism were significantly altered in cirrhosis patients. The mean predicted contribution of CYP and UGT-enzymes in overall carvedilol metabolism were reduced from 76 % and 23% in healthy adults to 32% and 66% in cirrhosis CP-C respectively (**Figure 3-5**). This finding indicate that drugs that can alter UGT enzymes activity (Kiang et al., 2005) will play a more significant role in cirrhotic patients when compared to healthy population where CYP metabolism predominates the overall carvedilol metabolism. This is important keeping in mind that patients with liver cirrhosis have often multiple comorbidities that require a concurrent administration of different drugs with a higher potential for DDI's and eventually, ADR's (Franz et al., 2012). By using the developed PBPK model, clinically possible "what if" scenarios can be explored and DDI's between carvedilol and other co-administered drugs (e.g. UGT inhibitors) can be predicted,

which can eventually help in optimizing the drug therapy and preventing ADR's in liver cirrhosis population.

There is no doubt that the clinical use of carvedilol has been extensively studied in cirrhosis patients with portal hypertension (Forrest et al., 1996; Stanley et al., 1999; Tripathi et al., 2002; Hobolth et al., 2014), but after looking closely at participants of these clinical trials, some shortcomings and question marks can be identified that may have undermined their findings. Firstly, the number of participating cirrhosis patients with respect to CP classes were different in every clinical trial, so the findings from these clinical studies may not be generalized for all the cirrhosis patients with different CP classes. Moreover, in every clinical study, the same carvedilol dose was administered to cirrhosis patients regardless of the CP class, which may have resulted in different drug exposures and could have potentially impaired the associated clinical benefits with its use in these patients. These potential changes in the drug exposure were explored and quantified with the presented model, and the results indicate the need of dose adaptation if the same drug exposure is to be achieved in all patients.

In the present work, the developed model after its evaluation with the CP–C population was used to predict carvedilol exposure in CP-A and B populations, where no clinical data were available and it was seen that, in order to have similar total (bound and unbound) drug exposure as achieved after administering 25 mg oral carvedilol in healthy population, the administered doses should be reduced to 12.5 mg, 6.25 mg, and 3.125 mg in in CP–A, CP–B, and CP–C populations, respectively (**Figure 3-6**). Since, carvedilol is a drug that is extensively bound to

plasma proteins (f_{uP} of 0.0054) and the changes occurring in its CL and free fraction in liver cirrhosis patients can affect its PD response, therefore, measuring/predicting its unbound systemic concentration in liver cirrhosis patients is very important. Keeping this in mind, the developed model was used to predict unbound systemic carvedilol concentrations in healthy and cirrhosis (CP-A–C) populations. It was seen that in liver cirrhosis patients, the unbound systemic concentration of carvedilol increases more markedly in comparison to that of total systemic concentration of carvedilol (~7-fold increase in total exposure vs. ~13-fold increase in unbound exposure between healthy and CP–C population). This relative increase in unbound drug exposure may be the potential underlying reason for the intolerance seen in cirrhosis patients after administering 25 mg daily doses of oral carvedilol (Stanley et al., 1999). As a result, on the basis of simulated unbound carvedilol exposure, a further 25% reduction in administered carvedilol dose was required and the final suggested drug doses were 9.375 mg in CP–A, 4.68 mg in CP–B and 2.34 mg in CP–C population. Nevertheless, the above-suggested dose reductions should be considered in light of the information that carvedilol is commercially available in strengths of 3.125 mg, 6.25 mg, 12.5 mg, and 25 mg, and that for these recommendations, manipulation of the available dosage forms may be required.

.

X. Final Summary of the thesis and perspectives

This thesis was aimed to improve the clinical use of carvedilol, a high hepatic extraction drug, in CHF and liver cirrhosis populations by developing PBPK drug-disease models. In order to understand the pharmacokinetic differences associated with use of carvedilol in healthy and diseases populations, a systematic model building strategy was adopted. In this modeling strategy, the developed models were first evaluated in healthy populations and after incorporation of disease related data, they were tested in diseased populations. In order to propose model based drug dosing and to explore complex clinical scenarios, after evaluation of these developed drug-disease models with the available clinical data sets, they were extrapolated to other populations, where no clinical data was available. The developed PBPK models have the capacity to be extended to predict ADME of other high hepatic extraction drugs in diseased populations and they can be used to optimize current dosing schemes in these diseased populations.

In the first part of the thesis, the hemodynamic changes occurring in hepatic and renal blood flow in CHF were incorporated in two-PBPK models and the model predictions were compared with the available clinical data in adult and pediatric CHF patients. The model predictions in adult CHF population who were classified according to NYHA classification of CHF, were significantly improved with incorporation of reduced organ blood flows and a strong connection was seen between decrease in hepatic clearance of carvedilol with increased disease severity. The predictions in pediatric CHF patients were not improved with organ blood flow reductions and it was hypothesized that the pediatric system of

assessing severity of heart failure, the Ross score, was not very well correlated with the organ blood flow reductions occurring in the disease as the NYHA system. Since, majority of pediatric patients in the clinical trial were diagnosed with mild heart failure (Ross score 3-6), it was assumed that the pathophysiology of the disease is different in mild CHF, this assumption was further strengthened when the organ blood flow reductions in children above 17 years of age, assessed by NYHA system, resulted in improvement in predicted pharmacokinetic parameters. These results cannot be generalized to all the pediatric CHF patients taking into consideration the small sample size of the pediatric clinical trial data used for model development and secondly, in terms of severity of disease the participants were not evenly distributed throughout the pediatric age range. In order to make a definite conclusion regarding the role of reduced organ blood flows in children, there is a need for further evaluation with additional clinical pharmacokinetic data of pediatric patients with different degrees of CHF.

In the second part of the thesis a PBPK model was developed to predict stereo-selective disposition of carvedilol in CHF populations, after incorporating more relevent pathophysiological changes in blood flow to limbs, adipose, skin and muscle. After evaluation in adult CHF patients, the model was scaled to pediatric CHF patients to see if the same tissue/organ blood flow changes can also be adopted for children. The developed model has successfully described PK of carvedilol enantiomers in healthy adults and in patients after the incorporation of reduced organ blood flows. In comparison to systemic concentration of R-carvedilol, there was a relative increase in S-carvedilol systemic concentration in adult CHF population. This relative increase in S-carvedilol systemic concentration

is expected to widen with the increase in severity of CH. In contrast to adults, pediatric patients up to 12 years of age were better described without the reductions in organ blood flow, whereas older pediatric patients were better described after incorporating organ blood flow reductions. These findings indicate that the incorporated blood flow reductions in the adult model cannot be directly adopted in pediatrics, at least for the young ones; however, in order to draw definite conclusions, more data is still needed.

The last part of thesis was aimed to develop and evaluate a PBPK-carvedilol-cirrhosis model with the available clinical data in liver cirrhosis patients and to recommend model based drug dosing after exploring the underlying differences in unbound and total (bound and unbound) systemic carvedilol concentrations with the different disease stages. The model predictions in different cirrhosis populations (CP-A–C) showed that UGT-enzymes predominate drug metabolism in CP–C populations and therefore, the concomitant use of UGT inhibitors with carvedilol in cirrhosis patients can lead to clinically relevant DDI's. Since, both drug regulatory agencies (FDA and EMA) recommend studying drug PK with respect to CP classification system in cirrhosis populations, dose optimization was recommended based on predicted unbound drug exposure in different cirrhosis CP classes (A–C). The presented model generated-data can guide the optimization of administered carvedilol doses in cirrhosis patients with respect to disease severity and can help improve the design of some necessary clinical studies in the drug development process

Because of the mechanistic nature of the presented PBPK models, they can be extended to other high extraction drugs in chronic heart failure and liver cirrhosis populations. These models can also serve as a basis to develop PBPK models for carvedilol and similar high extraction drugs in special populations like geriatrics and renal failure. By exploring underlying pathophysiological differences between adult and pediatric CHF populations, the developed PBPK models can help in suggesting required carvedilol doses in pediatric CHF patients.

XI. References

U.S. Food and Drug Administration Guidance for industry: pharmacokinetics in patients with impaired hepatic function. Study design, and impact on dosing and labeling. Rockville (MD): FDA, May, 2003.

The Criteria Committee of the New York Heart Association (1994). Nomenclature and Criteria for Diagnosis of Diseases of the Heart and Great Vessels. Boston: Little, Brown and Company.

European Medicines Agency Committee for Medicinal Products for Human Use. Guideline on the evaluation of the pharmacokinetics of medicinal products in patients with impaired hepatic function. London: European Medicines Agency, February, 2005.

Abdelaziz A, al-Araby M, Mahran L, and Spahn-Langguth H (2009) Active metabolites formed during hepatic first-pass: simulations featuring their contribution to the overall effect in altered liver clearance and drug-drug interactions. *BMC Pharmacology* **9:**A38.

Abduljalil K, Cain T, Humphries H, and Rostami-Hodjegan A (2014) Deciding on success criteria for predictability of pharmacokinetic parameters from in vitro studies: an analysis based on in vivo observations. *Drug metabolism and disposition: the biological fate of chemicals* **42:**1478-1484.

Aiba T, Ishida K, Yoshinaga M, Okuno M, and Hashimoto Y (2005) Pharmacokinetic characterization of transcellular transport and drug interaction of digoxin

in Caco-2 cell monolayers. *Biological & pharmaceutical bulletin* **28:**114-119.

Anderson GD (2010) Developmental pharmacokinetics. *Seminars in pediatric neurology* **17:**208-213.

Bachmakov I, Werner U, Endress B, Auge D, and Fromm MF (2006) Characterization of beta-adrenoceptor antagonists as substrates and inhibitors of the drug transporter P-glycoprotein. *Fundamental & clinical pharmacology* **20:**273-282.

Behn F (2001) Pharmakokinetik, Pharmakodynamik und Pharmakogenetik von Carvedilol in Abhängigkeit vom Lebensalter bei pädiatrischen Patienten mit Herzinsuffizienz. *Dissertation zur Erlangung des Doktorgrades des Fachbereichs Chemie der Universität Hamburg*.

Berezhkovskiy LM (2004) Volume of distribution at steady state for a linear pharmacokinetic system with peripheral elimination. *Journal of pharmaceutical sciences* **93:**1628-1640.

Berkowitz D, Groll MN, and Likoff W (1963) Malabsorption as a complication of congestive heart failure. *The American Journal of Cardiology* **11:**43-47.

Birkett DJ (1989) Racemates or enantiomers: regulatory approaches. *Clinical and experimental pharmacology & physiology* **16:**479-483.

Bosch J (2013) Carvedilol: the beta-blocker of choice for portal hypertension? *Gut* **62:**1529-1530.

Bosch J, Berzigotti A, Garcia-Pagan JC, and Abraldes JG (2008) The management of portal hypertension: Rational basis, available treatments and future options. *Journal of Hepatology* **48, Supplement 1:**S68-S92.

Boucher BA, Wood GC, and Swanson JM (2006) Pharmacokinetic changes in critical illness. *Critical care clinics* **22:**255-271, vi.

Caron G, Steyaert G, Pagliara A, Reymond F, Crivori P, Gaillard P, Carrupt P-A, Avdeef A, Comer J, Box KJ, Girault HH, and Testa B (1999) Structure-Lipophilicity Relationships of Neutral and Protonated β-Blockers, Part I, Intra- and Intermolecular Effects in Isotropic Solvent Systems. *Helvetica Chimica Acta* **82:**1211-1222.

Cubitt HE, Yeo KR, Howgate EM, Rostami-Hodjegan A, and Barter ZE (2011) Sources of interindividual variability in IVIVE of clearance: an investigation into the prediction of benzodiazepine clearance using a mechanistic population-based pharmacokinetic model. *Xenobiotica* **41:**623-638.

Davis SS, Hardy JG, and Fara JW (1986) Transit of pharmaceutical dosage forms through the small intestine. *Gut* **27:**886-892.

De Buck SS, Sinha VK, Fenu LA, Nijsen MJ, Mackie CE, and Gilissen RA (2007) Prediction of human pharmacokinetics using physiologically based modeling: a retrospective analysis of 26 clinically tested drugs. *Drug metabolism and disposition: the biological fate of chemicals* **35:**1766-1780.

de Franchis R (2010) Revising consensus in portal hypertension: Report of the Baveno V consensus workshop on methodology of diagnosis and therapy in portal hypertension. *Journal of Hepatology* **53:**762-768.

Edginton AN and Willmann S (2008) Physiology-based simulations of a pathological condition: prediction of pharmacokinetics in patients with liver cirrhosis. *Clinical pharmacokinetics* **47:**743-752.

Fleming S, Thompson M, Stevens R, Heneghan C, Pluddemann A, Maconochie I, Tarassenko L, and Mant D (2011) Normal ranges of heart rate and respiratory rate in children from birth to 18 years of age: a systematic review of observational studies. *Lancet* **377:**1011-1018.

Forrest EH, Bouchier IA, and Hayes PC (1996) Acute haemodynamic changes after oral carvedilol, a vasodilating beta-blocker, in patients with cirrhosis. *J Hepatol* **25:**909-915.

Franz C, Egger S, Born C, Rätz Bravo A, and Krähenbühl S (2012) Potential drug-drug interactions and adverse drug reactions in patients with liver cirrhosis. *Eur J Clin Pharmacol* **68:**179-188.

Fujimaki M, Murakoshi Y, and Hakusui H (1990) Assay and disposition of carvedilol enantiomers in humans and monkeys: evidence of stereoselective presystemic metabolism. *Journal of pharmaceutical sciences* **79:**568-572.

Gehr TW, Tenero DM, Boyle DA, Qian Y, Sica DA, and Shusterman NH (1999) The pharmacokinetics of carvedilol and its metabolites after single and multiple dose oral administration in patients with hypertension and renal insufficiency. *European journal of clinical pharmacology* **55:**269-277.

Gertz M, Houston JB, and Galetin A (2011) Physiologically based pharmacokinetic modeling of intestinal first-pass metabolism of CYP3A substrates with high

intestinal extraction. *Drug metabolism and disposition: the biological fate of chemicals* **39:**1633-1642.

Giacomini KM, Huang SM, Tweedie DJ, Benet LZ, Brouwer KL, Chu X, Dahlin A, Evers R, Fischer V, Hillgren KM, Hoffmaster KA, Ishikawa T, Keppler D, Kim RB, Lee CA, Niemi M, Polli JW, Sugiyama Y, Swaan PW, Ware JA, Wright SH, Yee SW, Zamek-Gliszczynski MJ, and Zhang L (2010) Membrane transporters in drug development. *Nature reviews Drug discovery* **9:**215-236.

Giannelli V, Lattanzi B, Thalheimer U, and Merli M (2014) Beta-blockers in liver cirrhosis. *Annals of gastroenterology : quarterly publication of the Hellenic Society of Gastroenterology* **27:**20-26.

Giessmann T, Modess C, Hecker U, Zschiesche M, Dazert P, Kunert-Keil C, Warzok R, Engel G, Weitschies W, Cascorbi I, Kroemer HK, and Siegmund W (2004) CYP2D6 genotype and induction of intestinal drug transporters by rifampin predict presystemic clearance of carvedilol in healthy subjects. *Clin Pharmacol Ther* **75:**213-222.

Hanioka N, Tanaka S, Moriguchi Y, and Narimatsu S (2012) Stereoselective glucuronidation of carvedilol in human liver and intestinal microsomes. *Pharmacology* **90:**117-124.

Hemstreet BA (2004) Evaluation of Carvedilol for the Treatment of Portal Hypertension. *Pharmacotherapy: The Journal of Human Pharmacology and Drug Therapy* **24:**94-104.

Hobolth L, Bendtsen F, Hansen EF, and Moller S (2014) Effects of carvedilol and propranolol on circulatory regulation and oxygenation in cirrhosis: a randomised study. *Digestive and liver disease : official journal of the Italian Society of Gastroenterology and the Italian Association for the Study of the Liver* **46:**251-256.

Hsu DT and Pearson GD (2009) Heart Failure in Children: Part I: History, Etiology, and Pathophysiology. *Circulation: Heart Failure* **2:**63-70.

Jamei M, Bajot F, Neuhoff S, Barter Z, Yang J, Rostami-Hodjegan A, and Rowland-Yeo K (2014) A mechanistic framework for in vitro-in vivo extrapolation of liver membrane transporters: prediction of drug-drug interaction between rosuvastatin and cyclosporine. *Clinical pharmacokinetics* **53:**73-87.

Jamei M, Marciniak S, Feng K, Barnett A, Tucker G, and Rostami-Hodjegan A (2009a) The Simcyp population-based ADME simulator. *Expert opinion on drug metabolism & toxicology* **5:**211-223.

Jamei M, Turner D, Yang J, Neuhoff S, Polak S, Rostami-Hodjegan A, and Tucker G (2009b) Population-based mechanistic prediction of oral drug absorption. *The AAPS journal* **11:**225-237.

Jiang XL, Zhao P, Barrett JS, Lesko LJ, and Schmidt S (2013) Application of physiologically based pharmacokinetic modeling to predict acetaminophen metabolism and pharmacokinetics in children. *CPT: pharmacometrics & systems pharmacology* **2:**e80.

Johnson T, Rostami-Hodjegan A, and Tucker G (2006) Prediction of the Clearance of Eleven Drugs and Associated Variability in Neonates, Infants and Children. *Clin Pharmacokinet* **45:**931-956.

Johnson TN, Boussery K, Rowland-Yeo K, Tucker GT, and Rostami-Hodjegan A (2010) A semi-mechanistic model to predict the effects of liver cirrhosis on drug clearance. *Clinical pharmacokinetics* **49:**189-206.

Johnson TN and Rostami-Hodjegan A (2011) Resurgence in the use of physiologically based pharmacokinetic models in pediatric clinical pharmacology: parallel shift in incorporating the knowledge of biological elements and increased applicability to drug development and clinical practice. *Paediatric anaesthesia* **21:**291-301.

Jones HM, Mayawala K, and Poulin P (2013) Dose Selection Based on Physiologically Based Pharmacokinetic (PBPK) Approaches. *The AAPS journal* **15:**377-387.

Jones HM, Parrott N, Jorga K, and Lave T (2006) A novel strategy for physiologically based predictions of human pharmacokinetics. *Clinical pharmacokinetics* **45:**511-542.

Kaijser M, Johnsson C, Zezina L, Backman U, Dimeny E, and Fellstrom B (1997) Elevation of cyclosporin A blood levels during carvedilol treatment in renal transplant patients. *Clinical transplantation* **11:**577-581.

Khalil F and Laer S (2011) Physiologically based pharmacokinetic modeling: methodology, applications, and limitations with a focus on its role in

pediatric drug development. *Journal of biomedicine & biotechnology* **2011:**907461.

Khalil F and Laer S (2014) Physiologically based pharmacokinetic models in the prediction of oral drug exposure over the entire pediatric age range-sotalol as a model drug. *The AAPS journal* **16:**226-239.

Kiang TK, Ensom MH, and Chang TK (2005) UDP-glucuronosyltransferases and clinical drug-drug interactions. *Pharmacology & therapeutics* **106:**97-132.

Kilford PJ, Stringer R, Sohal B, Houston JB, and Galetin A (2009) Prediction of drug clearance by glucuronidation from in vitro data: use of combined cytochrome P450 and UDP-glucuronosyltransferase cofactors in alamethicin-activated human liver microsomes. *Drug metabolism and disposition: the biological fate of chemicals* **37:**82-89.

Laer S, Mir TS, Behn F, Eiselt M, Scholz H, Venzke A, Meibohm B, and Weil J (2002) Carvedilol therapy in pediatric patients with congestive heart failure: a study investigating clinical and pharmacokinetic parameters. *American heart journal* **143:**916-922.

Lee R, Beard J, and Aldoori M (1993) Blood flow to the limbs, in: *Cardiac Output and Regional Flow in Health and Disease* (Salmasi A-M and Iskandrian A eds), pp 505-522, Springer Netherlands.

Leithe ME, Margorien RD, Hermiller JB, Unverferth DV, and Leier CV (1984) Relationship between central hemodynamics and regional blood flow in normal subjects and in patients with congestive heart failure. *Circulation* **69:**57-64.

Li GF, Wang K, Chen R, Zhao HR, Yang J, and Zheng QS (2012) Simulation of the pharmacokinetics of bisoprolol in healthy adults and patients with impaired renal function using whole-body physiologically based pharmacokinetic modeling. *Acta pharmacologica Sinica* **33:**1359-1371.

Marsousi N, Daali Y, Rudaz S, Almond L, Humphries H, Desmeules J, and Samer CF (2014) Prediction of Metabolic Interactions With Oxycodone via CYP2D6 and CYP3A Inhibition Using a Physiologically Based Pharmacokinetic Model. *CPT: Pharmacometrics & Systems Pharmacology* **3:**1-8.

Meng F, Yin X, Ma X, Guo XD, Jin B, and Li H (2013) Assessment of the value of serum cholinesterase as a liver function test for cirrhotic patients. *Biomedical reports* **1:**265-268.

Morgan DJ and McLean AJ (1995) Clinical pharmacokinetic and pharmacodynamic considerations in patients with liver disease. An update. *Clinical pharmacokinetics* **29:**370-391.

Nakamura H, Ishii M, Sugimura T, Chiba K, Kato H, and Ishizaki T (1994) The kinetic profiles of enalapril and enalaprilat and their possible developmental changes in pediatric patients with congestive heart failure. *Clin Pharmacol Ther* **56:**160-168.

Neugebauer G, Akpan W, Kaufmann B, and Reiff K (1990) Stereoselective disposition of carvedilol in man after intravenous and oral administration of the racemic compound. *Eur J Clin Pharmacol* **38:**S108-S111.

Neugebauer G, Akpan W, von Mollendorff E, Neubert P, and Reiff K (1987) Pharmacokinetics and disposition of carvedilol in humans. *Journal of cardiovascular pharmacology* **10 Suppl 11:**S85-88.

Neugebauer G, Gabor M, and Reiff K (1988) Pharmacokinetics and Bioavailability of Carvedilol in Patients with Liver Cirrhosis. *Drugs* **36:**148-154.

Neugebauer G and Neubert P (1991) Metabolism of carvedilol in man. *European journal of drug metabolism and pharmacokinetics* **16:**257-260.

Nies AS, Shand DG, and Wilkinson GR (1976) Altered hepatic blood flow and drug disposition. *Clinical pharmacokinetics* **1:**135-155.

Noda T, Todani T, Watanabe Y, and Yamamoto S (1997) Liver volume in children measured by computed tomography. *Pediatric radiology* **27:**250-252.

Ogawa R, Stachnik JM, and Echizen H (2013) Clinical pharmacokinetics of drugs in patients with heart failure: an update (part 1, drugs administered intravenously). *Clinical pharmacokinetics* **52:**169-185.

Ogawa R, Stachnik JM, and Echizen H (2014) Clinical pharmacokinetics of drugs in patients with heart failure: an update (part 2, drugs administered orally). *Clinical pharmacokinetics* **53:**1083-1114.

Ohno A, Saito Y, Hanioka N, Jinno H, Saeki M, Ando M, Ozawa S, and Sawada J (2004) Involvement of human hepatic UGT1A1, UGT2B4, and UGT2B7 in the glucuronidation of carvedilol. *Drug metabolism and disposition: the biological fate of chemicals* **32:**235-239.

Oldham HG and Clarke SE (1997) In vitro identification of the human cytochrome P450 enzymes involved in the metabolism of R(+)- and S(-)-carvedilol. *Drug metabolism and disposition: the biological fate of chemicals* **25:**970-977.

Pugh RN, Murray-Lyon IM, Dawson JL, Pietroni MC, and Williams R (1973) Transection of the oesophagus for bleeding oesophageal varices. *The British journal of surgery* **60:**646-649.

Rasool MF, Khalil F, and Laer S (2015) A Physiologically Based Pharmacokinetic Drug-Disease Model to Predict Carvedilol Exposure in Adult and Paediatric Heart Failure Patients by Incorporating Pathophysiological Changes in Hepatic and Renal Blood Flows. *Clinical pharmacokinetics* **54:**943-962.

Reiberger T, Ulbrich G, Ferlitsch A, Payer BA, Schwabl P, Pinter M, Heinisch BB, Trauner M, Kramer L, and Peck-Radosavljevic M (2013) Carvedilol for primary prophylaxis of variceal bleeding in cirrhotic patients with haemodynamic non-response to propranolol. *Gut* **62:**1634-1641.

Ross RD (2012) The Ross classification for heart failure in children after 25 years: a review and an age-stratified revision. *Pediatric cardiology* **33:**1295-1300.

Ross RD, Bollinger RO, and Pinsky WW (1992) Grading the severity of congestive heart failure in infants. *Pediatric cardiology* **13:**72-75.

Rowland Yeo K, Aarabi M, Jamei M, and Rostami-Hodjegan A (2011) Modeling and predicting drug pharmacokinetics in patients with renal impairment. *Expert review of clinical pharmacology* **4:**261-274.

Salem F, Johnson TN, Abduljalil K, Tucker GT, and Rostami-Hodjegan A (2014) A re-evaluation and validation of ontogeny functions for cytochrome P450 1A2 and 3A4 based on in vivo data. *Clinical pharmacokinetics* **53:**625-636.

Salem F, Johnson TN, Barter ZE, Leeder JS, and Rostami-Hodjegan A (2013) Age Related Changes in Fractional Elimination Pathways for Drugs: Assessing the Impact of Variable Ontogeny on Metabolic Drug–Drug Interactions. *The Journal of Clinical Pharmacology* **53:**857-865.

Sandek A, Bauditz J, Swidsinski A, Buhner S, Weber-Eibel J, von Haehling S, Schroedl W, Karhausen T, Doehner W, Rauchhaus M, Poole-Wilson P, Volk HD, Lochs H, and Anker SD (2007) Altered intestinal function in patients with chronic heart failure. *Journal of the American College of Cardiology* **50:**1561-1569.

Sayama H, Takubo H, Komura H, Kogayu M, and Iwaki M (2014) Application of a Physiologically Based Pharmacokinetic Model Informed by a Top-Down Approach for the Prediction of Pharmacokinetics in Chronic Kidney Disease Patients. *The AAPS journal*.

Sehrt D, Meineke I, Tzvetkov M, Gultepe S, and Brockmoller J (2011) Carvedilol pharmacokinetics and pharmacodynamics in relation to CYP2D6 and ADRB pharmacogenetics. *Pharmacogenomics* **12:**783-795.

Sica DA (2003) Pharmacotherapy in congestive heart failure: drug absorption in the management of congestive heart failure: loop diuretics. *Congestive heart failure (Greenwich, Conn)* **9:**287-292.

Sinagra E, Perricone G, D'Amico M, Tine F, and D'Amico G (2014) Systematic review with meta-analysis: the haemodynamic effects of carvedilol compared with propranolol for portal hypertension in cirrhosis. *Alimentary pharmacology & therapeutics* **39:**557-568.

Spahn H, Henke W, Langguth P, Schloos J, and Mutschler E (1990) Measurement of carvedilol enantiomers in human plasma and urine using S-naproxen chloride for chiral derivatization. *Archiv der Pharmazie* **323:**465-469.

Stanley AJ, Therapondos G, Helmy A, and Hayes PC (1999) Acute and chronic haemodynamic and renal effects of carvedilol in patients with cirrhosis. *J Hepatol* **30:**479-484.

Takekuma Y, Yagisawa K, and Sugawara M (2012) Mutual inhibition between carvedilol enantiomers during racemate glucuronidation mediated by human liver and intestinal microsomes. *Biological & pharmaceutical bulletin* **35:**151-163.

Tanaka H, Monahan KD, and Seals DR (2001) Age-predicted maximal heart rate revisited. *Journal of the American College of Cardiology* **37:**153-156.

Tenero D, Boike S, Boyle D, Ilson B, Fesniak HF, Brozena S, and Jorkasky D (2000) Steady-state pharmacokinetics of carvedilol and its enantiomers in patients with congestive heart failure. *Journal of clinical pharmacology* **40:**844-853.

Tian Y, He Y, Hu H, Wang L, and Zeng S (2012) Determination of the enantioselectivity of six chiral aryloxy aminopropanol drugs transport across Caco-2 cell monolayers. *Acta Pharmaceutica Sinica B* **2:**168-173.

Tripathi D, Therapondos G, Lui HF, Stanley AJ, and Hayes PC (2002) Haemodynamic effects of acute and chronic administration of low-dose carvedilol, a vasodilating beta-blocker, in patients with cirrhosis and portal hypertension. *Alimentary pharmacology & therapeutics* **16:**373-380.

Tucker GT and Lennard MS (1990) Enantiomer specific pharmacokinetics. *Pharmacology & therapeutics* **45:**309-329.

Verbeeck RK (2008) Pharmacokinetics and dosage adjustment in patients with hepatic dysfunction. *European journal of clinical pharmacology* **64:**1147-1161.

Vogt W (2014) Evaluation and optimisation of current milrinone prescribing for the treatment and prevention of low cardiac output syndrome in paediatric patients after open heart surgery using a physiology-based pharmacokinetic drug-disease model. *Clinical pharmacokinetics* **53:**51-72.

von Mollendorff E, Reiff K, and Neugebauer G (1987) Pharmacokinetics and bioavailability of carvedilol, a vasodilating beta-blocker. *European journal of clinical pharmacology* **33:**511-513.

Wessler JD, Grip LT, Mendell J, and Giugliano RP (2013) The P-glycoprotein transport system and cardiovascular drugs. *Journal of the American College of Cardiology* **61:**2495-2502.

World Health Organization Position Paper: Paediatric Age Categories to be Used in Differentiating Between Listing on a Model Essential Medicines List for Children.

Wilkinson GR and Shand DG (1975) Commentary: a physiological approach to hepatic drug clearance. *Clin Pharmacol Ther* **18:**377-390.

Zhou HH and Wood AJ (1995) Stereoselective disposition of carvedilol is determined by CYP2D6. *Clin Pharmacol Ther* **57:**518-524.

XII. Appendix

Appendix 1   Observed and predicted data used for model evaluation in healthy adults after intravenous carvedilol administration

Appendix 2   Observed and predicted data used for model evaluation in healthy adults after oral carvedilol administration

Appendix 3   Observed/predicted ratios for the pharmacokinetic parameters in adults

Appendix 4   Observed and predicted data used for model evaluation in adult chronic heart failure patients after oral carvedilol administration

Appendix 5   Observed/predicted ratios for the pharmacokinetic parameters in NYHA III and NYHA IV adult chronic heart failure patients

Appendix 6   Observed and predicted data used for model evaluation in pediatric chronic heart failure patients after oral carvedilol administration

Appendix 7   Observed and predicted data used for model evaluation in pediatric chronic heart failure patients after oral carvedilol administration

Appendix 8   Observed and predicted data used for model evaluation in healthy adults after administering 12.5 mg intravenous racemic carvedilol

Appendix 9   Observed and predicted data used for model evaluation in healthy adults after administering 50mg oral racemic carvedilol

Appendix 10   Observed and predicted data used for model evaluation in healthy adults (n=7), after administering 0.09mg/kg oral racemic carvedilol.

Appendix 11   Observed and predicted data used for model evaluation in extensive and poor metabolizers of CYP2D6 after administering 25mg oral racemic carvedilol

Appendix 1. Observed and predicted data used for model evaluation in healthy adults after intravenous carvedilol administration

Time (hour)	Systemic carvedilol concentration (µg/L)			Route	Dose	Study
	Observed*	Model-1 predicted	Model-2 predicted			
0.37	112.0	109.4	113.8	iv	12.5	1
0.60	136.0	126.4	133.5	iv	12.5	1
0.84	160.0	139.5	147.9	iv	12.5	1
1.00	177.5	145.2	154.4	iv	12.5	1
1.08	88.5	74.1	82.6	iv	12.5	1
1.25	72.8	60.7	68.7	iv	12.5	1
1.33	65.3	53.8	61.0	iv	12.5	1
1.50	54.8	49.0	55.6	iv	12.5	1
1.75	48.2	42.7	48.6	iv	12.5	1
2.00	42.3	36.4	42.5	iv	12.5	1
2.50	34.0	31.0	36.0	iv	12.5	1
3.00	30.3	27.0	31.8	iv	12.5	1
3.50	26.2	23.6	28.1	iv	12.5	1
4.00	22.1	20.0	24.5	iv	12.5	1
6.00	13.7	12.6	16.2	iv	12.5	1
8.00	9.4	7.9	10.7	iv	12.5	1
10.00	6.2	5.1	7.3	iv	12.5	1
12.00	4.0	3.5	5.1	iv	12.5	1
14.00	2.8	2.4	3.5	iv	12.5	1
0.25	37.3	40.8	42.0	iv	5	2
0.50	48.8	49.0	51.4	iv	5	2
0.75	58.7	55.2	58.4	iv	5	2
1.00	54.7	60.2	64.3	iv	5	2
1.33	26.8	22.8	26.3	iv	5	2
1.75	22.1	18.1	21.1	iv	5	2
2.00	19.6	16.2	19.1	iv	5	2
2.40	16.3	13.6	16.3	iv	5	2
2.89	14.1	11.7	14.3	iv	5	2
4.00	10.8	8.8	11.1	iv	5	2
6.00	7.0	5.4	7.3	iv	5	2

Study 1: (Neugebauer et al., 1987), Study 2: (Giessmann et al., 2004)

*The observed data was digitized by using the publication figure. Therefore, it is possible to have small differences between digitized and source data.

Appendix 2. Observed and predicted data used for model evaluation in healthy adults after oral carvedilol administration

Time (hour)	Observed*	Model-1 predicted	Model-2 predicted	Route	Dose	Study
0.25	5.1	19.1	14.8	oral	25 mg	1
0.75	10.4	29.4	23.1	oral	25 mg	1
1.00	15.5	36.3	29.8	oral	25 mg	1
1.25	19.4	38.1	31.0	oral	25 mg	1
1.50	22.2	38.5	30.2	oral	25 mg	1
1.75	20.8	35.8	30.0	oral	25 mg	1
2.00	19.1	31.8	27.5	oral	25 mg	1
2.50	17.0	26.8	23.8	oral	25 mg	1
3.00	14.9	23.1	20.8	oral	25 mg	1
3.50	12.5	20.8	18.9	oral	25 mg	1
4.50	10.8	16.9	15.7	oral	25 mg	1
6.00	6.6	11.5	10.8	oral	25 mg	1
8.00	5.2	7.4	7.2	oral	25 mg	1
10.00	4.0	4.5	4.6	oral	25 mg	1
12.00	3.1	3.0	3.3	oral	25 mg	1
14.00	3.2	2.1	2.2	oral	25 mg	1
0.25	8.6	24.5	18.6	oral	50 mg	1
0.75	41.0	58.8	46.2	oral	50 mg	1
1.00	47.0	72.5	59.5	oral	50 mg	1
1.50	51.5	76.9	60.4	oral	50 mg	1
1.75	51.5	71.6	60.1	oral	50 mg	1
2.00	50.2	63.5	55.1	oral	50 mg	1
2.50	45.2	53.7	47.5	oral	50 mg	1
3.00	38.3	46.3	41.6	oral	50 mg	1
3.50	32.1	41.6	37.8	oral	50 mg	1
4.50	27.1	33.7	31.4	oral	50 mg	1
6.00	18.6	22.9	21.7	oral	50 mg	1
8.00	15.1	14.7	14.4	oral	50 mg	1
10.00	10.4	9.0	9.1	oral	50 mg	1
12.00	7.6	6.1	6.5	oral	50 mg	1
14.00	6.8	4.2	4.4	oral	50 mg	1
0.25	3.5	11.5	8.1	oral	0.09mg/kg	2
0.50	7.9	17.6	12.6	oral	0.09mg/kg	2
0.75	9.5	17.7	12.8	oral	0.09mg/kg	2
1.00	9.4	13.9	10.6	oral	0.09mg/kg	2
1.50	9.3	9.5	7.6	oral	0.09mg/kg	2
2.00	8.4	7.0	5.8	oral	0.09mg/kg	2
2.50	7.2	5.4	4.6	oral	0.09mg/kg	2
3.00	6.1	4.5	3.9	oral	0.09mg/kg	2

Time (hour)	Systemic carvedilol concentration (μg/L)			Route	Dose	Study
	Observed*	Model-1 predicted	Model-2 predicted			
4.00	4.0	3.3	3.0	oral	0.09mg/kg	2
5.00	2.7	2.6	2.4	oral	0.09mg/kg	2
6.00	1.9	1.9	1.9	oral	0.09mg/kg	2
8.00	1.4	1.2	1.2	oral	0.09mg/kg	2
12.00	0.7	0.5	0.6	oral	0.09mg/kg	2

Study 1: (Neugebauer et al., 1987), Study 2: (Behn, 2001)

*The observed data was digitized by using the publication figure. Therefore, it is possible to have small differences between digitized and source data.

Appendix 3. Observed/predicted ratios for the pharmacokinetic parameters in adults

PK-Parameter	Model-2	Model-1	Model-2	Model-1	Model-2	Model-1	Model-2	Model-1
	CHF-R		CHF-N		oral		iv	
AUC_{last}	1.0	0.8	2.6	2.3	1.1	0.8	1.0	1.1
	1.0	0.7	2.5	2.2	0.7	0.6	1.0	1.1
	1.0	0.8	2.6	2.3	0.9	0.8		
	1.2	0.9	3.0	2.6	1.0	1.1		
C_{max}	1.2	0.8	2.6	2.0	0.8	0.5	1.2	1.2
	1.1	0.7	2.3	1.8	0.7	0.6	0.9	1.0
	1.2	0.8	2.6	2.0	0.8	0.7		
	1.3	0.9	2.8	2.1	1.3	1.1		
CL	1.0	1.0	0.4	0.4	0.9	1.2	1.1	0.9
	1.0	1.0	0.4	0.4	1.3	1.4	1.0	0.9
	1.0	1.0	0.3	0.3	1.0	1.1		
	0.9	0.9	0.3	0.3	1.0	1.0		

CHF: chronic heart failure, iv: intravenous, CHF-R: simulations with incorporation of reductions in organ blood flows, CHF-N: simulations with normal healthy organ blood flows, AUC_{last}: area under the plasma concentration-time curve, C_{max}: the maximum concentration and CL: clearance

Appendix 4. Observed and predicted data used for model evaluation in adult chronic heart failure patients after oral carvedilol administration

Time (hour)	Tenero et al.*	Model-1 predicted	Model-2 predicted	Route	Dose (mg)	Study
		Systemic carvedilol concentration (µg/L)				
0.00	6.5	5.6	5.0	oral	6.25	1
0.33	11.2	13.7	10.0	oral	6.25	1
0.67	16.4	21.4	14.9	oral	6.25	1
1.00	21.4	28.2	19.8	oral	6.25	1
1.50	24.2	28.8	20.6	oral	6.25	1
2.00	21.2	26.6	19.4	oral	6.25	1
2.50	18.2	24.7	18.3	oral	6.25	1
3.00	16.4	22.3	16.8	oral	6.25	1
4.00	15.1	18.3	14.3	oral	6.25	1
6.00	7.6	13.1	10.7	oral	6.25	1
8.00	8.2	9.7	8.2	oral	6.25	1
12.00	5.8	5.6	5.0	oral	6.25	1
0.00	12.3	11.1	10.0	oral	12.5	1
0.33	13.8	27.4	20.0	oral	12.5	1
0.67	30.9	42.8	29.9	oral	12.5	1
1.00	41.7	56.4	39.5	oral	12.5	1
1.50	43.7	57.6	41.1	oral	12.5	1
2.00	39.0	53.2	38.9	oral	12.5	1
2.50	37.2	49.3	36.6	oral	12.5	1
3.00	33.2	44.6	33.7	oral	12.5	1
4.00	28.0	36.7	28.6	oral	12.5	1
6.00	18.9	26.2	21.4	oral	12.5	1
8.00	14.7	19.5	16.5	oral	12.5	1
12.00	10.4	11.1	10.0	oral	12.5	1
0.00	29.3	22.3	20.1	oral	25.0	1
0.33	33.1	54.8	40.0	oral	25.0	1
0.67	70.8	85.5	59.8	oral	25.0	1
1.00	97.8	112.8	79.0	oral	25.0	1
1.50	92.4	115.2	82.2	oral	25.0	1
2.00	81.4	106.4	77.7	oral	25.0	1
2.50	74.3	98.7	73.2	oral	25.0	1
3.00	66.3	89.2	67.4	oral	25.0	1
4.00	55.2	73.4	57.2	oral	25.0	1
6.00	38.2	52.5	42.8	oral	25.0	1
8.00	31.9	38.9	32.9	oral	25.0	1
12.00	21.6	22.3	20.1	oral	25.0	1
0.00	62.0	44.5	40.1	oral	50.0	1
0.33	72.0	109.6	79.9	oral	50.0	1

0.67	131.9	171.1	119.5	oral	50.0	1
1.00	160.5	225.7	158.1	oral	50.0	1
1.50	178.1	230.5	164.4	oral	50.0	1
2.00	164.4	212.8	155.5	oral	50.0	1
2.50	148.3	197.3	146.3	oral	50.0	1
3.00	136.9	178.4	134.7	oral	50.0	1
4.00	120.7	146.8	114.4	oral	50.0	1
6.00	82.7	104.9	85.6	oral	50.0	1
8.00	68.9	77.8	65.8	oral	50.0	1
12.00	42.3	44.5	40.1	oral	50.0	1

*The observed data was digitized by using the publication figure. Therefore, it is possible to have small differences between digitized and source data.

Appendix 5. Observed/predicted ratios for the pharmacokinetic parameters in NYHA III and NYHA IV adult chronic heart failure patients

PK-Parameter	Model-2	Model-1	Model-2	Model-1	Model-2	Model-1	Model-2	Model-1
	NYHA IV-R		NYHA III-R		NYHA IV-N		NYHA III-N	
AUC$_{last}$	1.3	1.0	0.6	0.6	3.5	3.1	1.7	1.5
	1.2	0.9	0.7	0.6	3.1	2.7	1.8	1.6
	1.1	0.9	0.9	0.7	3.1	2.8	2.1	1.8
	1.1	0.9	0.8	0.7	3.2	2.8	2.2	1.9
C$_{max}$	1.4	1.2	1.1	1.0	3.3	2.5	2.4	1.8
	1.7	1.2	1.0	0.9	3.4	2.6	2.2	1.7
	1.4	1.1	1.2	1.0	3.2	2.5	2.6	2.0
	1.2	1.0	1.3	1.1	2.9	2.2	2.7	2.0
CL	1.0	1.0	1.7	1.7	0.3	0.3	0.7	0.7
	1.1	0.9	1.6	1.6	0.4	0.4	0.6	0.6
	1.1	0.9	1.4	1.4	0.4	0.4	0.6	0.5
	1.1	0.9	1.4	1.4	0.4	0.4	0.5	0.5

NYHA III and IV: New York Heart Association chronic heart failure class III and IV, NYHA-R: simulations with incorporation of reductions in organ blood flows,NYHA-N: simulations with normal healthy organ blood flows, AUC$_{last}$: area under the plasma concentration-time curve, C$_{max}$: the maximum concentration and CL: clearance

Appendix 6. Observed and predicted data used for model evaluation in pediatric chronic heart failure patients after oral carvedilol administration

Patient age (years)	time (hour)	Systemic carvedilol concentration (µg/L)		
		Observed	Predicted-N	Predicted-R
0.12	0.50	21.3	26.4	35.0
	0.75	15.3	26.2	34.0
	1.00	10.6	22.3	29.1
	1.50	9.2	15.3	20.5
	2.00	4.9	11.6	15.9
	2.50	3.0	9.1	12.7
	3.00	3.3	7.1	10.3
	4.00	1.8	4.7	6.9
	6.00	0.4	2.3	3.4
	7.00	0.2	1.6	2.4
0.15	0.75	1.0	24.4	30.9
	1.00	1.5	21.0	25.7
	1.50	2.1	14.5	18.4
	2.00	1.9	11.0	13.9
	2.50	2.5	8.6	11.1
	3.00	2.3	6.9	9.1
	4.00	1.5	4.6	6.5
	7.00	0.5	1.6	2.4
0.5	0.25	2.6	13.2	16.0
	0.50	12.3	23.8	29.4
	0.75	7.8	23.5	31.0
	1.00	10.4	20.6	27.8
	1.50	8.3	14.1	19.7
	2.00	5.1	10.1	14.3
	2.50	3.9	7.9	10.7
	3.00	3.2	6.3	8.5
	4.00	2.2	4.2	5.9
	5.00	1.9	2.8	4.3
	6.00	1.1	1.9	3.2
	7.00	0.8	1.3	2.3
	8.00	0.8	0.9	1.7
	12.00	0.4	0.2	0.5
0.75	0.25	2.9	9.5	13.0
	0.50	5.4	18.0	23.8
	0.75	5.6	19.4	25.4
	1.00	5.0	17.8	23.4
	1.50	3.9	12.3	16.9
	2.00	3.7	8.7	12.0

Patient age (years)	time	Systemic carvedilol concentration (µg/L)		
	(hour)	Observed	Predicted-N	Predicted-R
	2.50	2.7	6.6	9.0
	3.00	1.7	5.2	7.2
	4.00	1.2	3.5	5.1
	6.00	0.8	1.6	2.7
	8.00	0.6	0.9	1.5
	12.00	0.3	0.2	0.5
1.25	0.25	21.2	11.5	12.9
	0.50	28.4	19.3	22.1
	0.75	22.2	19.5	23.9
	1.00	26.6	18.6	22.3
	1.50	18.4	12.5	15.9
	2.00	20.9	9.3	11.5
	2.50	11.5	6.9	8.6
	3.00	6.0	5.3	6.9
	4.00	4.2	3.6	4.8
	5.00	2.4	2.5	3.5
	6.00	1.9	1.7	2.6
	8.00	1.5	0.9	1.5
1.5	0.25	2.3	8.2	17.2
	0.50	8.0	15.8	32.3
	0.75	12.7	17.8	35.6
	1.00	14.4	16.1	32.6
	1.50	10.1	11.2	25.0
	2.00	8.1	7.6	18.4
	2.50	7.0	5.8	14.7
	3.00	5.7	4.5	12.1
	4.00	2.9	3.0	9.0
	5.00	2.2	2.1	7.0
	6.00	1.9	1.5	5.6
	7.00	1.3	1.1	4.6
3.5	0.25	10.1	8.7	12.7
	0.50	24.4	15.5	22.0
	0.75	23.4	16.3	23.0
	1.00	12.8	14.7	20.8
	1.50	9.9	10.6	15.5
	2.00	5.0	7.4	11.3
	2.50	4.5	5.6	8.5
	3.00	3.6	4.3	6.8
	4.00	2.4	2.9	4.7
	5.00	1.6	2.0	3.5

Patient age (years)	time	Systemic carvedilol concentration (µg/L)		
	(hour)	Observed	Predicted-N	Predicted-R
	6.00	1.1	1.5	2.6
	7.00	0.8	1.1	1.9
	12.00	0.4	0.2	0.5
5.5	0.25	6.9	8.9	12.1
	0.50	15.6	15.1	19.6
	0.75	16.8	15.3	19.7
	1.00	15.6	13.7	18.1
	1.50	13.9	10.0	13.7
	2.00	9.9	7.2	10.3
	2.50	6.0	5.5	7.9
	3.00	4.8	4.4	6.4
	4.00	4.2	3.0	4.4
	5.00	3.3	2.1	3.2
	6.00	2.3	1.5	2.3
	7.00	1.9	1.1	1.7
	8.00	0.9	0.8	1.2
	12.00	0.6	0.2	0.4
7.5	0.25	7.1	8.7	11.7
	0.50	15.3	14.7	19.2
	0.75	13.5	15.0	19.4
	1.00	12.2	13.3	17.5
	1.50	8.1	9.8	13.3
	2.00	6.5	7.2	10.1
	2.50	4.5	5.6	8.0
	3.00	3.7	4.5	6.4
	4.00	2.0	3.1	4.5
	5.00	1.6	2.1	3.2
	6.00	2.1	1.5	2.3
	7.00	1.7	1.0	1.7
	8.00	0.7	0.7	1.2
	12.00	0.4	0.2	0.3
8.25	0.25	7.1	8.6	17.0
	0.50	9.5	14.4	27.2
	0.75	6.6	15.0	27.4
	1.00	7.9	13.3	24.8
	1.50	7.8	9.8	19.0
	2.00	6.6	7.2	15.1
	2.50	3.5	5.7	12.2
	3.00	2.7	4.5	10.3
	4.00	5.7	3.1	7.6

Patient age (years)	time (hour)	Systemic carvedilol concentration (µg/L)		
		Observed	Predicted-N	Predicted-R
	5.00	2.4	2.1	5.9
	6.00	1.2	1.5	4.6
	7.00	0.9	1.1	3.7
	8.00	0.5	0.7	2.9
10.75	0.25	9.7	8.2	11.1
	0.50	13.7	13.8	18.3
	0.75	12.6	14.1	19.1
	1.00	10.5	13.0	17.8
	1.50	10.8	9.5	13.4
	2.00	7.5	7.0	10.0
	3.00	3.9	4.1	6.5
	4.00	3.2	2.8	4.5
	6.00	2.2	1.2	2.2
	8.00	1.6	0.6	1.1
11.6	0.25	0.5	9.0	13.4
	0.50	17.7	14.7	22.3
	0.75	31.7	15.3	23.3
	1.00	23.6	14.2	20.8
	1.50	18.6	9.8	15.1
	2.00	16.0	6.9	10.9
	2.50	8.7	5.1	8.2
	3.00	7.4	4.0	6.6
	4.00	4.7	2.6	4.7
	5.00	3.3	1.8	3.4
	6.00	2.7	1.3	2.6
	7.00	1.9	0.9	1.9
	8.00	1.6	0.6	1.4
11.8	0.25	3.3	8.0	
	0.50	8.7	13.5	
	0.75	11.7	13.7	
	1.00	11.8	12.8	
	1.50	8.8	9.2	
	2.00	6.4	6.7	
	2.50	4.9	5.1	
	3.00	4.0	4.0	
	4.00	2.0	2.7	
	5.00	1.7	1.8	
	6.00	1.3	1.3	
	7.00	0.7	0.9	
	8.00	0.6	0.6	

Patient age (years)	time	Systemic carvedilol concentration (µg/L)		
	(hour)	Observed	Predicted-N	Predicted-R
17.5	0.25	16.0	7.9	11.7
	0.50	36.4	12.8	18.1
	0.75	32.5	12.8	18.6
	1.00	26.8	11.0	16.1
	1.50	23.0	8.1	11.2
	2.00	17.8	5.9	8.5
	2.50	12.9	4.9	6.9
	3.00	11.7	4.1	6.0
	4.00	6.2	3.1	4.7
	5.00	4.6	2.4	3.7
	6.00	3.8	1.9	3.0
	8.00	2.6	1.1	2.0
	12.00	1.3	0.4	0.9
17.8	0.25	2.8	7.9	17.7
	0.50	16.4	12.7	27.1
	0.75	13.3	12.8	27.0
	1.00	11.7	11.2	23.6
	1.50	9.3	8.1	16.4
	2.00	6.4	5.9	12.5
	2.50	4.2	4.8	10.3
	3.00	4.5	4.1	9.1
	4.00	4.0	3.1	7.4
	5.00	3.3	2.4	6.3
	6.00	2.3	1.9	5.4
	7.00	1.6	1.4	4.6
	8.00	1.4	1.1	4.0
19.3	0.25	29.4	7.5	16.6
	0.5	35.6	12.0	26.6
	0.75	33.0	13.0	28.4
	1	22.3	11.7	25.7
	1.5	18.8	8.4	18.7
	2	14.2	6.2	14.1
	2.5	10.9	5.0	11.4
	3	9.0	4.1	9.9
	4	5.7	3.1	8.1
	6	3.5	2.0	5.9
	7	1.8	1.6	5.1
	8	1.2	1.3	4.5

Predicted-N: simulations with normal healthy organ blood flows, Predicted-R: simulations with incorporation of reductions in organ blood flows. Observed clinical data: (Behn, 2001)

Appendix 7. Observed/predicted ratios for the pharmacokinetic parameters in pediatric chronic heart failure patients

Pharmacokinetic parameter	19.3 years patient				All pediatric patients			
	Model-2-R	Model-1-R	Model-2-N	Model-1-N	Model-2-R	Model-1-R	Model-2-N	Model-1-N
AUC_{last}	0.9	0.7	2.2	1.9	0.4	0.4	0.5	0.6
					0.1	0.1	0.2	0.2
					0.4	0.2	0.5	0.7
					0.3	0.3	0.4	0.4
					1.2	1.1	1.5	1.8
					0.4	0.3	0.9	0.9
					0.6	0.6	1.0	1.0
					0.9	0.8	1.3	1.2
					0.7	0.6	0.9	0.9
					0.4	0.3	0.8	0.7
					0.8	0.6	1.1	0.9
					1.1	0.9	1.7	1.5
					1.6	1.5	0.9	0.7
					0.4	0.4	0.9	0.9
							2.3	2.4
C_{max}	1.2	0.9	2.7	2.4	0.6	0.6	0.8	0.8
					0.1	0.1	0.1	0.1
					0.4	0.3	0.5	0.6
					0.2	0.2	0.3	0.3
					1.2	1.1	1.4	1.5
					0.4	0.3	0.8	0.8
					1.1	0.9	1.5	1.3
					0.8	0.7	1.1	0.9
					0.8	0.6	1.0	0.8
					0.3	0.3	0.6	0.5

Pharmacokinetic parameter	19.3 years patient				All pediatric patients			
	Model-2-R	Model-1-R	Model-2-N	Model-1-N	Model-2-R	Model-1-R	Model-2-N	Model-1-N
					0.7	0.6	1.0	0.8
					1.4	1.0	2.0	1.8
					0.6	0.5	0.8	0.7
					1.9	1.7	1.2	1.0
							2.2	2.3
CL	1.4	1.5	0.5	0.5	2.9	2.6	2.1	1.8
					7.4	7.6	5.6	5.5
					2.5	4.3	1.8	1.4
					3.5	3.6	2.4	2.3
					0.8	0.9	0.6	0.6
					3.0	3.7	1.1	1.1
					1.5	1.7	1.0	1.0
					1.1	1.3	0.8	0.8
					1.5	1.7	1.1	1.2
					3.0	3.7	1.3	1.4
					1.1	1.6	0.8	1.1
					0.9	1.2	0.5	0.7
					2.7	2.5	1.2	1.4
					0.6	0.6	1.1	1.1
							0.4	0.4

Model-1-N: simulations with normal healthy organ blood flows, Model-1-R: simulations with incorporation of reductions in organ blood flows, Model-2-N: simulations with normal healthy organ blood flows, Model-2-R: simulations with incorporation of reductions in organ blood flows.

Appendix 8. Observed and predicted data used for model evaluation in healthy adults after administering 12.5 mg intravenous racemic carvedilol

Time	Systemic R-carvedilol concentration (µg/L)			Time	Systemic S-carvedilol concentration (µg/L)		
(hour)	Predicted	Neugebauer et al*	Spahn et al*	(hour)	Predicted	Neugebauer et al*	Spahn et al*
0.25	51.8	54.3	34.6	0.25	43.5	47.7	30.5
0.50	62.4	70.0	44.8	0.50	50.9	58.5	41.2
0.75	69.9	70.2	61.5	0.75	56.3	58.1	55.2
1.00	71.2	84.6	71.5	1.00	56.8	70.6	65.5
1.15	33.1		46.6	1.15	23.8		35.4
1.25	29.4		31.0	1.25	21.1		29.0
1.50	24.0	37.8	25.8	1.50	17.3	27.4	22.4
2.00	19.2	29.0	21.1	1.75	14.8		18.9
2.50	16.1		17.5	2.00	13.6	21.8	19.9
3.00	13.6	15.6	17.9	2.50	11.3		15.2
3.50	11.9		15.6	3.00	9.6	11.3	14.6
4.00	10.6	10.4	12.4	3.50	8.4		11.5
6.00	6.5	5.0	9.6	4.00	7.3	8.0	12.6
8.00	4.1	3.4	6.4	6.00	4.3	4.4	8.5
10.00	2.6	2.4		8.00	2.7	2.5	5.2
12.00	1.7	1.4		10.00	1.7	1.5	
14.00	1.1	0.8					

*The observed data was digitized by using the publication figure. Therefore, it is possible to have small differences between digitized and source data.

Appendix 9. Observed and predicted data used for model evaluation in healthy adults after administering 50mg oral racemic carvedilol

Time	Systemic R-carvedilol concentration (µg/L)			Time	Systemic S-carvedilol concentration (µg/L)		
(hour)	Predicted	Neugebauer et al*	Spahn et al*	(hour)	Predicted	Neugebauer et al*	Spahn et al*
0.25	30.5	7.8		0.25	8.6	3.1	
0.50	53.8		5.4	0.50	14.3	23.7	4.5
0.75	60.4	50.9	28.1	0.75	15.6	21.5	11.8
1.00	60.1	65.6	50.9	1.00	17.9	21.0	20.5
1.50	49.1	54.6	54.7	1.50	17.6	16.9	20.1
2.00	37.9	45.0	54.7	2.00	14.0	13.6	21.1
2.50	30.4		59.7	2.50	13.2		23.4
3.00	24.6	24.0	40.5	3.00	12.1	7.5	15.0
3.50	20.2		28.6	3.50	10.6		11.8
4.00	17.6	15.7	22.9	4.00	9.1	5.0	10.7
6.00	10.5	6.8	13.0	6.00	5.5	2.6	6.0
8.00	6.4	3.9	7.6	8.00	3.5	1.9	5.2
10.00	4.2	2.6		10.00	2.1	1.1	
12.00	2.8	1.7		12.00	1.3	1.0	
24.00	0.2	0.4		14.00	0.9	0.5	

*The observed data was digitized by using the publication figure. Therefore, it is possible to have small differences between digitized and source data.

Appendix 10. Observed and predicted data used for model evaluation in healthy adults (n=7), after administering 0.09mg/kg oral racemic carvedilol.

Time (hour)	Systemic R-carvedilol concentration (µg/L) Predicted	Behn, 2001						
0.25	4.2	2.1	1.5	3.5	4.4	4.5	5.8	0.2
0.50	7.3	5.3	2.8	8.6	6.5	9.9	7.8	0.5
0.75	8.1	8.7		11.6	6.8	10.3	8.0	1.1
1.00	8.0	9.6	2.5	12.3	7.4	9.6	8.2	1.8
1.50	6.5	7.6	2.6	13.5	6.8	9.7	5.6	2.4
2.00	5.0	7.0	2.2	10.7	5.3	11.4	5.4	2.5
2.50	3.9	5.8	1.5	7.9	4.6	13.8	4.4	2.7
3.00	3.1	4.4		5.9		9.0	2.3	2.2
3.50	2.6					9.1		
4.00	2.3	3.0	0.7	3.7	2.6	7.2	1.3	2.1
5.00	1.7	1.8	0.5	2.7	1.7	3.5	1.5	1.4
6.00	1.3	1.2	0.4	1.6	1.2	3.1		1.1
7.00	1.0							0.5
8.00	0.8		0.4	0.8	0.7	2.3		0.8
10.00	0.5	0.5						
12.00	0.3			0.3	1.2			
24.00	0.0				0.3			

Time (hour)	Systemic S-carvedilol concentration (µg/L) Predicted	Behn, 2001						
0.25	1.0	0.2	2.3	1.4	1.2	1.4	1.2	3.0
0.50	1.9	0.3	4.0	3.0	2.4	1.5	1.6	3.6
0.75	2.4	0.5	3.6	3.9	3.2	1.6	1.3	3.2
1.00	2.6	0.8	3.3	5.3	3.5	1.6	1.4	3.1
1.50	2.5	0.8	3.2	4.2	2.9	1.4	1.2	2.0
2.00	2.2	0.8	4.2	3.1	2.8	1.2		2.1
2.50	1.9	0.8	5.6	2.6	2.7	1.0	0.8	1.8
3.00	1.6	0.6	3.4	1.7	1.8			1.0
4.00	1.2	0.7	2.4	1.3	1.5	0.7	0.5	0.7
5.00	0.9	0.6	1.1	1.0	0.9	0.6	0.5	0.9
6.00	0.7	0.5	1.1	0.7	0.8	0.5	0.4	
8.00	0.4	0.5	1.0	0.5		0.4	0.5	
10.00	0.2				0.5			
12.00	0.1		0.7			0.3		

Appendix 11. Observed and predicted data used for model evaluation in extensive and poor metabolizers of CYP2D6 after administering 25mg oral racemic carvedilol

Time	Systemic R-carvedilol concentration (µg/L)				Time	Systemic S-carvedilol concentration (µg/L)			
(hour)	EM-P	EM*	PM-P	PM*	(hour)	EM-P	EM*	PM-P	PM*
0.25	16.2	20.4	29.1	12.6	0.25	3.9	11.1	5.0	6.2
0.50	27.9	35.5	58.2	40.4	0.50	7.3	18.8	12.8	16.5
0.75	31.7	35.4	69.2	65.3	0.75	9.4	15.1	15.7	23.0
1.00	31.9	33.4	72.0	72.2	1.00	10.0	13.2	17.4	21.7
1.25	28.1	35.9	68.6	74.2	1.25	10.0	14.3	18.4	20.2
1.50	25.2	34.8	63.1	72.0	1.50	9.5	13.6	17.9	18.8
2.00	19.6	30.9	51.9	63.1	2.00	8.3	11.5	16.1	14.3
2.50	15.5	25.5	43.3	52.8	2.50	7.0	9.6	14.5	11.5
3.00	12.3	22.3	37.5	49.7	3.00	5.9	8.1	12.5	11.0
4.00	8.8	15.9	30.3	38.1	4.00	4.4	6.2	9.3	8.2
6.00	5.2	7.8	22.7	24.1	6.00	2.6	3.3	5.4	5.1
8.00	3.2	4.3	15.0	15.2	8.00	1.6	2.4	3.4	3.2
10.00	1.9	2.8	10.8	12.6	10.00	0.9	1.8	2.2	2.9

EM-P: model predicted values in extensive metabolizers, EM: observed data in extensive metabolizers, PM-P: model predicted values in poor metabolizers, PM: observed data in poor metabolizers. EM and PM: Observed data from (Zhou and Wood, 1995).

*The observed data was digitized by using the publication figure. Therefore, it is possible to have small differences between digitized and source data.

Appendix 12. Observed/predicted ratios for the pharmacokinetic parameters in adults after administering racemic carvedilol

PK-Parameter	R-carvedilol					S-carvedilol				
	iv	oral				iv	oral			
	12.5 mg	50 mg	25 mg-EM	25 mg-PM	0.09 mg/kg	12.5 mg	50 mg	25 mg-EM	25 mg-PM	0.09 mg/kg
C_{max}	1.1	1.1	1.1	1.0	1.0	0.9	1.3	1.8	1.2	1.3
	0.9	1.0				1.1	1.3			
CL	0.9	1.1	0.7	0.9	1.0	1.2	1.3	0.6	1.0	1.1
	0.9	0.9				0.8	0.8			

iv: intravenous, EM: extensive metabolizers, PM: poor metabolizers.

Appendix 13. Observed and predicted data used for model evaluation in adult CHF patients after administering steady state doses of oral racemic carvedilol

Time	Systemic R-carvedilol concentration (µg/L)		Systemic S-carvedilol concentration (µg/L)		Dose
(hour)	Predicted	Tenero et al*	Predicted	Tenero et al.*	(mg)
0.00	2.6	4.8	1.7	2.2	6.25
0.33	6.6	7.8	3.5	3.9	6.25
0.67	11.3	11.7	5.5	5.3	6.25
1.00	13.6	14.9	6.6	6.5	6.25
1.50	14.3	15.9	7.2	6.7	6.25
2.00	13.5	13.7	7.0	5.4	6.25
2.50	12.1	12.1	6.6	5.0	6.25
3.00	10.7	11.0	6.0	4.7	6.25
4.00	8.3	9.5	5.0	4.0	6.25
6.00	5.6	4.4	3.6	2.6	6.25
8.00	4.2	5.7	2.7	2.6	6.25
12.00	2.6	3.7	1.7	2.0	6.25
0.00	5.1	8.8	3.4	4.1	12.5
0.33	13.3	9.1	7.0	4.5	12.5
0.67	22.5	18.5	10.9	9.7	12.5
1.00	27.2	27.6	13.1	12.8	12.5
1.50	28.5	30.3	14.2	13.6	12.5
2.00	26.8	26.8	13.9	11.7	12.5
2.50	24.0	25.3	13.0	10.7	12.5
3.00	21.1	22.4	11.9	9.8	12.5
4.00	16.4	19.2	9.8	8.1	12.5
6.00	11.0	12.6	6.9	5.8	12.5
8.00	8.2	10.2	5.3	5.0	12.5
12.00	5.1	6.5	3.4	3.7	12.5
0.0	10.1	19.1	6.5	9.1	25

Time	Systemic R-carvedilol concentration (µg/L)		Systemic S-carvedilol concentration (µg/L)		Dose
(hour)	Predicted	Tenero et al*	Predicted	Tenero et al.*	(mg)
0.33	26.4	22.2	13.7	10.6	25
0.67	44.6	47.9	21.5	22.3	25
1.00	53.8	65.2	25.7	30.3	25
1.50	56.4	61.4	27.7	26.8	25
2.00	52.9	56.1	27.0	23.0	25
2.50	47.4	49.7	25.2	21.7	25
3.00	41.7	45.4	22.9	18.6	25
4.00	32.3	36.7	18.8	15.5	25
6.00	21.6	25.5	13.1	12.2	25
8.00	16.2	20.7	10.0	10.5	25
12.00	10.1	13.2	6.5	7.6	25
0.0	19.9	41.1	12.2	20.3	50
0.33	52.2	45.0	26.3	25.1	50
0.67	87.3	88.6	41.3	45.1	50
1.00	104.3	109.9	49.2	52.6	50
1.50	108.8	120.7	52.4	56.0	50
2.00	102.1	103.6	50.6	49.6	50
2.50	91.7	94.6	46.9	46.7	50
3.00	81.0	89.1	42.6	42.7	50
4.00	63.0	84.0	34.8	37.8	50
6.00	41.9	56.7	24.2	26.3	50
8.00	31.5	37.1	18.5	22.0	50
12.00	19.9	29.3	12.2	16.9	50

*The observed data was digitized by using the publication figure. Therefore, it is possible to have small differences between digitized and source data.

Appendix 14. Observed/predicted ratios for the pharmacokinetic parameters in adult CHF patients

R-carvedilol			S-carvedilol		
C_{max}	AUC	CL/F	C_{max}	AUC	CL/F
1.2	1.2	0.8	0.9	1.0	1.0
1.1	1.2	0.8	1.0	1.1	0.9
1.2	1.3	0.8	1.1	1.1	0.9
1.1	1.2	0.6	1.1	1.3	0.8

Appendix 15. Observed and predicted data used for model evaluation in pediatric CHF patients after administering 0.09mg/kg of oral racemic carvedilol

Patient age Group/years	Time (hour)	Systemic R-carvedilol concentration (µg/L) Predicted	Individual patients; Behn, 2001							Time (hour)	Systemic S-carvedilol concentration (µg/L) Predicted	Individual patients; Behn, 2001						
Infants	0.25	4.8				1.8				0.25	1.3				0.7			
	0.50	9.0	10.0	2.8		7.9	4.0		1.7	0.50	2.7	3.5	2.1		2.6	1.8		1.1
	0.75	9.9	6.3		0.5	6.8	3.6	17.1		0.75	3.5	2.4		0.4	2.2	1.9	7.3	
	1.00	9.1	3.6	3.2	0.9	6.1	3.2	14.7	9.0	1.00	3.7	1.5	2.8	0.6	1.8	1.3	6.5	4.1
	1.50	6.6	3.5	2.0	1.2	5.3	2.7	11.9	6.8	1.50	3.2	1.5	1.6	0.9	1.7	1.5	4.9	2.7
	2.00	4.4	2.3	1.6	1.1	4.3		11.4	4.6	2.00	2.4	1.1	1.1	0.8	1.4		4.6	2.4
	2.50	3.2	1.6	1.1	1.5	2.8		7.4	3.7	2.50	1.8	0.9	1.0	1.0	1.0		3.2	1.8
	3.00	2.3	1.2	2.3	1.3	1.7		3.9	3.0	3.00	1.3	0.7	2.0	1.0	0.8		1.9	1.8
	4.00	1.4	1.3	1.8	0.8	1.2	0.8	2.7	1.5	4.00	0.8	0.7	1.4	0.7	0.5	0.6	1.4	1.0
	5.00	0.9				1.0			1.3	5.00	0.5				0.6			0.9
	6.00	0.5		1.1		0.7	0.4	0.8		6.00	0.3		0.7		0.4	0.4	0.6	
	8.00	0.2						0.6		8.00	0.1						0.7	
Young children	0.25	4.3	6.2	3.5						0.25	1.1	2.8	2.9					
	0.50	7.6	13.2	8.3						0.50	2.2	5.1	5.4					
	0.75	7.9	12.2	10.5						0.75	2.7	4.4	6.5					
	1.00	7.5	9.0	9.3						1.00	2.8	3.3	5.8					
	1.50	6.0	6.1	9.4						1.50	2.5	2.2	5.7					
	2.00	4.2	3.3	5.7						2.00	2.0	1.2	3.5					
	2.50	3.0	2.3	4.0						2.50	1.6	0.9	2.5					
	3.00	2.2	1.5	2.7						3.00	1.2	0.7	2.0					
	4.00	1.3	0.7	1.9						4.00	0.7	0.5	1.5					
	5.00	0.8	0.5	2.0						5.00	0.5	0.4	1.6					
	6.00	0.5	0.3	1.6						6.00	0.3	0.3	1.4					
	8.00	0.2		0.5						8.00	0.1		0.5					
Children	0.25	4.4	5.0		2.4					0.25	1.1	2.2		0.9				

Patient age Group/years	Time (hour)	Systemic R-carvedilol concentration (µg/L)				Time (hour)	Systemic S-carvedilol concentration (µg/L)			
		Predicted	Individual patients; Behn, 2001				Predicted	Individual patients; Behn, 2001		
	0.50	7.5	6.7	11.4	6.5	0.50	2.1	3.0	5.0	2.1
	0.75	7.9	4.5	19.8	9.7	0.75	2.5	1.7	6.8	3.2
	1.00	7.7	5.6	19.0	8.8	1.00	2.6	2.4	6.1	2.4
	1.50	6.2	5.7		7.0	1.50	2.6	2.4		1.7
	2.00	4.8	4.5	9.5	5.1	2.00	2.3	2.4	3.0	1.5
	2.50	3.6	2.4	6.6	4.0	2.50	1.9	1.2	2.6	1.0
	3.00	2.8	1.7	4.7	3.0	3.00	1.5	1.0	1.7	0.9
	4.00	1.7	0.9	2.5	1.6	4.00	0.9	0.6	1.1	1.0
	5.00	1.0	0.7		1.6	5.00	0.6	0.6		0.8
	6.00	0.6	0.6		1.3	6.00	0.4	0.6		0.7
	8.00	0.3			0.6	8.00	0.2			0.5
Adolescents	0.25	3.9	11.2	1.9		0.25	1.1	6.0	0.8	
	0.50	7.0	27.6	10.4		0.50	2.1	12.4	3.8	
	0.75	8.4	24.2	10.5		0.75	2.5	8.6	3.8	
	1.00	8.3	21.7	8.7		1.00	2.7	7.2	3.2	
	1.50	7.0	18.8	6.1		1.50	2.7	6.4	2.1	
	2.00	5.4	13.7	4.5		2.00	2.3	4.3	1.6	
	2.50	4.3	10.3	3.2		2.50	2.0	3.5	1.2	
	3.00	3.5	9.6	2.0		3.00	1.6	3.0	0.9	
	4.00	2.4	5.2	2.1		4.00	1.2	1.3	1.0	
	5.00	1.7	4.0	1.7		5.00	0.8	1.2	1.0	
	6.00	1.2	3.2	1.0		6.00	0.6	1.0	0.7	
	7.00	0.9		1.1		7.00	0.4		0.8	
	8.00	0.7	2.1			8.00	0.3	0.8		
17.5-years*	0.25	4.1	11			0.25	1.7	6.0		
	0.50	7.9	28			0.50	3.2	12.4		
	0.75	10.0	24			0.75	4.1	8.6		
	1.00	10.6	22			1.00	4.5	7.2		
	1.50	10.3	19			1.50	4.7	6.4		

Patient age	Time	Systemic R-carvedilol concentration (µg/L)		Time	Systemic S-carvedilol concentration (µg/L)	
Group/years	(hour)	Predicted	Individual patients; Behn, 2001	(hour)	Predicted	Individual patients; Behn, 2001
	2.00	9.0	14	2.00	4.5	4.3
	2.50	7.5	10	2.50	4.0	3.5
	3.00	6.3	9.6	3.00	3.5	3.0
	4.00	4.6	5.2	4.00	2.7	1.3
	5.00	3.6	4	5.00	2.2	1.2
	6.00	2.9	3.2	6.00	1.8	1.0
	8.00	1.9	2.1	8.00	1.2	0.8
19.3-years*	0.25	4.9	19	0.25	2.6	9.7
	0.50	10.3	25	0.50	5.3	12.2
	0.75	13.1	14	0.75	7.1	5.9
	1.00	14.6	19	1.00	8.0	8.5
	1.50	14.4	13	1.50	8.4	5.6
	2.00	13.5	7.6	2.00	8.2	3.0
	2.50	11.9	5.5	2.50	7.5	2.4
	3.00	10.3	5.5	3.00	6.7	3.3
	4.00	7.5	3.4	4.00	5.0	2.0
	5.00	5.9	2.8	5.00	4.0	2.5
	6.00	4.8	1.4	6.00	3.2	1.3
	8.00	3.5	0.6	8.00	2.4	2.0

*Predictions with incorporation of reduced organ/tissue blood flows

Appendix 16. Observed/predicted ratios for the pharmacokinetic parameters in pediatric CHF patients

	PK-Parameter	All Patients	19.3 year*	19.3 year	17.8 year	17.5 year*	17.5 year	Children	Young Children	Infants
R-carvedilol	Cmax	1.2	1.7	3.2	1.2	2.5	3.4	1.3	1.5	0.8
	CL	1.1	1.7	0.6	1.1	0.7	0.4	0.9	0.8	1.2
S-carvedilol	Cmax	1.2	1.4	4.7	1.3	2.6	4.9	1.2	2.0	0.8
	CL	1.0	1.5	0.3	0.7	1.0	0.4	0.9	0.7	1.4

* Predictions with incorporation of reduced organ/tissue blood flows

Appendix 17. Observed and predicted data used for model evaluation in healthy and cirrhosis patients after administering iv and oral carvedilol.

Time	Systemic carvedilol concentration (µg/L)		Route	Dose (mg)	Population
(hour)	Predicted	Neugebauer et al*.	Route	Dose (mg)	Population
0.37	106.2	112.0	iv	12.50	Healthy
0.60	126.4	136.0	iv	12.50	Healthy
0.84	144.4	160.0	iv	12.50	Healthy
1.00	142.3	177.5	iv	12.50	Healthy
1.08	74.4	88.5	iv	12.50	Healthy
1.25	68.3	72.8	iv	12.50	Healthy
1.33	60.6	65.3	iv	12.50	Healthy
1.50	50.0	54.8	iv	12.50	Healthy
1.75	44.1	48.2	iv	12.50	Healthy
2.00	40.1	42.3	iv	12.50	Healthy
2.50	34.0	34.0	iv	12.50	Healthy
3.00	29.9	30.3	iv	12.50	Healthy
3.50	26.8	26.2	iv	12.50	Healthy
4.00	23.4	22.1	iv	12.50	Healthy
6.00	15.5	13.7	iv	12.50	Healthy
8.00	10.3	9.4	iv	12.50	Healthy
10.00	6.9	6.2	iv	12.50	Healthy
12.00	4.9	4.0	iv	12.50	Healthy
14.00	3.4	2.8	iv	12.50	Healthy
24.00	0.6	0.5	iv	12.50	Healthy
0.50	116.7	128.0	iv	12.50	Cirrhosis
0.75	133.9	149.2	iv	12.50	Cirrhosis
1.00	151.6	100.0	iv	12.50	Cirrhosis
2.00	54.8	41.8	iv	12.50	Cirrhosis
4.00	40.2	22.5	iv	12.50	Cirrhosis
8.00	27.4	17.4	iv	12.50	Cirrhosis
12.00	19.3	13.9	iv	12.50	Cirrhosis
24.00	7.1	6.2	iv	12.50	Cirrhosis
32.00	3.6	2.4	iv	12.50	Cirrhosis
0.25	10.8	1.0	oral	25.00	Healthy
0.50	16.5	7.8	oral	25.00	Healthy
0.75	22.7	13.7	oral	25.00	Healthy
1.00	26.1	17.2	oral	25.00	Healthy
1.50	28.1	21.9	oral	25.00	Healthy
2.00	26.8	18.4	oral	25.00	Healthy
2.50	24.3	17.8	oral	25.00	Healthy
3.00	21.4	14.8	oral	25.00	Healthy
3.50	19.1	12.7	oral	25.00	Healthy

Time	Systemic carvedilol concentration (µg/L)		Route	Dose (mg)	Population
(hour)	Predicted	Neugebauer et al*.	Route	Dose (mg)	Population
4.00	16.8	10.1	oral	25.00	Healthy
6.00	10.6	6.7	oral	25.00	Healthy
8.00	7.2	4.3	oral	25.00	Healthy
10.00	4.7	3.2	oral	25.00	Healthy
12.00	3.3	2.7	oral	25.00	Healthy
14.00	2.3	1.8	oral	25.00	Healthy
0.25	30.2	50.5	oral	25.00	Cirrhosis
0.75	71.7	98.6	oral	25.00	Cirrhosis
1.25	112.0	103.0	oral	25.00	Cirrhosis
2.25	116.5	79.4	oral	25.00	Cirrhosis
4.25	89.9	54.1	oral	25.00	Cirrhosis
8.50	57.3	36.7	oral	25.00	Cirrhosis
13.00	39.0	22.6	oral	25.00	Cirrhosis
24.00	14.5	12.0	oral	25.00	Cirrhosis
32.00	7.3	5.5	oral	25.00	Cirrhosis

*The observed data was digitized by using the publication figure. Therefore, it is possible to have small differences between digitized and source data.

Appendix 18. Unbound and total area under the curve (AUC) for carvedilol in healthy and cirrhosis populations

AUC Total				AUC Unbound			
Administered carvedilol dose: 25mg							
Healthy	CP-A	CP-B	CP-C	Healthy	CP-A	CP-B	CP-C
76.8	215.2	466.4	682.1	0.4	1.3	3.4	6.7
107.4	298.6	675.4	1017.9	0.5	1.7	4.7	9.5
299.0	918.3	2039.3	2905.7	1.4	4.5	11.9	22.7
129.9	328.0	693.3	1022.7	0.8	2.6	7.2	14.4
240.7	671.5	1318.6	1672.3	1.2	3.6	8.7	15.0
818.3	1732.5	2491.5	2620.4	4.0	9.5	16.8	23.8
185.1	438.7	957.5	1515.4	1.2	3.6	10.5	22.5
202.8	566.8	1141.1	1520.4	0.9	2.6	6.2	11.0
78.4	208.3	464.2	684.9	0.5	1.6	4.9	9.8
78.5	248.1	598.5	1000.5	0.4	1.7	5.2	11.8
156.6	381.5	868.4	1300.7	0.7	2.5	7.3	14.9
156.2	471.2	929.8	1230.9	0.8	2.9	7.3	13.0
55.1	177.9	432.1	744.6	0.3	1.2	3.6	8.3
278.6	684.3	1211.4	1832.3	1.2	2.8	8.1	16.3
275.6	584.6	1144.7	1433.1	1.4	4.4	11.3	19.1
236.4	619.3	1371.4	2176.8	1.2	3.5	9.7	20.7
207.0	586.1	1255.4	1764.2	1.0	3.2	8.6	16.3
231.7	578.3	1168.9	1612.7	1.3	3.7	9.4	17.5
86.3	225.7	530.8	882.3	0.4	1.5	4.5	10.0
171.1	447.5	952.3	1371.9	1.0	3.0	8.1	15.9
110.4	274.2	631.2	975.6	0.6	1.7	4.8	9.8
127.1	341.3	627.1	797.4	0.7	2.1	4.8	8.2
191.0	152.5	363.4	597.5	1.1	1.0	3.0	6.5
359.7	843.5	1400.3	2010.8	2.2	6.3	13.8	21.8
21.8	59.7	145.9	249.7	0.1	0.4	1.3	3.0
196.1	383.2	805.0	1182.6	1.1	2.2	5.8	11.3
163.2	547.0	1237.6	1992.2	0.8	2.7	7.2	15.5
140.9	402.0	903.3	1495.2	0.7	2.3	7.0	15.6
251.7	870.1	1870.7	2597.0	1.4	4.6	12.0	22.3
64.6	183.0	440.7	755.0	0.4	1.5	5.0	11.7
338.6	864.1	1883.3	2732.0	2.0	6.6	19.0	37.7
96.8	279.0	671.0	1031.7	0.5	1.8	5.6	11.8
467.8	1172.9	1933.6	2085.7	2.0	5.1	9.8	14.1
164.3	343.0	719.9	1020.2	0.8	2.1	5.5	10.3
210.8	287.4	582.7	819.6	1.2	2.0	5.3	10.1
300.7	438.8	902.3	1257.5	1.6	3.0	8.0	14.9
142.9	419.7	1104.4	1855.8	0.7	2.5	8.2	18.6
218.4	557.3	1408.9	2117.9	1.3	2.4	6.9	13.7
142.1	326.9	717.8	1181.6	0.8	2.2	6.2	12.4
110.4	192.7	462.7	773.8	0.6	1.4	4.5	10.1

AUC Total				AUC Unbound			
Administered carvedilol dose: 25mg							
120.8	336.2	834.5	1407.9	0.6	1.7	5.0	11.1
65.5	181.6	422.7	671.3	0.4	1.2	3.5	7.5
168.9	496.8	1035.1	1409.7	0.8	3.3	8.7	16.0
132.0	325.0	805.1	2021.8	0.6	2.1	6.7	14.6
79.3	228.3	545.6	872.2	0.5	1.6	4.9	10.5
133.4	653.7	1572.2	2429.9	0.7	2.7	7.4	15.2
162.2	346.4	757.7	1121.5	0.9	2.3	6.3	12.6
441.3	391.9	837.4	1216.3	2.4	2.1	5.4	10.4
713.0	483.1	1038.8	1429.0	3.4	3.0	8.1	15.0
118.8	673.8	1484.0	2160.8	0.6	3.4	9.1	17.6
194.7	408.9	896.6	1324.8	0.9	2.5	6.9	13.6
68.9	616.2	948.7	1101.2	0.4	4.5	9.0	14.0
163.4	430.7	949.6	1379.7	1.0	2.1	5.6	10.7
396.9	434.4	851.1	1133.1	2.2	2.7	6.8	12.1
189.5	646.8	1247.3	1680.0	1.0	3.7	8.7	15.6
172.4	269.3	535.4	787.4	0.7	1.8	4.4	8.7
156.6	160.6	412.3	994.7	0.8	1.2	3.9	8.6
305.4	844.7	1644.4	2102.8	1.7	4.0	9.3	15.9
177.0	214.6	529.7	876.7	1.1	1.3	3.9	8.7
388.4	455.5	966.7	1478.2	1.8	3.4	9.5	19.7
385.0	290.3	645.9	991.0	2.1	1.7	4.7	9.7
94.0	524.4	1061.8	1304.3	0.5	3.3	8.4	15.8
199.2	476.9	1112.1	1731.6	1.0	2.6	7.6	15.7
84.8	266.2	608.0	952.4	0.4	1.4	3.8	7.9
76.2	332.4	755.7	1137.4	0.4	2.0	5.6	11.5
149.6	499.3	1234.0	1857.6	0.8	2.2	6.5	13.1
260.8	688.1	1439.2	2027.2	1.5	3.5	8.9	16.7
176.6	558.5	1097.5	1452.1	0.7	3.7	9.1	16.2
125.5	326.7	772.4	1232.8	0.7	1.9	5.7	12.2
190.4	384.3	750.5	1001.0	1.1	2.9	7.5	13.4
267.6	661.3	1532.3	2194.9	1.4	3.9	11.1	21.4
600.7	252.3	689.5	1422.9	3.5	1.5	5.1	11.2
147.2	336.1	696.9	970.2	0.9	2.5	6.7	12.7
89.2	227.0	570.3	995.3	0.6	1.4	4.5	10.6
265.0	583.6	1125.9	1521.1	1.4	3.5	8.6	15.4
252.9	593.3	1224.8	1675.8	1.2	3.0	7.4	13.5
37.3	269.0	720.8	1264.2	0.2	1.4	4.6	10.8
284.7	634.1	1318.1	1758.7	1.5	4.1	10.7	19.4
57.7	345.3	754.9	1173.1	0.3	2.1	5.6	11.7
114.0	330.2	837.3	1403.2	0.5	1.7	5.1	11.4
294.4	609.0	1202.2	1615.7	1.5	3.6	8.8	15.9
247.1	610.5	1296.9	1814.0	1.2	3.1	8.1	15.1
69.9	185.9	480.2	767.4	0.4	1.3	4.2	9.0
430.1	989.9	1785.9	2246.0	2.3	5.7	12.7	21.4

AUC Total				AUC Unbound			
Administered carvedilol dose: 25mg							
114.8	314.7	737.1	1125.2	0.6	1.7	5.0	10.2
133.8	288.9	595.9	833.8	0.7	1.7	4.4	8.4
253.3	609.5	1264.2	1731.5	1.3	3.4	8.7	15.9
81.6	210.0	524.3	916.9	0.4	1.3	4.0	9.3
81.5	245.0	646.6	1204.9	0.4	1.3	4.0	10.0
327.7	747.6	1548.1	2168.0	1.6	4.1	10.4	19.5
104.9	284.3	644.7	963.8	0.5	1.6	4.4	8.9
240.6	474.6	824.7	1041.9	1.5	3.8	8.9	15.2
148.1	391.5	763.2	1022.0	0.7	2.2	5.5	10.0
386.4	811.4	1351.5	1612.2	2.0	4.7	9.6	15.4
749.7	1566.7	2332.2	2608.9	4.0	9.7	18.2	27.5
98.4	354.6	833.4	890.9	0.6	1.9	5.3	12.0
102.5	255.4	565.8	873.6	0.5	1.5	4.1	8.5
228.2	629.8	1466.7	2060.7	1.0	3.1	8.6	18.5
85.2	234.3	505.4	706.7	0.4	1.3	3.6	6.8
122.3	351.1	857.2	1305.9	0.7	2.3	7.2	14.8

Appendix 19. Unbound and total area under the curve (AUC) for carvedilol in healthy and cirrhosis populations after first reductions in administered doses.

AUC Total				AUC Unbound			
25mg Healthy	12.5mg CP-A	6.25mg CP-B	3.125mg CP-C	25mg Healthy	12.5mg CP-A	6.25mg CP-B	3.125mg CP-C
76.8	107.6	79.4	85.3	0.4	0.6	0.9	0.8
107.4	866.3	131.6	127.2	0.5	4.8	1.2	1.2
299.0	29.9	394.1	363.2	1.4	0.2	3.0	2.8
129.9	143.7	135.6	127.8	0.8	1.0	1.8	1.8
240.7	107.3	264.0	209.0	1.2	0.6	2.2	1.9
818.3	238.4	458.8	327.6	4.0	1.3	4.2	3.0
185.1	166.2	177.2	189.4	1.2	1.0	2.6	2.8
202.8	279.2	218.2	190.1	0.9	1.8	1.5	1.4
78.4	192.1	93.1	85.6	0.5	1.5	1.2	1.2
78.5	172.7	123.1	125.1	0.4	1.0	1.3	1.5
156.6	459.2	151.1	162.6	0.7	2.3	1.8	1.9
156.2	335.8	167.0	153.9	0.8	1.8	1.8	1.6
55.1	201.0	86.2	93.1	0.3	1.2	0.9	1.0
278.6	209.9	229.4	229.0	1.2	1.3	2.0	2.0
275.6	248.4	235.0	179.1	1.4	1.6	2.8	2.4
236.4	326.9	264.2	272.1	1.2	1.3	2.4	2.6
207.0	262.2	220.9	220.5	1.0	1.6	2.1	2.0
231.7	305.3	222.6	201.6	1.3	1.6	2.4	2.2
86.3	237.3	94.5	110.3	0.4	1.9	1.1	1.3
171.1	177.3	177.9	171.5	1.0	0.9	2.0	2.0
110.4	293.1	123.9	122.0	0.6	1.6	1.2	1.2
127.1	112.9	108.2	99.7	0.7	0.7	1.2	1.0
191.0	170.7	72.6	74.7	1.1	1.0	0.7	0.8
359.7	273.5	270.7	251.3	2.2	1.3	3.4	2.7
21.8	163.5	27.0	31.2	0.1	1.1	0.3	0.4
196.1	196.0	157.1	147.8	1.1	1.0	1.4	1.4
163.2	217.2	229.7	249.0	0.8	1.4	1.8	1.9
140.9	126.1	183.3	186.9	0.7	0.8	1.8	2.0
251.7	92.9	358.8	324.6	1.4	0.6	3.0	2.8
64.6	195.8	82.3	94.4	0.4	1.1	1.3	1.5
338.6	164.0	371.5	341.5	2.0	1.3	4.7	4.7
96.8	235.6	133.8	129.0	0.5	1.5	1.4	1.5
467.8	89.0	362.8	260.7	2.0	0.6	2.5	1.8
164.3	76.3	137.3	127.5	0.8	0.5	1.4	1.3
210.8	171.5	97.4	102.5	1.2	1.0	1.3	1.3
300.7	219.4	176.2	157.2	1.6	1.5	2.0	1.9
142.9	90.8	228.0	232.0	0.7	0.6	2.1	2.3
218.4	113.5	260.3	264.7	1.3	0.7	1.7	1.7
142.1	783.4	136.2	147.7	0.8	4.9	1.6	1.6
110.4	175.6	85.6	96.7	0.6	1.2	1.1	1.3

| AUC Total | | | | AUC Unbound | | | |
25mg Healthy	12.5mg CP-A	6.25mg CP-B	3.125mg CP-C	25mg Healthy	12.5mg CP-A	6.25mg CP-B	3.125mg CP-C
120.8	219.4	160.2	176.0	0.6	1.8	1.2	1.4
65.5	421.7	84.9	83.9	0.4	3.2	0.9	0.9
168.9	91.5	209.3	176.2	0.8	0.8	2.2	2.0
132.0	278.7	156.1	252.7	0.6	1.2	1.7	1.8
79.3	114.1	102.2	109.0	0.5	0.8	1.2	1.3
133.4	422.3	290.5	303.7	0.7	2.0	1.9	1.9
162.2	227.8	143.1	140.2	0.9	1.7	1.6	1.6
441.3	163.4	162.4	152.1	2.4	1.0	1.3	1.3
713.0	122.5	208.8	178.6	3.4	0.6	2.0	1.9
118.8	142.1	282.4	270.1	0.6	0.8	2.3	2.2
194.7	149.3	174.9	165.6	0.9	0.8	1.7	1.7
68.9	168.1	175.9	137.7	0.4	0.8	2.2	1.8
163.4	173.2	190.4	172.5	1.0	1.1	1.4	1.3
396.9	241.6	163.4	141.6	2.2	1.5	1.7	1.5
189.5	204.4	233.4	210.0	1.0	1.3	2.2	2.0
172.4	323.4	104.4	98.4	0.7	1.8	1.1	1.1
156.6	80.3	83.7	124.4	0.8	0.6	1.0	1.1
305.4	330.7	302.2	262.9	1.7	1.9	2.3	2.0
177.0	157.4	98.3	109.6	1.1	0.9	1.0	1.1
388.4	405.7	172.2	184.8	1.8	2.3	2.4	2.5
385.0	104.1	132.1	123.9	2.1	0.8	1.2	1.2
94.0	309.7	209.6	163.0	0.5	1.8	2.1	2.0
199.2	432.0	223.5	216.5	1.0	3.3	1.9	2.0
84.8	139.5	120.6	119.1	0.4	0.9	0.9	1.0
76.2	96.3	149.8	142.2	0.4	0.7	1.4	1.4
149.6	344.0	241.6	232.2	0.8	1.8	1.6	1.6
260.8	168.1	269.8	253.4	1.5	1.2	2.2	2.1
176.6	134.5	223.1	181.5	0.7	0.7	2.3	2.0
125.5	317.1	153.7	154.1	0.7	2.0	1.4	1.5
190.4	304.7	148.1	125.1	1.1	1.7	1.9	1.7
267.6	283.4	299.0	274.4	1.4	1.3	2.8	2.7
600.7	124.1	139.8	177.9	3.5	0.8	1.3	1.4
147.2	190.8	129.2	121.3	0.9	1.3	1.7	1.6
89.2	342.2	108.0	124.4	0.6	1.4	1.1	1.3
265.0	215.4	218.7	190.1	1.4	1.1	2.1	1.9
252.9	134.7	220.6	209.5	1.2	0.9	1.9	1.7
37.3	291.8	154.1	158.0	0.2	1.8	1.2	1.3
284.7	495.0	255.3	219.8	1.5	2.8	2.7	2.4
57.7	105.0	133.2	146.6	0.3	0.6	1.4	1.5
114.0	314.9	157.0	175.4	0.5	1.5	1.3	1.4
294.4	292.3	220.3	202.0	1.5	2.2	2.2	2.0
247.1	289.1	254.1	226.8	1.2	1.8	2.0	1.9
69.9	223.7	97.8	95.9	0.4	1.5	1.0	1.1

AUC Total				AUC Unbound			
25mg Healthy	12.5mg CP-A	6.25mg CP-B	3.125mg CP-C	25mg Healthy	12.5mg CP-A	6.25mg CP-B	3.125mg CP-C
430.1	137.1	347.3	280.8	2.3	0.8	3.2	2.7
114.8	435.0	140.3	140.7	0.6	2.3	1.2	1.3
133.8	336.9	114.1	104.2	0.7	1.7	1.1	1.1
253.3	308.1	239.8	216.4	1.3	2.2	2.2	2.0
81.6	373.8	101.6	114.6	0.4	2.0	1.0	1.2
81.5	127.7	134.1	150.6	0.4	0.7	1.0	1.3
327.7	117.2	294.5	271.0	1.6	0.7	2.6	2.4
104.9	191.6	124.6	120.5	0.5	1.1	1.1	1.1
240.6	586.4	150.1	130.3	1.5	2.5	2.2	1.9
148.1	162.5	149.3	127.8	0.7	1.1	1.4	1.3
386.4	145.2	272.4	201.5	2.0	0.9	2.4	1.9
749.7	133.1	456.1	326.1	4.0	0.7	4.6	3.4
98.4	249.6	178.8	111.4	0.6	1.1	1.3	1.5
102.5	296.6	104.7	109.2	0.5	1.5	1.0	1.1
228.2	165.1	255.5	257.6	1.0	0.8	2.2	2.3
85.2	304.5	101.5	88.3	0.4	1.8	0.9	0.8
122.3	144.4	163.1	163.2	0.7	0.9	1.8	1.9

Appendix 20. Unbound and total area under the curve (AUC) for carvedilol in healthy and cirrhosis populations after further 25% reductions in administered doses.

Total AUC				Unbound AUC			
25mg Healthy	9.375mg CP-A	4.68mg CP-B	2.34mg CP-C	25mg Healthy	9.375mg CP-A	4.68mg CP-B	2.34mg CP-C
76.8	80.7	87.3	63.8	0.4	0.5	0.6	0.6
107.4	112.0	126.4	95.3	0.5	0.6	0.9	0.9
299.0	344.4	381.7	272.0	1.4	1.7	2.2	2.1
129.9	123.0	129.8	95.7	0.8	1.0	1.4	1.4
240.7	251.8	246.8	156.5	1.2	1.4	1.6	1.4
818.3	649.7	466.5	245.3	4.0	3.6	3.2	2.2
185.1	164.5	179.3	141.8	1.2	1.4	2.0	2.1
202.8	212.6	213.6	142.3	0.9	1.0	1.2	1.0
78.4	78.1	86.9	64.1	0.5	0.6	0.9	0.9
78.5	93.1	112.0	93.7	0.4	0.6	1.0	1.1
156.6	143.1	162.6	121.8	0.7	0.9	1.4	1.4
156.2	176.7	174.1	115.2	0.8	1.1	1.4	1.2
55.1	66.7	80.9	69.7	0.3	0.4	0.7	0.8
278.6	256.6	226.8	171.5	1.2	1.1	1.5	1.5
275.6	219.2	214.3	134.1	1.4	1.7	2.1	1.8
236.4	232.3	256.8	203.8	1.2	1.3	1.8	1.9
207.0	219.8	235.0	165.1	1.0	1.2	1.6	1.5
231.7	216.9	218.8	150.9	1.3	1.4	1.8	1.6
86.3	84.7	99.4	82.6	0.4	0.6	0.8	0.9
171.1	167.8	178.3	128.4	1.0	1.1	1.5	1.5
110.4	102.8	118.2	91.3	0.6	0.6	0.9	0.9
127.1	128.0	117.4	74.6	0.7	0.8	0.9	0.8
191.0	57.2	68.0	55.9	1.1	0.4	0.6	0.6
359.7	316.3	262.1	188.2	2.2	2.4	2.6	2.0
21.8	22.4	27.3	23.4	0.1	0.2	0.2	0.3
196.1	143.7	150.7	110.7	1.1	0.8	1.1	1.1
163.2	205.1	231.7	186.5	0.8	1.0	1.4	1.5
140.9	150.8	169.1	140.0	0.7	0.9	1.3	1.5
251.7	326.3	350.2	243.1	1.4	1.7	2.2	2.1
64.6	68.6	82.5	70.7	0.4	0.6	0.9	1.1
338.6	324.0	352.6	255.7	2.0	2.5	3.6	3.5
96.8	104.6	125.6	96.6	0.5	0.7	1.1	1.1
467.8	439.8	362.0	195.2	2.0	1.9	1.8	1.3
164.3	128.6	134.8	95.5	0.8	0.8	1.0	1.0
210.8	107.8	109.1	76.7	1.2	0.8	1.0	0.9
300.7	164.6	168.9	117.7	1.6	1.1	1.5	1.4
142.9	157.4	206.8	173.7	0.7	0.9	1.5	1.7
218.4	209.0	263.8	198.2	1.3	0.9	1.3	1.3
142.1	122.6	134.4	110.6	0.8	0.8	1.2	1.2

	Total AUC				Unbound AUC		
25mg Healthy	9.375mg CP-A	4.68mg CP-B	2.34mg CP-C	25mg Healthy	9.375mg CP-A	4.68mg CP-B	2.34mg CP-C
110.4	72.3	86.6	72.4	0.6	0.5	0.8	0.9
120.8	126.1	156.2	131.8	0.6	0.6	0.9	1.0
65.5	68.1	79.1	62.8	0.4	0.4	0.7	0.7
168.9	186.3	193.8	131.9	0.8	1.2	1.6	1.5
132.0	121.9	150.7	189.2	0.6	0.8	1.3	1.4
79.3	85.6	102.1	81.6	0.5	0.6	0.9	1.0
133.4	245.1	294.3	227.4	0.7	1.0	1.4	1.4
162.2	129.9	141.8	105.0	0.9	0.9	1.2	1.2
441.3	147.0	156.7	113.9	2.4	0.8	1.0	1.0
713.0	181.2	194.5	133.8	3.4	1.1	1.5	1.4
118.8	252.7	277.8	202.3	0.6	1.3	1.7	1.7
194.7	153.3	167.8	124.0	0.9	0.9	1.3	1.3
68.9	231.1	177.6	103.1	0.4	1.7	1.7	1.3
163.4	161.5	177.8	129.1	1.0	0.8	1.0	1.0
396.9	162.9	159.3	106.1	2.2	1.0	1.3	1.1
189.5	242.6	233.5	157.3	1.0	1.4	1.6	1.5
172.4	101.0	100.2	73.7	0.7	0.7	0.8	0.8
156.6	60.2	77.2	93.1	0.8	0.4	0.7	0.8
305.4	316.8	307.8	196.8	1.7	1.5	1.8	1.5
177.0	80.5	99.2	82.1	1.1	0.5	0.7	0.8
388.4	170.8	181.0	138.4	1.8	1.3	1.8	1.8
385.0	108.9	120.9	92.8	2.1	0.6	0.9	0.9
94.0	196.6	198.8	122.1	0.5	1.2	1.6	1.5
199.2	178.8	208.2	162.1	1.0	1.0	1.4	1.5
84.8	99.8	113.8	89.2	0.4	0.5	0.7	0.7
76.2	124.7	141.5	106.5	0.4	0.7	1.1	1.1
149.6	187.2	231.0	173.9	0.8	0.8	1.2	1.2
260.8	258.0	269.4	189.8	1.5	1.3	1.7	1.6
176.6	209.4	205.5	135.9	0.7	1.4	1.7	1.5
125.5	122.5	144.6	115.4	0.7	0.7	1.1	1.1
190.4	144.1	140.5	93.7	1.1	1.1	1.4	1.3
267.6	248.0	286.9	205.5	1.4	1.5	2.1	2.0
600.7	94.6	129.1	133.2	3.5	0.6	1.0	1.1
147.2	126.0	130.5	90.8	0.9	0.9	1.3	1.2
89.2	85.1	106.8	93.2	0.6	0.5	0.9	1.0
265.0	218.8	210.8	142.4	1.4	1.3	1.6	1.4
252.9	222.5	229.3	156.9	1.2	1.1	1.4	1.3
37.3	100.9	134.9	118.3	0.2	0.5	0.9	1.0
284.7	237.8	246.8	164.6	1.5	1.5	2.0	1.8
57.7	129.5	141.3	109.8	0.3	0.8	1.1	1.1
114.0	123.8	156.8	131.3	0.5	0.6	1.0	1.1
294.4	228.4	225.0	151.2	1.5	1.3	1.7	1.5
247.1	229.0	242.8	169.8	1.2	1.2	1.5	1.4

Total AUC				Unbound AUC			
25mg Healthy	9.375mg CP-A	4.68mg CP-B	2.34mg CP-C	25mg Healthy	9.375mg CP-A	4.68mg CP-B	2.34mg CP-C
69.9	69.7	89.9	71.8	0.4	0.5	0.8	0.8
430.1	371.2	334.3	210.2	2.3	2.1	2.4	2.0
114.8	118.0	138.0	105.3	0.6	0.7	0.9	1.0
133.8	108.3	111.6	78.1	0.7	0.6	0.8	0.8
253.3	228.5	236.7	162.1	1.3	1.3	1.6	1.5
81.6	78.7	98.2	85.8	0.4	0.5	0.7	0.9
81.5	91.9	121.1	112.8	0.4	0.5	0.8	0.9
327.7	280.4	289.8	202.9	1.6	1.5	1.9	1.8
104.9	106.6	120.7	90.2	0.5	0.6	0.8	0.8
240.6	178.0	154.4	97.5	1.5	1.4	1.7	1.4
148.1	146.8	142.9	95.7	0.7	0.8	1.0	0.9
386.4	304.3	253.0	150.9	2.0	1.8	1.8	1.4
749.7	587.5	436.6	244.2	4.0	3.6	3.4	2.6
98.4	133.0	156.0	83.4	0.6	0.7	1.0	1.1
102.5	95.8	105.9	81.8	0.5	0.6	0.8	0.8
228.2	236.2	274.6	192.9	1.0	1.2	1.6	1.7
85.2	87.9	94.6	66.2	0.4	0.5	0.7	0.6
122.3	131.7	160.5	122.2	0.7	0.9	1.4	1.4

XIII. Curriculum vitae

Personal Information

Name:	Muhammad Fawad
Surname:	Rasool
Date of birth:	10.01.1982
Address:	Kaiserswertherstraße 82B, 47249 Duisburg
Phone number:	+4917684366064
E-mail address:	fawad.rasool@uni-duesseldorf.de/
	fawadrasool@bzu.edu.pk

Work Experience

04.2014 – to date	Research Assistant modelling and simulation LENA Project, HHU, Düsseldorf, Germany
05.2013 – 03.2014	Teaching Assistant HHU, Düsseldorf, Germany
12.2007 – 07.2012	Lecturer in Department of Pharmacy, Bahauddin Zakariya University, Multan, Pakistan
04.2006 – 12.2007	Incharge Pharmacy in Bakhtawar Amin Memorial Trust Hospital, Multan, Pakistan.

Basic Education

01.2005 – 06.2007	M.Phil (Pharmaceutics) Department of Pharmacy, Bahauddin Zakariya University, Multan, Pakistan
11.2000 – 12.2004	B.Pharmacy, Department of Pharmacy, Bahauddin Zakariya University, Multan, Pakistan

Achievements/Awards

2015	Awarded runners-up prize, for the most informative scientific report at Simcyp consortium meeting, Sheffield, UK.
2012	Govt. of Pakistan funded PhD merit scholarship for doing PhD in an technologically advanced country (Prime Minister's Program)
2005	Best Sportsman of the year, Bahauddin Zakariya University, Multan, Pakistan (Gold Medal)

Languages

Urdu	Mother tongue
Punjabi	Bilingual proficiency
English	Bilingual proficiency
German	Limited working proficiency (Level A2)

Courses/Workshops attended

No.	Month/Year	Course/Workshop
1	Aug-Oct, 2012	A1 German Language Course (IDAF), Düsseldorf.
2	Sept, 2012	Simcyp hands on experience with automated model-based drug development: incorporating population variability into

		mechanistic prediction of PK and modelling PK-PD at Sheffield, UK.
3	Sept, 2012	Simcyp focused workshop on predicting age related changes to pharmacokinetics and drug-drug interactions including associated variability: linking this information to drug response in the pediatric population at Sheffield, UK.
4	Nov, 2012	Introduction to good scientific practice at iGRAD (HHU), Düsseldorf.
5	Nov, 2012	Fundamentals of Project Management at iGRAD (HHU), Düsseldorf.
6	Oct, 2012 to Jan, 2013	A1/A2 German Language Course (HHU), Düsseldorf.
7	April, 2013	Introduction to R-Statistical package (HHU), Düsseldorf.
8	June, 2013	Global research in pediatrics: Road show in Salzburg, Austria.
9	July, 2013	Management of research grants and projects at iGRAD (HHU), Düsseldorf.
10	Sept, 2013	Presenting science I–comprehensive, competent and convincing at iGRAD (HHU), Dusseldorf.
11	Sept, 2013	Simcyp focused workshop on the ABC of modelling drug transporter data: mechanistic approaches to predict the impact of drug transport proteins on ADME/pharmacokinetics and toxicity at Sheffield, UK.

12	Oct, 2013	20th Intermediate Workshop on PK/PD Data Analysis, Rome, Italy (Phoenix WinNonLin).
13	Jan, 2014	In-house Training: Introduction to "Good Laboratory Practice" (Klinkner & Partner), HHU, Düsseldorf.
14	March, 2015	Training on SPE and HPLC in proteomics and peptide analysis by Sigma at HHU, Düsseldorf.
15	April, 2015	Certara-Phoenix WinNonLin® Road Show, Frankfurt.
16	April, 2015	Get into teaching for Doctoral Researchers, iGRAD (HHU), Düsseldorf.
17	May, 2015	Simcyp workshop on hands on experience with model-based drug development: incorporating population variability into mechanistic prediction of PK and modelling PK-PD at Cambridge, UK.
18	June, 2015	Bioanalysis of Therapeutic and Endogenous Peptides: Understanding and Overcoming the Challenges of Working with Large Molecules by waters® in Köln.
19	June, 2015	Global research in pediatrics: Road show in Belgrade, Serbia.
20	Sept, 2015	Simcyp focused workshop on a systems pharmacology approach to modelling and simulation: Accelerating model building and covariate recognition in drug development by combining top down and bottom up modelling of pharmacokinetics linked to drug response at Sheffield, UK:

21   Jan, 2016   Visible & influential: making the most of self-marketing and networking, iGRAD (HHU), Düsseldorf.

Presentations in Conferences/Meetings

1. Rasool MF, Läer S. Physiologically based pharmacokinetic modelling of carvedilol. 1st Pharmacometrics in NRW, 2013; Cologne, Germany (Poster).

2. Rasool MF, Läer S. Prediction of carvedilol-paroxetine DDI by mechanism based inhibition of CYP2D6 using Simcyp®. 2nd Pharmacometrics in NRW, 2013; Cologne, Germany (Workshop).

3. Rasool MF, Läer S. Approaches for physiologically based pharmacokinetic modelling of carvedilol. 14th ESDPPP Congress, 2013, Salzburg, Austria (Poster).

4. Rasool MF, Khalil F, Läer S. A PBPK model for assessing impact of reduced organ blood flows on carvedilol exposure in heart failure. 3rd Pharmacometrics in NRW, 2014; Düsseldorf, Germany (Poster).

5. Rasool MF, Khalil F, Läer S. A PBPK approach for predicting carvedilol exposure in chronic heart failure. 4th Pharmacometrics in NRW, 2015; Münster, Germany (oral presentation).

6. Rasool MF, Khalil F, Läer S. Investigation of altered organ blood flow on carvedilol disposition in adult and pediatric chronic heart failure patients by using PBPK modelling. DPhG, 2015; Düsseldorf, Germany (Poster).

7. Rasool MF, Khalil F, Läer S. Physiologically based pharmacokinetic models for adult and paediatric chronic heart failure patients using the example of

carvedilol treated patients. 15th ESDPPP Congress, 2015, Belgrade, Serbia (oral presentation).

8. Rasool MF, Khalil F, Läer S. A Physiologically Based Pharmacokinetic Drug-Disease Model to Predict Carvedilol Exposure in Adult and Paediatric Heart Failure Patients, 6th Annual Simcyp Virtual Seminar on Applications of Population-based IVIVE and PBPK, 2015 (online presentation).

9. Rasool MF, Khalil F, Läer S. Optimizing clinical use of carvedilol in liver cirrhosis–a physiologically based pharmacokinetic approach. 5th Pharmacometrics in NRW, 2016; Bonn, Germany (oral presentation).

10. Rasool MF, Khalil F, Läer S. Investigating the role of altered organ blood flows on enantiomeric disposition of carvedilol in adult and pediatric chronic heart failure patients by using a physiologically based pharmacokinetic approach. 50th AEPC Congress, 2016; Rome, Italy (Poster).

M.Phil Thesis Supervised

1. Effect of Different Hydrophilic Binders On the Dissolution Profile of Mefenamic Acid (2011)

2. A multifactorial intervention in diabetic patients to enhance compliance, A prospective study (2012)

Publications

1. Arshad MS**, Rasool MF**, et al. Evaluation of antibiotic use behavior in cold and flu amongst the students of bahauddin zakariya university multan pakistan. Pak. J. Pharm. 20-23 (1 & 2) 15-22. (2010)

2. Sial AR, **Rasool MF** et al. Effect of Different Hydrophillic Binders on the Dissolution Profiles of Mefenamic Acid. Lat. Am. J. Pharm. 31 (3): 362-7 (2012)

3. Samtia AM, **Rasool MF** et al. A Multifactorial Intervention to Enhance Adherence to Medications and Disease-Related Knowledge in Type 2 Diabetic Patients in Southern Punjab, Pakistan. Trop J Pharm Res, 12 (5):851-856 (2013)

4. Majeed A, Ranjha NM, **Rasool MF** et al. Adherence to drug therapy in psychiatric patients in Nishtar Hospital, Multan (Pakistan) Journal of Pharmacy and Alternative Medicine www.iiste.org ISSN 2222-4807 (Online) Vol. 3, No. 1, 2014

5. Imtiaz S, Hashmat Ullah, **Rasool MF** et al. ASSESSMENT OF COMPLIANCE OF DIABETIC PATIENTS AT NISHTAR HOSPITAL MULTAN, PAKISTAN. Gomal Journal of Medical Sciences April-June 2014, Vol. 12, No. 2

6. **Rasool MF**, Khalil F, Laer S. A Physiologically Based Pharmacokinetic Drug-Disease Model to Predict Carvedilol Exposure in Adult and Paediatric Heart Failure Patients by Incorporating Pathophysiological Changes in Hepatic and Renal Blood Flows. Clinical pharmacokinetics. 2015 Sep;54(9):943-62.

7. **Rasool MF**, Khalil F, and Läer S. Physiologically Based Pharmacokinetic Models for Adult and Paediatric Chronic Heart Failure Patients Using the Example of Carvedilol Treated Patients. Archives of disease in childhood 101: e1 (Abstract).

8. **Rasool MF**, Khalil F, Läer S. Author's Reply to Zheng et al.: A Physiologically Based Pharmacokinetic Drug–Disease Model to Predict Carvedilol

Exposure in Adult and Paediatric Heart Failure Patients by Incorporating Pathophysiological Changes in Hepatic and Renal Blood Flows. Clinical Pharmacokinetics. 2015 2015/12/09:1-3.

9. **Rasool MF**, Khalil F, Läer S. Predicting stereo-selective disposition of carvedilol in adult and pediatric chronic heart failure patients by incorporating pathophysiological changes in organ blood flows–A physiologically based pharmacokinetic approach. (Drug Metabolism and Disposition: DMD Fast Forward. Published on April 11, 2016 as DOI: 10.1124/dmd.115.068858).

10. **Rasool MF**, Khalil F, Läer S. Optimizing the clinical use of carvedilol in liver cirrhosis using a physiologically based pharmacokinetic modeling approach. (accepted in European Journal of Drug Metabolism and Pharmacokinetics June, 2016).

Software skills

1. Microsoft Word, Excel, Powerpoint and Publisher

2. Graphpad Prism®

3. Simcyp®

4. Origin®

5. Phoenix WinNonLin®

6. R statistical package (basic proficiency)

7. MATLAB Simbiology (basic proficiency)

_____

Muhammad Fawad Rasool